



National Library
of Canada

Acquisitions and
Bibliographic Services Branch

395 Wellington Street
Ottawa, Ontario
K1A 0N4

Bibliothèque nationale
du Canada

Direction des acquisitions et
des services bibliographiques

395, rue Wellington
Ottawa (Ontario)
K1A 0N4

Your lib. / Votre référence

Our lib. / Notre référence

NOTICE

The quality of this microform is heavily dependent upon the quality of the original thesis submitted for microfilming. Every effort has been made to ensure the highest quality of reproduction possible.

If pages are missing, contact the university which granted the degree.

Some pages may have indistinct print especially if the original pages were typed with a poor typewriter ribbon or if the university sent us an inferior photocopy.

Reproduction in full or in part of this microform is governed by the Canadian Copyright Act, R.S.C. 1970, c. C-30, and subsequent amendments.

AVIS

La qualité de cette microforme dépend grandement de la qualité de la thèse soumise au microfilmage. Nous avons tout fait pour assurer une qualité supérieure de reproduction.

S'il manque des pages, veuillez communiquer avec l'université qui a conféré le grade.

La qualité d'impression de certaines pages peut laisser à désirer, surtout si les pages originales ont été dactylographiées à l'aide d'un ruban usé ou si l'université nous a fait parvenir une photocopie de qualité inférieure.

La reproduction, même partielle, de cette microforme est soumise à la Loi canadienne sur le droit d'auteur, SRC 1970, c. C-30, et ses amendements subséquents.

Canada

University of Alberta

Stochastic Models for Turbulent Diffusion

by



Shuming Du

A thesis

submitted to the Faculty of Graduate Studies and Research
in partial fulfilment of the requirements for the degree of
Doctor of Philosophy

Department of Earth and Atmospheric Sciences

Edmonton, Alberta

Fall 1995



National Library
of Canada

Acquisitions and
Bibliographic Services Branch

395 Wellington Street
Ottawa, Ontario
K1A 0N4

Bibliothèque nationale
du Canada

Direction des acquisitions et
des services bibliographiques

395, rue Wellington
Ottawa (Ontario)
K1A 0N4

Your file Votre référence

Our file Notre référence

THE AUTHOR HAS GRANTED AN
IRREVOCABLE NON-EXCLUSIVE
LICENCE ALLOWING THE NATIONAL
LIBRARY OF CANADA TO
REPRODUCE, LOAN, DISTRIBUTE OR
SELL COPIES OF HIS/HER THESIS BY
ANY MEANS AND IN ANY FORM OR
FORMAT, MAKING THIS THESIS
AVAILABLE TO INTERESTED
PERSONS.

L'AUTEUR A ACCORDE UNE LICENCE
IRREVOCABLE ET NON EXCLUSIVE
PERMETTANT A LA BIBLIOTHEQUE
NATIONALE DU CANADA DE
REPRODUIRE, PRETER, DISTRIBUER
OU VENDRE DES COPIES DE SA
THESE DE QUELQUE MANIERE ET
SOUS QUELQUE FORME QUE CE SOIT
POUR METTRE DES EXEMPLAIRES DE
CETTE THESE A LA DISPOSITION DES
PERSONNE INTERESSEES.

THE AUTHOR RETAINS OWNERSHIP
OF THE COPYRIGHT IN HIS/HER
THESIS. NEITHER THE THESIS NOR
SUBSTANTIAL EXTRACTS FROM IT
MAY BE PRINTED OR OTHERWISE
REPRODUCED WITHOUT HIS/HER
PERMISSION.

L'AUTEUR CONSERVE LA PROPRIETE
DU DROIT D'AUTEUR QUI PROTEGE
SA THESE. NI LA THESE NI DES
EXTRAITS SUBSTANTIELS DE CELLE-
CI NE DOIVENT ETRE IMPRIMES OU
AUTREMENT REPRODUITS SANS SON
AUTORISATION.

ISBN 0-612-06204-X

Canada

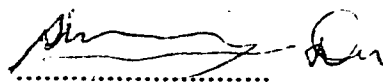
University of Alberta

Library Release Form

Name of Author: Shuming Du
Title of Thesis: Stochastic Models for Turbulent Diffusion
Degree: Doctor of Philosophy
Year this Degree Granted: 1995

Permission is hereby granted to The University of Alberta Library to reproduce single copies of this thesis and to lend or sell such copies for private, scholarly, or scientific research purposes only.

The author reserves all other publication and other rights in association with the copyright in the thesis, and except as hereinbefore provided, neither the thesis nor any substantial portion thereof may be printed or otherwise reproduced in any material form whatever without the author's prior written permission.

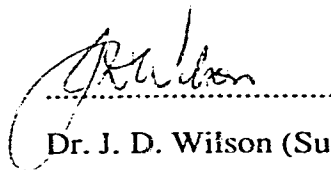


10-602
8 Bei Yin Yang Ying
Nanjing, 210024
P. R. CHINA

August 28, 1995
.....

THE UNIVERSITY OF ALBERTA
FACULTY OF GRADUATE STUDIES AND RESEARCH

The undersigned certify that they have read, and recommended to the Faculty of Graduate Studies and Research for acceptance, a thesis entitled STOCHASTIC MODELS OF TURBULENT DIFFUSION submitted by SHUMING DU in partial fulfilment of the requirements for the degree of DOCTOR OF PHILOSOPHY.



Dr. J. D. Wilson (Supervisor)



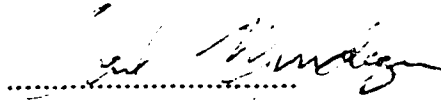
Dr. D. J. Wilson (Co-supervisor)



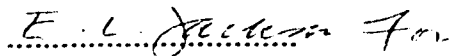
Dr. E. P. Lozowski




Dr. R. G. Ironside



Dr. C. A. Mendoza



Dr. F. T. M. Nieuwstadt (External examiner)



Dr. G. W. Reuter

DATE: 28 August 1995

This work is dedicated to my wife, parents and parents-in-law.

Abstract

This thesis develops a group of Lagrangian Stochastic (LS) turbulent dispersion models, and applies those models to study some problems of theoretical and/or practical importance.

By invoking the maximum missing information (mmi) principle, an mmi pdf of vertical velocity is constructed for non-Gaussian turbulence and the LS model implied by that pdf is derived. With this model, the effects of higher Eulerian velocity moments on the mean concentration distribution is studied and some earlier predictions of the small time behaviour of spread from a source are re-examined. The moments approximation method for developing LS models is also examined, and shown to be inferior to the standard method.

A second-order model for decaying isotropic turbulence was developed. By applying it to wind tunnel and water channel grid turbulent flows, and by applying a well established first-order model to wind tunnel and atmospheric boundary layer turbulence, the universal constant for the Lagrangian velocity structure function in the inertial subrange is determined to be 3.0 ± 0.5 .

With these stochastic techniques two other problems are also studied: the droplet collision probability in turbulent clouds - it is found that the effect of turbulence on enhancing collision probability can be very strong if the sizes of droplets are not substantially different, and the rate of upcrossing over a specified threshold level of concentration at a given spatial point - the model result accords with the Dugway field experiment data very well.

Acknowledgements

I would like to thank firstly my supervisor Dr. John D. Wilson, to whom I am very grateful for his support, patience and encouragement; and my co-supervisor Dr. David J. Wilson, who helped greatly with respect to several aspects of my research.

I thank also my external examiner, Dr. Frans T. M. Nieuwstadt (Delft University of Technology, Netherlands); supervisory committee members, Drs. Edward P. Lozowski and Gerhard W. Reuter; examining committee members, Drs. Robert G. Ironside and Carl A. Mendoza; and the Graduate Chair, Dr. Edgar L. Jackson.

It is a pleasure to acknowledge assistance in many matters from Dr. Thomas K. Flesch, Ms. Laura Smith, and Mr. Terry Thompson (of the former Geography Department); and Mr. Wayne Pittman (Mechanical Engineering Department). And finally I am grateful to Drs. Brian L. Sawford (CSIRO Division of Atmospheric Research, Australia), Eugene Yee (Defence Research Establishment Suffield), and Nathan Dinar (Israel Institute for Biological Research) for their kind assistance on academic matters.

Table of Contents

Chapter 1

INTRODUCTION: REVIEW OF LAGRANGIAN STOCHASTIC MODELS AND OUTLINE OF PRESENT CONTRIBUTION.....	1
1.1 History.....	1
1.2 Markovian Hypothesis.....	8
1.3 Review of the modern basis for LS models.....	8
1.4 Contribution of the present thesis.....	11
Bibliography.....	12

Chapter 2.

CONSTRUCTING A P.D.F., AND A FIRST-ORDER MODEL. FOR NON- GAUSSIAN TURBULENCE	16
2.1. Probability density function for velocity in the convective boundary layer, and implied trajectory models.....	17
2.1.1. Introduction.....	17
2.1.2. Criteria in constructing a pdf.....	17
2.1.3. Pdf's for vertical velocity (w) in the CBL.....	20
2.1.4. LS models for the CBL, from bi-Gaussian and mmi pdf's.....	22
2.1.5. Conclusion.....	25
Bibliography.....	26
2.2. On the moments approximation for constructing a Lagrangian stochastic model.....	34
2.2.1. Introduction.....	34
2.2.2. The exact model and the approximate model.....	35
2.2.3. Comparison of the exact and approximate models.....	39
2.2.4. Forming an optional Lagrangian model from partial information on Eulerian velocity statistics.....	48
2.2.5. Conclusion.....	51

Appendix 2.2. Eulerian velocity pdf implied by the moments approximation.....	53
Bibliography.....	54
2.3. The effects of higher Eulerian velocity moments on the mean concentration distribution.....	64
2.3.1. Introduction.....	64
2.3.2. Vertical velocity (w) moments in the Convective Boundary Layer	65
2.3.3. Eulerian vertical velocity pdf and the corresponding LS model	56
2.3.4. Sensitivity of the mean concentration distribution to the skewness and kurtosis of the vertical velocity.....	68
2.3.5. Small time behaviour of vertical dispersion.....	72
2.3.6. Conclusions.....	75
Appendix 2.3. An algorithm to generate random numbers with given pdf	77
Bibliography.....	78

Chapter 3

ON THE UNIVERSALITY OF THE KOLMOGOROV CONSTANT FOR THE LAGRANGIAN VELOCITY STRUCTURE FUNCTION.....	96
3.1. Estimation of the Kolmogorov constant (C_0) for the Lagrangian structure function, using a second-order Lagrangian model of grid turbulence	97
3.1.1. Introduction.....	97
3.1.2. Sawford's second-order model.....	99
3.1.3. Extension of the Sawford model to decaying turbulence.....	102
3.1.4. The magnitude of C_0	103
3.1.5. First-order Lagrangian stochastic model.....	108
3.1.6. Conclusion.....	109

Appendix 3.1. The pdf for fixed-point acceleration.....	109
Bibliography.....	110
3.2. Universality of the Kolmogorov constant for the Lagrangian velocity structure function across different kinds of turbulence.....	117
3.2.1. Introduction.....	117
3.2.2. C_0 in Grid Turbulence.....	119
3.2.3. C_0 from a Wind Tunnel Boundary Layer.....	119
3.2.4. C_0 in the Neutral Atmospheric Surface Layer: Project Prairie Grass (PPG).....	112
3.2.5. Criterion to Determine C_0 in the Neutral Atmospheric Boundary Layer.....	123
3.2.6. Conclusions.....	124
Bibliography.....	125

Chapter 4

OTHER APPLICATIONS OF STOCHASTIC METHODS.....	132
4.1. Modelling the effect of turbulence on the collision of cloud droplets...	133
4.1.1. Introduction.....	133
4.1.2. Relevant scales in the cloud droplet collision problem.....	134
4.1.3. First-order two-particle LS model for the collisions between large droplets.....	136
4.1.4. The collision probability and the collection kernel.....	141
4.1.5. Results.....	142
4.1.6. Conclusion.....	144
Appendix 4.1. Three droplet trajectory models.....	146
Bibliography.....	147
4.2. A stochastic model of concentration fluctuations in plumes	154
4.2.1. Introduction.....	154
4.2.2. A stochastic model of the concentration time series.....	155
4.2.3. Application of the present model to an intermittent concentration	

time series.....	158
4.2.4. Comparison of stochastic model with the Dugway data.....	159
4.2.5. Sensitivity of N^+ to the shape of the concentration pdf.....	160
4.2.6. Conditional standard deviation of concentration time derivative	160
4.2.7. Considerations to improve the model.....	161
4.2.8. Conclusions.....	162
Bibliography.....	163

Chapter 5

CONCLUDING REMARKS.....	172
Bibliography.....	175

Nomenclature

$\mathbf{a}(\mathbf{u}, \mathbf{x}, t)$:	mean acceleration of particles conditioned on $\mathbf{u}, \mathbf{x}, t$,
$a(A^+, W^+, Z^+, t)$:	rate of change of the Lagrangian acceleration conditioned on A^+, W^+, Z^+ ,
a_0 :	dimensionless constant appeared in the expression of Eulerian acceleration variance,
A :	(everywhere except section 3.1) fractional area occupied by thermals, (in section 3.1) Eulerian acceleration,
A^+ :	Lagrangian acceleration,
b_1 :	coefficient in the expression $\sigma_w = b_1 u_*$,
b_2 :	coefficient in the expression $T_L = b_2 Z / \sigma_w$,
\tilde{b}_{ij} :	coefficient of random forcing in Langevin equations,
B :	fractional area occupied by downdrafts,
c :	instantaneous concentration,
c_t :	threshold concentration,
c_* :	non-dimensional concentration defined as $c_* = Q/hU(h)$,
C :	the mean concentration,
C_k :	the coefficient of the k-th order term in the moment-approximation for $a(w, z)$,
C_p :	conditional (in-plume) mean concentration,
C_0 :	Kolmogorov's constant for Lagrangian velocity structure function,
$C_0^{\text{effective}}$:	effective Kolmogorov's constant in low Reynolds number flow,
$CWIC$:	cross-wind integrated concentration,
d :	separation between two cloud droplets,
d_0 :	zero-plane displacement height,
$d\zeta$:	Gaussian random variable with zero mean and variance dt ;
D_H :	horizontal separation between two cloud droplets,
$D_{ij}(\Delta t)$:	Lagrangian velocity structure function,
$E(R, r)$:	collection efficiency,
g :	gravitational acceleration,

h :	height of line source,
$H(p)$:	missing information when choosing a pdf p ,
\hat{i}_p :	(in-plume) conditional concentration fluctuation intensity,
K :	kurtosis factor for velocity fluctuations,
K_r :	horizontal distribution function of collection kernel,
K_s :	scalar eddy diffusivity,
$K(V,v)$:	collection kernel,
L :	Lagrangian integral length scale,
L_E :	Eulerian integral length scale,
M_k :	k -th order of vertical velocity moment,
N :	total number of known moments,
$N(V,t)$:	cloud droplet number density function,
N^* :	rate of upcrossing concentration threshold level c_* ,
p :	Lagrangian pdf for velocity,
$p_{z t}$:	conditional pdf of concentration derivative conditioned on c_t ,
p_a :	(everywhere except in section 3.1) Eulerian pdf for velocity,
p_a :	(in section 3.1) Eulerian joint pdf for acceleration and velocity.
$p_c(c)$:	Eulerian pdf for concentration,
Q :	line source strength per unit length,
r :	radius of small cloud droplet,
R :	radius of large cloud droplet,
$R_c(\tau)$:	auto-correlation coefficient for concentration fluctuations,
Re :	Reynolds number,
Re_λ :	Reynolds number based on Taylor micro scale λ ,
Re_L :	Lagrangian Reynolds number defined by $16a_0^2 Re/C_0^4$.
R_{III} :	inhomogeneity index,
$R_L(\Delta t)$:	Lagrangian auto-correlation coefficient,
S :	skewness factor of velocity fluctuations,
t_η :	Kolmogorov micro time scale,
T_c :	integral time scale for concentration fluctuations,

T_L :	Lagrangian integral time scale or Lagrangian decorrelation time scale,
u :	velocity,
u_i :	the component of velocity in i -th direction,
u_* :	friction velocity,
U :	(everywhere except in section 3.1) mean downstream velocity,
U :	(in section 3.1) Eulerian (instantaneous) velocity,
U^* :	Lagrangian velocity,
v_t :	terminal velocity of cloud droplet in still air,
w_A :	the mean vertical velocity within thermals,
w_B :	the mean vertical velocity within downdraughts,
w_s :	scale for vertical velocity,
w_* :	scale for vertical velocity in CBL,
$\langle w^k \rangle$:	k -th order moment of vertical velocity,
x :	distance from source to the point of interest,
X :	(everywhere except in section 3.1) non-dimensional distance defined as xw_s/Z_iU ,
X :	(in section 3.1) downstream distance from the source to the point of interest,
X_0 :	distance from the grid to the source,
X_{max} :	non-dimensional distance from the source to the location of maximum ground-level concentration,
y :	crosswind distance from plume centreline to the point of interest,
z :	height from ground level,
z_0 :	roughness length,
z_s :	height for point source,
Z :	Eulerian space variable (in vertical direction),
Z^* :	Lagrangian position in vertical direction,
$\langle Z \rangle$:	mean plume height,
$\langle Z'^2 \rangle$:	variance of vertical spread (related to σ_z by $\langle Z'^2 \rangle^{1/2} = \sigma_z$),
Z_i :	depth of CBL,

δ_{ij} :	Kronecker delta function,
Δt :	time increment,
ϵ :	the mean rate of dissipation of turbulent kinetic energy,
η :	Kolmogorov micro scale,
Θ :	characteristic function of p_a ,
κ :	von Kármán constant,
λ :	Taylor micro scale,
λ_k :	Lagrangian multiplier,
ν :	molecular kinematic viscosity,
ρ :	correlation between Eulerian vertical velocity and acceleration,
ρ' :	derivative of ρ with respect to t ,
ρ_a :	fluid density,
σ_A :	(everywhere except in section 3.1) standard deviation of vertical velocity within thermals,
σ_A :	(in section 3.1) standard deviation of Eulerian acceleration,
σ_A' :	derivative of σ_A with respect to t ,
σ_B :	standard deviation of vertical velocity within downdrafts,
σ_U :	standard deviation of streamwise velocity fluctuations,
σ_w :	standard deviation of vertical velocity,
σ_w :	standard deviation of vertical velocity,
σ_w' :	derivative of standard deviation of vertical velocity with respect to t .,
σ_y :	standard deviation of cross-wind spread,
σ_z :	standard deviation of vertical spread,
τ :	time increment,
ϕ :	solution of $\partial\phi/\partial w = -\partial p_r/\partial z$.

Glossary of terms:

CBL:	convective boundary layer,
DNS:	direct numerical simulation,
FP:	Fokker-Planck equation,

LES:	large-eddy simulation,
LS:	Lagrangian stochastic,
mmi:	maximum missing information,
pdf:	probability density function,
TKE:	turbulent kinetic energy,
wmc:	well-mixed condition (or constraint).

List of Figures

- Figure 2.1.1. Kurtosis of the vertical velocity during unstable stratification at the Boulder Atmospheric Observatory tower. The solid line is $K = 3.0$, the kurtosis for Gaussian turbulence.....29
- Figure 2.1.2. Comparison of the "correct" pdf which maximizes the missing information with both the present and Baerentsen and Berkowitz bi-Gaussian pdfs for (a) $S = 0.2$; (b) $S = 0.65$, and (c) $S = 1.0$30
- Figure 2.1.3. Prediction of LS model corresponding to the mmi pdf for the CWIC distribution in the CBL for three release heights: (a) $z_s/Z_i=0.067$; (b) $z_s/Z_i=0.24$; and (c) z_s/Z_i31
- Figure 2.1.4. Prediction of LS model corresponding to the present bi-Gaussian pdf for the CWIC distribution in the CBL for three release heights: (a) $z_s/Z_i=0.067$; (b) $z_s/Z_i=0.24$; and (c) $z_s/Z_i=0.49$32
- Figure 2.2.1. Comparison of $a(w)$ in the exact model and the three term approximation model. The flow is homogeneous non-Gaussian.....56
- Figure 2.2.2. The predicted standard deviation by both the exact model and the three term approximation model in homogeneous non-Gaussian turbulence. Perfect reflection condition was applied at both top and bottom boundaries. 5,000 particles were released at $z_s=500$ m with initial velocity drawn from the Eulerian velocity distribution. In calculation, $\Delta t=0.01T_L$ 57
- Figure 2.2.3. (a) The evolution of concentration distribution from an initially well-mixed profile ($C=1$) predicted by the three term approximate model. (b) The probability density distribution of vertical velocity at $t^*=t/T_L=100$, calculated from both the exact model and three term approximation model. The solid line is the probability density function at $t=0$. In calculation, 50,000 particles were released with the "well-mixed" initial condition. In calculating the concentration distribution, perfect reflection condition was employed at both boundaries. In calculating the evolution of pdf, no

	reflection scheme was used.....	58
Figure 2.2.4.	(a) Comparison of the calculated standard deviation by the exact model and the approximate models in inhomogeneous non-Gaussian turbulence. The source height was $z_s=500$ m. T_{Lmax} is the maximum Lagrangian time scale in the computational domain. (b) Comparison of the calculated mean height of the dispersing particles by the exact model and approximate LS models.....	59
Figure 2.2.5.	The evolution of a well-mixed initial concentration profile in the inhomogeneous inhomogeneous non-Gaussian turbulence. The profiles are at $t=2T_{Lmax}$. In calculation, 50,000 particles were released.....	60
Figure 2.2.6.	The evolution of a well-mixed initial concentration profile ($C=1$) in the inhomogeneous turbulence when only two velocity moments are specified. The profiles are at $t=5T_{Lmax}$. In calculation, 50,000 particles were released.	61
Figure 2.2.7.	Comparison of the CWIC contours in the X-Z plane predicted by (a) the mmi model and (b) the modified Kaplan-Dinar model in the convective boundary layer. X is the dimensionless downwind distance defined as $X = xw_s/UZ_p$ and $Z = z/Z_p$	62
Figure 2.2.8.	Comparison of the calculated ground level CWIC from both the mmi model and the modified Kaplan-Dinar model with Willis and Deardorff's water tank experiment. The well-mixed value (which should obtain at large X) is $CWIC = 1$	63
Figure 2.3.1.	The variation of the shape of Eulerian pdf of vertical velocity with skewness and kurtosis. (a) For a given kurtosis, $K=3.0$, the variation of pdf with S; (b) For a given skewness, $S=0.5$, the variation of pdf with K....	81
Figure 2.3.2.	Test of the present LS model in Gaussian turbulence - the distribution of CWIC in the X-Z plane. Contour levels (from inner to outer) are 2.0, 1.5, 1.3, 1.1, 0.9, 0.6, and 0.3, respectively.....	82
Figure 2.3.3.	The variation of the cross-wind integrated concentration (CWIC) with skewness. (a) The variation of the maximum ground level CWIC with	

	skewness; (b) The variation of ground-level CWIC with the non-dimensional downstream distance X for different values of skewness...	83
Figure 2.3.4.	The variation of (a) the mean plume height and (b) the standard deviation of vertical spread with downstream distance X for different values of skewness.....	84
Figure 2.3.5.	CWIC contours in the X - Z plane for different values of skewness (holding $K=3.0$). Contour levels (from inner to outer) are 2.0, 1.5, 1.3, 1.1, 0.9, 0.6, and 0.3, respectively.....	85
Figure 2.3.6.	The variation of the cross-wind integrated concentration (CWIC) with kurtosis. (a) The variation of the maximum ground level CWIC with kurtosis; (b) The variation of ground-level CWIC with the non-dimensional downstream distance X for different values of kurtosis.....	87
Figure 2.3.7.	The variation of (a) the mean plume height and (b) the standard deviation of vertical spread with downstream distance X for different values of kurtosis.....	88
Figure 2.3.8.	CWIC contours in X - Z plane for different values of kurtosis (holding $S=0.5$). Contour levels (from inner to outer) are 2.0, 1.5, 1.3, 1.1, 0.9, 0.6, and 0.3, respectively.....	89
Figure 2.3.9.	The variation of the mean concentration distribution with different values of the Kolmogorov constant C_0 . In calculations, $S=0.5$, $K=3.0$. (a) CWIC contours in the X - Z plane, contour levels (from inner to outer) are 2.0, 1.5, 1.3, 1.1, 0.9, 0.6, and 0.3, respectively; (b) variation of ground-level CWIC with downstream distance, different symbols are used for different values of the Kolmogorov constant (2.0, 3.0 and 4.0).....	91
Figure 2.3.10.	Comparison of LS simulation with the Hunt perdition (eqn 2.3.13). (a) The mean plume height with travel time from the source; (b) The standard deviation of the particle spread with travel time from the source. The source height is $0.5Z_i$	92
Figure 2.3.11.	Comparison of LS simulation with the Hunt perdition (eqn 2.3.13). (a) The mean plume height with travel time from the source; (b) The standard	

deviation of the particle spread with travel time from the source. The source height $0.01Z_t$	93
Figure 2.3.12. Test of the Hunt inference (eqn 2.3.14): the standard deviation of the particle spread with travel distance from the source. (a) linear scale, (b) Logarithmic scale.	94
Figure 2.3.A. An example of the distribution of a large set of random numbers generated by the procedure given in the appendix, and the true pdf to which these random numbers are designed.....	95
Figure 3.1.1. Vertical dispersion from a tracer source in a water channel experiment, compared with simulations using a second-order LS model with different values of C_0 . Curves for Kolmogorov's constant C_0 from 2.0 to 4.0...	113
Figure 3.1.2. Vertical dispersion from a tracer source in a wind tunnel experiment, compared with simulations using a second-order LS model with different values of C_0 . Curves for Kolmogorov's constant C_0 from 2.0 to 4.0.	114
Figure 3.1.3. Vertical dispersion from a tracer source compared with simulations using a first-order model (with and without Reynolds number correction): (a) water channel, (b) wind tunnel. Curves for different effective Kolmogorov's constant $C_0^{effective}$	115
Figure 3.1.4. Reynolds number versus alongstream distance in the experimental grid turbulence: (a) water channel, (b) wind tunnel.....	116
Figure 3.2.1. Measured and simulated vertical spread of tracers, σ_z , for source height $h=6$ cm in a boundary layer with downstream distance x for wind tunnel data of Raupach and Legg (1983). Curves for the Kolmogorov constant C_0 from 2.5 to 10.0.....	127
Figure 3.2.2. Simulated vertical profiles of mean concentration with different values of C_0 in a wind tunnel boundary layer flow due to a line source of height $h = 6$ cm. c_* is defined by $c_* = Q/hU(h)$, where Q is the source strength per unit length.....	128
Figure 3.2.3. Measured and simulated ground-level mean concentration in the wind	

tunnel boundary layer flow (Raupach and Legg 1983) due to a line source of height $h = 6$ cm. c_s is defined by $c_s = Q/hU(h)$, where Q is the source strength perunit length. Curves for the Kolmogorov constant C_0 from 2.0 to 10.0.....	129
Figure 3.2.4. Measured and simulated vertical profiles of cross-wind integrated concentration for 6 neutral-stratification runs of the Project Prairie Grass. Curves for different values of the Kolmogorov constant 2.5 and 3.5, respectively.....	130
Figure 4.1.1. Distribution of the collection kernel according to models 1, 2, 3 for droplets of radii 50 μ m, 100 μ m in strong turbulence ($\sigma_v=2.0$ ms ⁻¹ ; $\epsilon=0.1$ m ² s ⁻³).....	149
Figure 4.1.2. Distribution of the collection kernel according to models 1, 2 for droplets of equal radii (50 μ m) in strong turbulence.....	150
Figure 4.1.3. Distribution of the collection kernel according to models 1, 2 for droplets of radii 50 μ m, 100 μ m in weak turbulence ($\sigma_v=0.5$ ms ⁻¹ ; $\epsilon=0.01$ m ² s ⁻³).	151
Figure 4.2.1. An example showing how essentially uncorrelated segments in the total time series become correlated in the conditional in-plume time series which is obtained by removing “zero” readings from the total time series. (a) total time series; (b) conditional time series.....	165
Figure 4.2.2. A family of the predicted upcrossing intensity from Log-normal concentration pdf. Also shown is the measured upcrossing intensity from Dugway experiment. Curves for different values of $T_{c,p}$	166
Figure 4.2.3. Comparison of model predicted upcrossing intensity with the Dugway field experiment data for two cut-off frequencies: 100 Hz and 5 Hz.....	167
Figure 4.2.4. The sensitivity of the upcrossing intensity to the non-linearity exponent α . Curves for α from -0.3 to 0.3.	168
Figure 4.2.5. Upcrossing intensity N^* predictions with different concentration pdf's: Log-normal pdf and Gamma pdf.....	169
Figure 4.2.6. A family of conditional standard deviation of concentration derivative (see	

text for the exact definition), $\sigma_{\xi}(c/C_p)$, obtained from model calculation with Log-normal pdf. Also shown is the Dugway data fit reported by Yee et al. (1993b). Curves for $T_{c,p}$ from 0.1 to 0.3 sec.....170

Figure 4.2.7. A family of conditional standard deviation of concentration derivative (see text for the exact definition), $\sigma_{\xi}(c/C_p)$, obtained from model calculation with Gamma pdf. Also shown is the Dugway data fit reported by Yee et al. (1993b). Curves for $T_{c,p}$ from 0.1 to 0.3 sec.....171

List of Tables

Table 2.1.1.	Location X_{\max} of maximum surface concentration according to LS models, and; WD water-tank experiment; Lamb LES/LS simulation; CONDORS field experiment.....	33
Table 4.1.1.	Collection kernels from models 1, 2, 3 for droplets of radii 50 μm and 100 μm in strong turbulence ($\sigma_v=2.0 \text{ ms}^{-1}$; $\epsilon=0.1 \text{ m}^2\text{s}^{-3}$). The pure gravitational collection kernel for this case is 0.02827. The unit is $10^{-6} \text{ m}^3\text{s}^{-1}$	152
Table 4.1.2.	Collection kernels from models 1, 2 for weak turbulence driving large droplets of (a) different radii (50 μm , 100 μm); and (b) equal radii (50 μm).The unit is $10^{-6} \text{ m}^3\text{s}^{-1}$	153

Chapter 1

Introduction: Review of Lagrangian Stochastic Models and Outline of Present Contribution

1.1 History

To protect the atmospheric environment, and to deal efficiently with environmental accidents, knowledge of how pollutants are transported and diffused in the atmospheric boundary layer is of great importance. The best means to expand and refine that knowledge is ongoing theoretical study, guided by experimental studies.

Over the last thirty years or so, many kinds of theoretical dispersion models have been advanced: among them being K-theory models (Egan and Mahoney 1972); higher-order closure models (Donaldson 1973); large-eddy simulation (LES) models (Nieuwstadt and de Valk 1987); direct numerical simulation (DNS) models (Pumir 1994); and, Lagrangian stochastic models (Wilson et al. 1981; Sawford 1985; Thomson 1987, 1990), which will be our topic here.

Lagrangian Stochastic (LS; or "Random Flight," or "Monte Carlo") simulation is the most natural means to describe turbulent diffusion, which is fundamentally a Lagrangian process: pollutants are carried by individual fluid elements. LS simulation has several advantages over the Eulerian approach, the most attractive being the avoidance of closure assumptions which involve the *joint* distribution of tracer concentration and fluid velocity. Closure assumptions of that character are essential to Eulerian methods, and are not very accurate except in simple cases where both the velocity statistics and the source distribution conspire to forgive the superficiality of the basic description; eg. the gradient-diffusion closure, $\langle u_j c' \rangle = -K_{sj} \partial C / \partial x_j$, introduces a scalar eddy diffusivity (K_{sj}), whose unknown "actual" value depends (in general) on the independent variables (x, t), the state of motion of the fluid, and on the source distribution; in practise, K_{sj} is usually little more

than a "calibrated function," tuned to observations. And Eulerian closures are barren in this sense, whether the context be (as in the example just given) to describe the mean concentration field, or to study statistics of the fluctuations. To reiterate then, the fundamental advantage of the Lagrangian method is that closure assumption(s) relate to the *velocity* field only; calculation of concentration statistics is a more-or-less exact process. Other notable merits of the LS method are the ability to correctly calculate the near field of a source; the absence of numerical problems (pseudo-diffusion); and the simplicity of coding.

The history of *numerical* LS simulation is not long. Thompson (1971) was perhaps the first work of the modern type reported in the literature; but the roots of the LS theory for turbulent dispersion extend back to the study of Brownian motion, by A. Einstein, P. Langevin, A. Fokker and M. Planck (for a historical review, see van Kampen 1981). G.I. Taylor (1921) was the first to use Lagrangian statistics to study turbulent diffusion. By noting the similarities between turbulent diffusion and the random "drunkard" walk, Taylor introduced into turbulent diffusion theory a focus on individual particle movement, and derived his famous formula for the spread of particles in unbounded homogeneous and stationary turbulence. That exact formulation by Taylor has been used extensively for various purposes - especially as a criterion to examine alternative or (putatively) more general theories/models of turbulent dispersion. For example it is with the aid of Taylor's theory that we can understand the failure of K-theory in the near source region; the theory proves that at such short range, the process (of spread) is "memory-dominated," *not* the manifestation of many independent random velocity choices, *ipso facto*, NOT actually "diffusive."

Obukhov (1959) introduced the Fokker-Planck (FP) equation to the field of research in turbulent diffusion. At the time many scholars were sceptical, but recent developments prove Obukhov's idea correct; its importance cannot be over-exaggerated. Early followers of Obukhov were Novikov (1963) and Lin and Reid (1963); while Lin (1960) pioneered the use of the Langevin equation, a stochastic differential equation (SDE) equivalent to the FP eqn.

While Thompson's (1971) "computer age" work was heuristic, and in the light of today's knowledge over-simplified, it showed how easily the effects of flow complexity (eg. wind shear) and topography can be incorporated into an LS model. After Thompson came others, eg. Hall (1975) and Reid (1979), who also used the LS model to study turbulent diffusion in the atmospheric boundary layer. Especially, Wilson et al. (1981, WTK) triggered many other studies, that greatly improved LS theory and enhanced the applicability of LS simulation; these authors noted that in inhomogeneous turbulence, tracer particles (in their heuristic formulation) erroneously aggregated in the region of lower turbulence intensity. To correct this tendency, they added a "mean drift velocity" term in their rescaled LS model, based on simple physical reasoning, and found more-plausible dispersion statistics. In the simpler case that turbulent velocity scale is height-invariant, WTK showed their model simulated field diffusion observations very satisfactorily.

Legg and Raupach (1982, LR) were perhaps the first to enunciate a crucial model design criterion: that tracer particles which are uniformly distributed should (according to the model) remain uniformly distributed (this criterion has proven pivotal in the development of LS theory). LR gave a rational argument for the addition (in any region where the turbulent velocity scale is variant) of a mean drift velocity to the Langevin equation, a correction differing from that of Wilson et al. (1981). Subsequently Wilson et al. (1983, WLT) investigated the difference between the WTK and LR models, and showed them equivalent in weakly inhomogeneous turbulence, but not in strongly inhomogeneous turbulence. WLT also proposed a new model, WTK'', a variant of WTK, which has subsequently been given theoretical foundation (Thomson 1984, 1987) and is now well-known to be useful even in strongly inhomogeneous (but Gaussian) turbulence. We re-emphasize that all the models mentioned so far (WTK, LR and WTK'') were in some manner heuristic.

In contrast, Thomson (1984) used the moment-generating function method to design an LS model *rigorously*. By requiring the Langevin model (in the form $dW = -Wdt/T + \mu$ which is assumed *a priori*) to produce the correct steady-state distribution of

tracer particles in phase space, he derived a set of constraints on the random forcing term (μ). Apart from the novel rigour brought to bear on the subject, a lasting finding of Thomson's study is that in *inhomogeneous Gaussian* turbulence the WTK" model (a re-scaled Langevin equation with Gaussian forcing) satisfies the design criterion,- whereas the LR Langevin model requires non-Gaussian forcing, which later studies show is not realizable.

Different, more-complex, but similarly profound, model design criteria were introduced by van Dop et al. (1985): a correct model should give correct small-time spread of tracer particles; and, Eulerian statistics implied by the LS model should be compatible with the hierarchy of *Eulerian* conservation equations. Given that guidance, but again taking a form of Langevin equation assumed *a priori*, van Dop et al. developed an LS model having Gaussian random forcing.

From essentially the same criterion used by Legg and Raupach (1982) and by Thomson (1984), namely that an initially well-mixed ~~state~~ should remain so, Sawford (1986) confirmed the findings of Thomson (1984) and of van Dop et al. (1985), and found further that in *inhomogeneous turbulence only models rescaled in the manner of Wilson et al. (1983) are "realizable."* Sawford also proved that the criteria of Thomson (1984) and van Dop et al. (1985) were equivalent.

In 1987 two exceptionally important papers in the LS field were published: Thomson (1987) and Pope (1987). The latter is less widely-cited. By arguing that the mean dissipation rate of turbulent kinetic energy (ϵ) is the only physical parameter that the random forcing is dependent on, Pope showed that the random forcing *must* be Gaussian, whatever the statistical nature of the turbulence, in order to contrive an LS model that is consistent with Kolmogorov's similarity hypothesis. Upon fixing the random term, Pope suggested that all flow complexity should be accommodated in the deterministic term. From the well-mixed criterion, that the model calculated (output) one-point pdf for velocity should equal the specified (input) pdf for velocity, which is in essence the same criterion used earlier by Legg and Raupach (1982), Thomson (1984) and Sawford (1986), Pope derived a constraint on the selection of the deterministic term of the Langevin

equation.

Thomson's (1987) contribution is essentially the same as Pope's: but his presentation is more general, and his work therefore more widely appreciated. Thomson collected all the LS model design criteria used in the literature, namely: (1) the well-mixed condition, ie., that the model should give the correct steady-state distribution of particles in the (position and velocity) phase space; (2) the model should produce correct small-time behaviour for a point source; (3) the model should imply Eulerian statistics compatible with the Eulerian equations; (4) when the Lagrangian time scale approaches zero, the model should reduce to a diffusion equation; and (5) the forward and backward formulations should be consistent. Thomson proved that criterion (1) is the most general, and that satisfying (1) ensures that *all (these) other* criteria are satisfied.

Upon proving in a rigorous way that the random forcing must be Gaussian, Thomson derived a mathematical expression of the well-mixed condition that constrains the selection of the deterministic term,- provided the Eulerian velocity pdf is known. It is noteworthy that the formulations of Thomson and Pope are identical; and that, to derive the LS model equation, the Eulerian pdf for velocity must be known (ie., the Eulerian turbulence must be specified in terms of its velocity pdf).

Thomson (1987) realized that in multi-dimensional problems the well-mixed constraint can not give a unique model. Sawford and Guest (1988) showed that this non-uniqueness is of practical consequence: different models derived from the same constraint give different predictions of particle spread. Borgas and Sawford (1994) showed that in *isotropic* turbulence a unique model can be derived (even in the multi-dimensional case). But for anisotropic turbulence, the non-uniqueness problem remains unsolved. Sawford and Guest (1988) raised another question: is the Kolmogorov constant (used in specifying the coefficient of the random forcing term) truly universal? This question will be answered in the present thesis (Chapter 2).

An important application of LS modelling is to study turbulent dispersion in the convective boundary layer (CBL), or more specifically, the mean concentration distribution in the CBL. The CBL is characterized by strong (vertical) inhomogeneity, and large

skewness of the vertical-velocity fluctuations. Baerentsen and Berkowicz (1984, BB) was the first modern attempt to simulate diffusion in the CBL by the Lagrangian method. BB approximated the skewed pdf of Eulerian velocity as a bi-Gaussian - a summation of two Gaussian pdf's, one representing the contribution from updrafts, and the other the downdrafts. In both the updrafts and the downdrafts the Legg-Raupach model (which is *not* well-mixed) was employed, but with different turbulence parameters. The bi-Gaussian pdf was also used by de Baas et al. (1986) and Sawford and Guest (1987) to study turbulent diffusion in the CBL, but these later models also were not well-mixed, violating Thomson's model selection criterion. Well-mixed models were later developed by Luhar and Britter (1989) and Weil (1990), both using BB's pdf, with slightly different specifications for the pdf parameters.

In all the above studies of the CBL, the bi-Gaussian pdf was used; but the basis for using that pdf is merely its empirical consistency with observations, - so further examination of the bi-Gaussian pdf, and the criterion for designing a pdf for velocity is needed. This will be addressed in the present work.

The 1990's have also seen much progress in LS simulation. Sawford (1991) proposed a second order (in velocity) LS model for steady, homogeneous turbulence, in order to examine Reynolds number effects on dispersion. He found that in low-Reynolds number turbulence (eg. grid turbulence) the Reynolds number effect is important, the primary effect being through the Lagrangian integral time scale. This implies the *apparent* non-uniqueness of the Kolmogorov constant (as judged from the enforcement of concordance of first-order LS models with dispersion observations) is at least partially due to Reynolds number effects. Extension of the Sawford model to unsteady (decaying) isotropic turbulence is another aspect of the present thesis.

Kaplan and Dinar (1993) gave a "moments approximation" method so that in constructing an LS model the background flow is specified by a (small) number of low order velocity moments, rather than the complete velocity pdf. This method will be examined in Chapter 2. Wilson and Flesch (1993) studied how to incorporate flow boundaries into an LS model, and how to make boundary conditions consistent with the

well-mixed condition. They showed that the (usually-used) perfect reflection algorithm is consistent with the well-mixed condition only in the case of homogeneous Gaussian turbulence; but that there exists no reflection scheme consistent with well-mixed condition in inhomogeneous and/or skewed turbulence. Borgas (1993) considered turbulence intermittency corrections to LS simulation, by means of a multifractal formalism; his major conclusion is that for single-particle Lagrangian statistics, the intermittency effect is negligible.

The above mentioned models are all "single particle" models: correlation between different particles is not considered. In parallel to the development of single-particle models, two-particle models (capable of predicting *relative* diffusion and concentration variance) have also been progressing. Since the present thesis deal mainly with single-particle models, two-particle simulation is only briefly reviewed here.

Durbin (1980) proposed the first two-particle LS model. Although the model is 1-dimensional, and very simple, it reproduces many known results. Sawford and Hunt (1986) extended Durbin's model to include molecular effects on relative movement between two dispersing particles. They found that molecular processes influence the spread of particle pairs in such a way that increasing viscosity enhances small-scale structure, while molecular diffusion tends to smooth it. Kaplan and Dinar (1988), by incorporating (in a heuristic way) the spatial correlation between two particles into the random forcing term of the Langevin equation, developed a 3-dimensional, 2-particle model. The advantage of a 3-dimensional model is that it can explicitly respect the incompressibility condition as an additional constraint, in contrast to 1- or 2-dimensional models. However Kaplan and Dinar's model was criticized by Thomson (1991) for its violation of Kolmogorov's similarity hypothesis. By further generalising the well-mixed condition to the case of particle pairs, Thomson (1990) constructed a 2-particle, 3-dimensional model for isotropic turbulence in which the two-point joint Eulerian velocity pdf is Gaussian. He compared his model results with laboratory measurements. Borgas and Sawford (1994) tried to develop constraints to select a unique model from the family of models introduced by Thomson, by requiring that two-particle models should correctly predict 1-particle statistics.

1.2 Markovian Hypothesis

The basic assumption in the LS method is that the evolution of the "state" of a fluid element/particle is Markovian, i.e., the change of the state of a particle is dependent on its present state, but not its earlier state. When the Reynolds number ($Re=VL/v$; V is the velocity scale, L is the length scale; v is kinematic viscosity) is sufficiently high, the "state" is defined as the particle's *joint* position and velocity (\mathbf{u}, \mathbf{x}). The basic assumption then is that the evolution of (\mathbf{u}, \mathbf{x}) is dependent on present (\mathbf{u}, \mathbf{x}) , but not (\mathbf{u}, \mathbf{x}) at earlier times.

This is a plausible assumption. According to the Kolmogorov similarity theory (Monin and Yaglom 1975), when the Reynolds number is sufficiently high, the variance of particle acceleration is of order ϵt_η^{-1} (ϵ is the mean rate of dissipation of turbulent kinetic energy, and $t_\eta=(\nu/\epsilon)^{1/2}$ is the Kolmogorov micro time scale), while the acceleration covariance over time lag Δt , is of order $\epsilon/\Delta t = \epsilon t_\eta^{-1}(t_\eta/\Delta t)$. Thus the auto-correlation coefficient for acceleration is of order $t_\eta/\Delta t$, and so over any time interval Δt satisfying $\Delta t \gg t_\eta$, the acceleration is only weakly auto-correlated: changes of a fluid element's velocity at two successive time instants separated by Δt are approximately independent. The evolution of a fluid element's velocity (over intervals $\Delta t \gg t_\eta$) can be taken as Markovian. And although this Markovian assumption has not been rigorously justified, the success of simulations based upon it suggests its adequacy.

1.3 Review of the modern basis for LS models

Under the assumption that the evolution of a fluid element's velocity and position is jointly Markovian, the movement of that fluid element is mathematically described by a set of stochastic differential equations (SDE's), our Lagrangian stochastic model equations

$$\begin{aligned} du_i &= a_i(\mathbf{u}, \mathbf{x}, t)dt + b_{ij}(\mathbf{u}, \mathbf{x}, t)d\zeta_j, \\ dx_i &= u_i dt. \end{aligned} \tag{1.1}$$

According to Thomson (1987) each component of the random forcing ($d\zeta$) is necessarily Gaussian (otherwise the model is either non-existent, or trajectories are discontinuous in phase space). It is usual to specify that $d\zeta$ has zero mean, and variance dt .

Equations (1.1) imply an equivalent deterministic equation, the Fokker-Planck equation, for the evolution of the transition pdf, $p(\mathbf{u}, \mathbf{x}, t | \mathbf{v}, \mathbf{y}, s)$ - the probability density for (\mathbf{u}, \mathbf{x}) at time t of a fluid element that at time s was in state (\mathbf{v}, \mathbf{y}) . The FP eqn can be written (Gardiner 1983)

$$\frac{\partial p}{\partial t} = - \frac{\partial}{\partial x_i} (u_i p) - \frac{\partial}{\partial u_i} (a_i p) + \frac{1}{2} \frac{\partial^2}{\partial u_i \partial u_j} (b_{ik} b_{jk} p). \quad (1.2)$$

Now, we introduce the well-mixed condition (Thomson 1987): if the Lagrangian pdf $p(\mathbf{v}, \mathbf{y}, s)$ is proportional to the single-point Eulerian pdf (p_a), ie., if we posit a special case in which the tracer particles are well-mixed with the background fluid, then at any later time t , the single-point Lagrangian pdf $p(\mathbf{u}, \mathbf{x}, t)$ must remain proportional to p_a , otherwise order will develop from disorder. Mathematical implementation of the well-mixed condition to obtain the implied constraint on the selection of LS models is straightforward: multiply (1.2) by $p(\mathbf{v}, \mathbf{y}, s)$ (assumed proportional to p_a); integrate w.r.t. \mathbf{v}, \mathbf{y} over all allowable \mathbf{v}, \mathbf{y} ; since (according to the well-mixed condition)

$$\int_{-\infty}^{\infty} \int_{-\infty}^{\infty} p(\mathbf{u}, \mathbf{x}, t | \mathbf{v}, \mathbf{y}, s) p_a(\mathbf{v}, \mathbf{y}, s) d\mathbf{v} d\mathbf{y} = p_a(\mathbf{u}, \mathbf{x}, t), \quad (1.3)$$

it follows from (1.2) that

$$\frac{\partial p_a}{\partial t} = - \frac{\partial}{\partial x_i} (u_i p_a) - \frac{\partial}{\partial u_i} (a_i p_a) + \frac{1}{2} \frac{\partial^2}{\partial u_i \partial u_j} (b_{ik} b_{jk} p_a). \quad (1.4)$$

Equation (1.4) exerts a constraint on the selection of functions $\mathbf{a}(\mathbf{u}, \mathbf{x}, t)$ and $\mathbf{b}(\mathbf{u}, \mathbf{x}, t)$.

Although the well-mixed constraint has been presented here in the context of a single-particle, first-order model, it is able to be generalised to other cases; eg., zero-order models, second-order models, 2-particle models.

We now determine the function $b(\mathbf{u}, \mathbf{x}, t)$. According Kolmogorov's theory, for time lags dt lying in the inertial subrange (ie., $t_n \ll dt \ll T_L$, where T_L is the decorrelation time scale) the Lagrangian structure function is of form (Monin and Yaglom 1975)

$$\langle [u_i(t+dt) - u_i(t)][u_j(t+dt) - u_j(t)] \rangle = C_0 \epsilon \delta_{ij} dt, \quad (1.5)$$

where C_0 is supposedly an universal constant. It follows from eqns 1.1 and 1.5 then

$$b_{ik} b_{jk} = C_0 \epsilon \delta_{ij} dt. \quad (1.6)$$

The simplest choice for b_{ij} is

$$b_{ij} = \sqrt{C_0 \epsilon} \delta_{ij}, \quad (1.7)$$

since it is $b_{ik} b_{jk}$ that determines the Lagrangian velocity statistics.

Naturally a question follows (Sawford 1985; Sawford and Guest 1988): is the constant C_0 *really* universal; and if so, what is it's numerical value? This question will be answered in Chapter 3.

Assuming the Eulerian pdf is known and that the function $b(\mathbf{u}, \mathbf{x}, t)$ has been chosen, the function $\mathbf{a}(\mathbf{u}, \mathbf{x}, t)$ is constrained by the Fokker-Planck equation (1.4). For a 1-dimensional model, $\mathbf{a}(\mathbf{u}, \mathbf{x}, t)$ can be uniquely determined from (1.4), but for a multi-dimensional problem $\mathbf{a}(\mathbf{u}, \mathbf{x}, t)$ cannot be determined solely from solving (1.4). Mathematically, this is because for an n -dimensional problem, the unknown vector function $\mathbf{a}(\mathbf{u}, \mathbf{x}, t)$ has n components, and those n components can not be determined by only one equation of constraint. Physically, the information contained in $\mathbf{a}(\mathbf{u}, \mathbf{x}, t)$ is much more than that contained in the single-point pdf p_a : the information about time variation is lost when (1.2) is integrated over the whole velocity-position space; or put it in another way: the LS model equation (1.1) is statistically equivalent to (1.2), ie., all the information contained in function $\mathbf{a}(\mathbf{u}, \mathbf{x}, t)$ is also contained in the transition pdf $p(\mathbf{u}, \mathbf{x}, t | \mathbf{v}, \mathbf{y}, s)$, so in principle, one can derive $p(\mathbf{u}, \mathbf{x}, t | \mathbf{v}, \mathbf{y}, s)$ from $\mathbf{a}(\mathbf{u}, \mathbf{x}, t)$, and can recover $\mathbf{a}(\mathbf{u}, \mathbf{x}, t)$ from the derived transition pdf $p(\mathbf{u}, \mathbf{x}, t | \mathbf{v}, \mathbf{y}, s)$ but not from any single-point pdf: the latter does not contain any information about time variation.

For the ideal case of homogeneous, isotropic and stationary turbulence, Borgas and Sawford (1994) show a unique LS model can be derived from (1.4). But for anisotropic turbulence, to make a multi-dimensional LS model unique, other physically-meaningful constraints must be discovered and employed.

1.4 Contribution of the present thesis.

This thesis will use "paper format," i.e. each section in the next three chapters will be self-contained. The work has three main parts.

1.4.1. *First-order single-particle model for non-Gaussian turbulence.*

Since Thomson's (1987) provision of the well-mixed constraint as the selection criterion for LS models, knowledge of the Eulerian velocity probability density function (pdf) has become a prerequisite for designing an LS model. However, the Eulerian pdf is usually not known, and what is available are a few low order moments of that pdf. In chapter 2 the maximum missing information (or maximum entropy) principle is used to construct an unbiased Eulerian velocity pdf, and a new LS model is derived from that pdf. The new model is used as the standard to examine the Kaplan-Dinar (1993) moments approximation method, which was claimed to yield a well-mixed model. The present study shows the latter does not satisfy the well-mixed constraint, and can give a poor prediction for dispersion. The effect of higher-order Eulerian velocity moments on the spatial distribution of the mean concentration is also studied.

1.4.2. *Universality (?) of Kolmogorov constant (C_0) of Lagrangian velocity structure function.*

Sawford and Guest (1988) found that, in order to achieve the best agreement between first-order LS model predictions and experimental measurements, different values

for C_0 had to be used for different flows. In chapter 3, evidence is presented that C_0 is indeed universal, and its value is estimated to be $C_0 = 3.0 \pm 0.5$.

These results are obtained (in part) by developing a second-order model for grid turbulence, in which the Reynolds number is fairly low. The second-order model takes that low Reynolds number explicitly into account. With the aid of this second-order model, it is also shown that the *effective*, $C_0^{\text{effective}}$, arising if a first-order model is applied to low- Re flows, is smaller than C_0 .

Constancy of C_0 is further examined across atmospheric and laboratory boundary layer flows: the optimal value is again found to be, $C_0 = 3.0 \pm 0.5$.

1.4.3. *Other applications of stochastic techniques.*

Chapter 4 gives two examples of the application of stochastic methods to other problems. In the first, we employ a two-particle model to study the effect of turbulence on collisions of cloud droplets, and to examine previous LS models of that process. In the second, a stochastic model for an Eulerian (rather than Lagrangian) problem is developed: the temporal evolution of the concentration of a contaminant *at a given spatial point*. The rate of upcrossing over any "threshold" level of concentration is studied; and the prediction of the stochastic model accords quite well with field measurement.

Bibliography

- Baerentsen, J.H. and R. Berkowicz, 1984: Monte Carlo simulation of plume dispersion in the convective boundary layer. *Atmos. Environ.* **18**, 701-712.
- Borgas, M.S., 1993: The multifractal Lagrangian nature of turbulence. *Phil. Trans. R. Soc. Lond. A* **342**, 379-411.
- Borgas, M.S. and B.L. Sawford, 1994: A family of stochastic models for two-particle dispersion in isotropic, homogeneous and stationary turbulence. *J. Fluid Mech.* **279**, 69-99.

- de Baas, A.F., H. van Dop and F.T.M. Nieuwstadt, An application of the Langevin equation for inhomogeneous conditions to dispersion in a convective boundary layer. *Quarterly J. Roy. Meteorol. Soc.* **112**, 165-180.
- Donaldson, C. du P., 1973: Construction of a dynamic model of the production of atmospheric turbulence and the dispersal of atmospheric pollutants. *Workshop on Micrometeorology*, ed. D. A. Haugen, American Meteorological Society.
- Durbin, P.A., 1980: A stochastic model of two-particle dispersion and concentration fluctuations in homogeneous turbulence. *J. Fluid Mech.* **100**, 279-302.
- Egan, B.A. and J.R. Mahoney 1972: Numerical modelling of advection and diffusion of urban area source pollutants. *J. Appl. Meteorol.* **11**, 312-322.
- Gardiner, C.W., 1983: *Handbook of Stochastic Methods for Physics, Chemistry and the Natural Sciences*. 2nd edition. Springer-Verlag.
- Hall, C.D., 1975: The simulation of particle motion in the atmosphere by a numerical random-walk model. *Quarterly J. Roy. Meteorol. Soc.* **101**, 235-244.
- Kaplan, H. and N. Dinar, 1988: A three-dimensional stochastic model for concentration fluctuation statistics in isotropic homogeneous turbulence. *J. Comp. Phys.* **79**, 317-335.
- Kaplan, H. and N. Dinar, 1993: A three-dimensional model for calculating concentration distribution in inhomogeneous turbulence. *Boundary-Layer Meteorol.* **62**, 217-245.
- Lin, C.C, 1960: On a theory of dispersion by continuous movements, I. *Proc. Nat. Acad. Sci., Wash.* **46**, 566-570.
- Lin, C.C. and Reid, W.H. Reid, 1963: Turbulent flow, theoretical aspects. *Handbuch der physik*, **VIII/2**, 438-523.
- Luhar, A.K. and R.E. Britter, 1989: A random walk model for dispersion in inhomogeneous turbulence in a convective boundary layer. *Atmos. Environ.* **23**, 1911-1924.
- Monin, A.S. and A.M. Yaglom, 1975: *Statistical Fluid Mechanics*, Vol 2. MIT Press.
- Novikov, E.A., 1963: Random force method in turbulence theory. *Sov. Phys. JETP* **17**,

1449-1454.

- Nieuwstadt, F.T.M. and J.P.J.M.M. de Valk 1987: A large eddy simulation of buoyant and non-buoyant plume dispersion in the atmospheric boundary layer. *Atmos. Environ.* **21**, 2573-2587.
- Obukhov, A.M., 1959: Description of turbulence in terms of lagrangian variables. *Adv. Geophys.* **6**, 113-116
- Pope, S.B., 1987: Consistency conditions for random-walk models of turbulent dispersion. *Phys. Fluids* **30**, 2374-2379.
- Pumir, A., 1994: A numerical study of the mixing of a passive scalar in three dimensions in the presence of a mean gradient. *Phys. Fluids* **6**, 2118-2132.
- Reid, J.D., 1979: Markov chain simulations of vertical dispersion in the neutral surface boundary layer. *Boundary-layer Meteorol.* **16**, 3-22.
- Sawford, B.L., 1985: Lagrangian statistical simulation of concentration mean and fluctuation fields. *J. Clim. Appl. Meteorol.* **24**, 1152-1166.
- Sawford, B.L., 1986: Generalized random forcing in random-walk turbulent dispersion models. *Phys. Fluids* **29**, 3582-3585.
- Sawford, B.L., 1991: Reynolds number effects in Lagrangian stochastic models of turbulent dispersion. *Phys. Fluid* **A3**, 1577-1586.
- Sawford, B.L. and F.M. Guest, 1987: Lagrangian stochastic analysis of flux-gradient relationships in the convective boundary layer. *J. Atmos. Sci.* **44**, 1152-1165.
- Sawford, B.L. and F.M. Guest, 1988: Uniqueness and universality of Lagrangian stochastic models of turbulent dispersion. *8th Symp. Turbulence and Diffusion*. American Meteorol. Soc.
- Sawford, B.L. and J.C.R. Hunt, 1986: Effects of turbulence structure, molecular diffusion and source size on scalar fluctuations in homogeneous turbulence. *J. Fluid Mech.* **165**, 373-400.
- Thompson, R., 1971: Numeric calculation of turbulent diffusion. *Quarterly J. Roy. Meteorol. Soc.* **97**, 93-98.
- Thomson, D.J., 1984: Random walk modelling of dispersion in inhomogeneous

- turbulence. *Quarterly J. Roy. Meteorol. Soc.* **110**, 1107-1120.
- Thomson, D.J., 1987: Criteria for the selection of stochastic models of particle trajectories in turbulent flows. *J. Fluid Mech.* **180**, 529-556.
- Thomson, D.J. 1990: A stochastic model for the motion of particle pairs in isotropic high-Reynolds-number turbulence, and its application to the problem of concentration variance. *J. Fluid Mech.* **210**, 113-153.
- Thomson, D.J., 1991: Comments on "Diffusion of an instantaneous cluster of particles in homogeneous turbulence" by Kaplan and Dinar (*Atmos. Environ.* 23, 1459-1463). *Atmos. Environ.* **25A**, 1725-1726.
- van Dop, H., F.T.M. Nieuwstadt and J.C.R. Hunt, 1985: Random walk models for particle displacements in inhomogeneous unsteady turbulent flows. *Phys. Fluids* **28**, 1639-1653.
- van Kampen, N.G., 1981: *Stochastic Processes in Physics and Chemistry*. North-Holland Publishing Company, Amsterdam.
- Weil, J.C., 1990: A diagnosis of the asymmetry in top-down and bottom-up diffusion using a Lagrangian stochastic model. *J. Atmos. Sci.* **47**, 501-515.
- Wilson, J.D. and T.K. Flesch, 1993: Flow boundaries in random-flight dispersion models: enforcing the well-mixed condition. *J. Appl. Meteorol.* **32**, 1695-1707.
- Wilson, J.D., B.J. Legg and D.J. Thomson, 1983: Calculation of particle trajectories in the presence of a gradient in turbulent-velocity variance. *Boundary-layer Meteorol.* **27**, 163-169.
- Wilson, J.D., G.W. Thurtell and G.E. Kidd, 1981: Numerical simulation of particle trajectories in inhomogeneous turbulence, II: Systems with variable turbulent velocity scale. *Boundary-Layer Meteorol.* **21**, 423-441.

Chapter 2.

CONSTRUCTING A P.D.F., AND A FIRST-ORDER LS MODEL, FOR NON-GAUSSIAN TURBULENCE

In this chapter, the maximum missing information (mmi) principle is used to construct the probability density function for Eulerian turbulent velocity from given (partial) information: known velocity moments. From the mmi pdf for Eulerian vertical velocity, a one-dimensional Lagrangian stochastic model is derived, and applied to the convective boundary layer. With the new model, the Kaplan-Dinar moments approximation is examined and is found to be inferior. The effect of higher-order velocity moments on the mean concentration distribution is also studied.

2.1. PROBABILITY DENSITY FUNCTION FOR VELOCITY IN THE CONVECTIVE BOUNDARY LAYER, AND IMPLIED TRAJECTORY MODELS¹

2.1.1. Introduction

When taking advantage of Thomson's (1987) well-mixed condition (w.m.c.) in designing Lagrangian stochastic (LS) models of trajectories in turbulent flow, we must specify the Eulerian probability density function (pdf) of the fluctuating velocity. Except in idealized flows, that pdf is not exactly known, so it is usual practise to assume a pdf, guided by experimental evidence. Flesch and Wilson (1992) showed that adding increasingly numerous moment constraints, to shape an ad hoc pdf so as to describe highly non-Gaussian turbulence, can result in deteriorating agreement between simulation and measurement. It is clear then, that criteria are needed in formulating the pdf, and we here investigate using the "maximum missing information" (mmi) pdf.

Though our point is general, we will discuss the choice of a pdf in the context of modelling vertical dispersion in the Convective Boundary Layer (CBL). Up to now, the most widely-used pdf for the CBL has been the bi-Gaussian (a linear combination of two Gaussian functions), proposed by Baerentsen and Berkowicz (1984), supported by atmospheric observations (Quintarelli 1990), and used to build a well-mixed LS model by Luhar and Britter (1989) and Weil (1990). Our considerations lead to an LS model that performs slightly better than its predecessors.

2.1.2. Criteria in constructing a pdf

Assume we require to choose a pdf $p(x)$ for a variable x , which is random on the

¹ A version of this section has been published. S. Du, J.D. Wilson and E. Yee, 1994, *Atmospheric Environment* **28**, 1211-1217.

range $(-\infty, \infty)$. According to information theory (Jaynes 1957), $p(x)$ should:

- (a) reflect all the information we actually have; and
- (b) subject to constraints implied by the given information, maximise the function

$$H(p) = - \int_{-\infty}^{\infty} p(x) \ln \left(\frac{p(x)}{P_o} \right) dx \quad (2.1.1)$$

Here P_o is a scale for probability density, quantitatively irrelevant to the maximisation of H . $H(p)$ quantifies missing information (Baierlein 1971; Guisasu 1977), ie. provides a numerical measure of the amount of additional information needed to determine the pdf correctly and uniquely. It may be surprising that the "amount of missing information," on first sight a qualitative concept, can be given a unique quantitative measure. We will attempt no formal justification, but perhaps the following words might help. We reduce our uncertainty about the pdf with the help of information given us (e.g., moment constraints). However uncertainty remains, because an infinite number of pdfs are consistent with the given (finite number of) constraints. The principle of scientific objectivity dictates that we be maximally *uncommitted* about what we do not know concerning the pdf, and the requirement that $p(x)$ maximizes $H(p)$ enforces that principle: by satisfying (b) in our choice of $p(x)$, we are "maximally non-committal with respect to missing information" (Jaynes 1957).

Now, we seek a pdf $p(x)$ that maximizes $H(p)$, subject to the constraints:

$$\int_{-\infty}^{\infty} x^j p(x) dx = M_j \quad (j=1,2,\dots,N) \quad (2.1.2)$$

and the normalization condition $\int_{-\infty}^{\infty} p(x) dx = 1$. We set $M_0 = 1$, without loss of generality. Introducing appropriate Lagrange multipliers $\{\lambda_k, k=0,\dots,N\}$, (Swokowski 1979), one maximises the functional $H^* = H^*(p)$ defined from

$$H^*(p) = - \int_{-\infty}^{\infty} p(x) \ln p(x) dx + (\lambda_0 - 1) \left(1 - \int_{-\infty}^{\infty} p(x) dx \right) + \sum_{k=1}^N \lambda_k \left(M_k - \int_{-\infty}^{\infty} x^k p(x) dx \right).$$

Functional variation with respect to the unknown pdf, $p(x)$,

$$\frac{\delta H^*(p)}{\delta p(x)} = 0, \quad (2.1.3)$$

yields the following mmi pdf:

$$p(x) = \exp \left(- \sum_{k=0}^N \lambda_k x^k \right). \quad (2.1.4)$$

where the $N+1$ unknown Lagrange multipliers are determined from the normalization condition and the given moments by the implicit relationships

$$\exp(\lambda_0) = \int_{-\infty}^{\infty} \exp \left(- \sum_{k=0}^N \lambda_k x^k \right) dx \equiv Z, \quad (2.1.5)$$

and

$$M_j = \frac{1}{Z} \int_{-\infty}^{\infty} x^j \exp \left(- \sum_{k=0}^N \lambda_k x^k \right) dx, \quad j=1,2,\dots,N. \quad (2.1.6)$$

If $N > 2$, analytical solution is impossible, because the numerator of (2.1.6) involves an integral which cannot in general be expressed in terms of elementary functions. We infer that:

- (I) If we seek the mmi pdf for a random variable x defined on $(-\infty, \infty)$, subject to constraints (i.e., available information) of the usual form (viz, a set of moment constraints), our search can succeed only if we have an *even* number of moment constraints.

- (II) From (2.1.4), to ensure the pdf reproduces the known moments and vanishes for very large $|x|$, we must require $\lambda_N > 0$, where N (necessarily even, from I) is the highest order imposed moment constraint.

2.1.3. Pdf's for vertical velocity (w) in the CBL

We assume available the information that:

$$\langle w \rangle = 0,$$

$$\langle w^3 \rangle = S \langle w^2 \rangle^{3/2},$$

$$\langle w^4 \rangle = 3.0 \langle w^2 \rangle^2.$$

where S is the skewness. A value of about 3 for the kurtosis is supported by data from the Boulder Atmospheric Observatory (see Figure 2.1.1), and by aircraft observations (Hanna 1982).

2.2.3.1 The mmi pdf

The mmi pdf, which is in principle to be preferred, is:

$$p_a(w, z) = \exp\left(-\sum_{k=0}^4 \lambda_k(z) w^k\right),$$

At each of ten heights within the CBL, we determined numerically the set of values $(\lambda_0, \lambda_1, \dots, \lambda_4)$ consistent with the four velocity-moment constraints, and the normalization condition.

2.1.3.2 Bi-Gaussian pdf

Baerentsen and Berkowicz (1984; hereafter BB) proposed to use in the CBL the pdf

$$p_a(w,z) = \frac{A}{\sqrt{2\pi}\sigma_A} \exp\left[-\frac{(w-w_A)^2}{2\sigma_A^2}\right] + \frac{B}{\sqrt{2\pi}\sigma_B} \exp\left[-\frac{(w+w_B)^2}{2\sigma_B^2}\right] \quad (2.1.7)$$

where A and B are the fractional areas occupied by thermals and the compensating downdrafts, and w_A (w_B) and σ_A (σ_B) are the mean and the standard deviation of the fluctuating vertical velocity within thermals (downdrafts). Making no use of information on the kurtosis, but assuming

$$\sigma_A = w_A, \quad \sigma_B = w_B \quad (2.1.8)$$

BB obtained the parameters:

$$\begin{aligned} \sigma_B = w_B &= \left[(\langle w^3 \rangle^2 + 8 \langle w^2 \rangle^3)^{1/2} - \langle w^3 \rangle \right] / 4 \langle w^2 \rangle, \\ \sigma_A = w_A &= \langle w^2 \rangle / 2 w_B, \\ A &= w_B / (w_A + w_B), \quad B = w_A / (w_A + w_B) \end{aligned} \quad (2.1.9)$$

Luhar and Britter (1989) used Eqs. (2.1.9) in their LS model. Weil (1990), assuming (rather than (2.1.8)) that $\sigma_A/w_A = \sigma_B/w_B = R$ (where R is an arbitrary constant taken as 1.5), used similar expressions. Note that in view of the discussion of Subsection (2.1.2), it is not possible to construct the mmi pdf corresponding to the bi-Gaussian (2.1.9).

One is quite at liberty to specify the parameters of the bi-Gaussian otherwise than (2.1.9). We are interested to see whether the bi-Gaussian can approximate the mmi pdf *that corresponds to the given information*. The mmi pdf, as stated, made use of the known kurtosis: so that information, if the comparison is to be fair, must be brought to bear in fitting the bi-Gaussian.

Invoking knowledge of the kurtosis, we require to solve

$$A + B = 1,$$

$$Aw_A - Bw_B = 0,$$

$$A(\sigma_A^2 + w_A^2) + B(\sigma_B^2 + w_B^2) = \langle w^2 \rangle. \quad (2.1.10)$$

$$A(3w_A\sigma_A^2 + w_A^3) - B(3w_B\sigma_B^2 + w_B^3) = \langle w^3 \rangle,$$

$$A(3\sigma_A^4 + 6w_A^2\sigma_A^2 + w_A^4) + B(3\sigma_B^4 + 6w_B^2\sigma_B^2 + w_B^4) = \langle w^4 \rangle.$$

Now the assumption (2.1.8) is not supported by experimental data (Lenschow and Stephens 1982), so we close the set of equations (2.1.10) by instead assuming

$$A = 0.4. \quad (2.1.11)$$

This is supported by many experiments (Hunt et al. 1988; Fritsch and Businger 1973; among others), but is not valid as stratification tends towards the neutral condition. Under this assumption, and provided $S \leq 1.12$ (which is usually the case; LeMone 1990), the solution is

$$\begin{aligned} A &= 0.4, & B &= 0.6 \\ w_A &= \langle w^3 \rangle^{1/3}, & w_B &= (2/3) \langle w^3 \rangle^{1/3} \\ \sigma_A &= (\langle w^2 \rangle - 0.280 \langle w^3 \rangle^{2/3})^{1/2}, & \sigma_B &= (\langle w^2 \rangle - 0.927 \langle w^3 \rangle^{2/3})^{1/2} \end{aligned} \quad (2.1.12)$$

Figure 2.1.2 compares the mmi pdf with the two bi-Gaussian pdf's, for $S=0.2$, $S=0.65$ and $S=1.0$. Not surprisingly, our alternate bi-Gaussian pdf generally approximates the mmi pdf better than does the BB bi-Gaussian pdf (pay particular attention to the pdf near the mode, whose value greatly affects the mean concentration field, Hunt et al. 1988).

2.1.4. LS models for the CBL, from bi-Gaussian and mmi pdf's

The well-mixed LS model corresponding to the Baerentsen and Berkowicz bi-

Gaussian pdf was derived by Luhar and Britter (1989), to whom the reader may refer. A similar derivation, based on our (alternatively fitted) bi-Gaussian, yields a similar model:

$$dw = \left[-\frac{\langle w^2 \rangle}{T_L} Q + \phi \right] \frac{dt}{P_a(w,z)} + \left(\frac{2\langle w^2 \rangle}{T_L} \right)^{1/2} d\zeta \quad (2.1.13)$$

(terms have the same meaning as in LB). Q and ϕ are given by:

$$Q = \frac{(w - w_A) A p_A}{\sigma_A^2} + \frac{(w + w_B) B p_B}{\sigma_B^2} \quad (2.1.14)$$

$$\begin{aligned} \phi = & -\frac{A}{2} \frac{\partial w_A}{\partial z} \operatorname{erf} \left(\frac{w - w_A}{\sqrt{2} \sigma_A} \right) \\ & + \left[\sigma_A \frac{\partial \sigma_A}{\partial z} + \frac{w(w - w_A)}{\sigma_A} \frac{\partial \sigma_A}{\partial z} + w \frac{\partial w_A}{\partial z} \right] P_A \\ & + \frac{B}{2} \frac{\partial w_B}{\partial z} \operatorname{erf} \left(\frac{w + w_B}{\sqrt{2} \sigma_B} \right) \\ & + \left[\sigma_B \frac{\partial \sigma_B}{\partial z} + \frac{w(w + w_B)}{\sigma_B} \frac{\partial \sigma_B}{\partial z} - w \frac{\partial w_B}{\partial z} \right] P_B \end{aligned} \quad (2.1.15)$$

In the case of the mmf pdf, we obtain the model equation:

$$dw = a(w,z)dt + \left(\frac{2\langle w^2 \rangle}{T_L} \right)^{1/2} d\zeta, \quad (2.1.16)$$

where

$$\begin{aligned} a(w,z) = & -\frac{\langle w^2 \rangle}{T_L} \sum_{k=1}^4 k \lambda_k(z) w^{k-1} \\ & + \left[\sum_{k=0}^4 \frac{d\lambda_k(z)}{dz} \int_{-\infty}^w w^{k+1} p_a(w,z) dw \right] / p_a(w,z). \end{aligned} \quad (2.1.17)$$

We adopted exactly the same turbulence statistics for the CBL as did LB, and we carried out LS trajectory simulations, using both the bi-Gaussian based models, and the mmi model, for tracer particles released at source heights $z_s = (0.067, 0.24, \text{ or } 0.49) Z_i$ (where Z_i is the CBL depth). Perfect reflection was imposed at the top and bottom boundaries, and the time step was taken to be $0.01 T_L$. The model based on the mmi pdf consumed at least an order of magnitude more computer time than the bi-Gaussian model.

The mmi-based model and our bi-Gaussian based model produce fields of Crosswind Integrated Concentration (CWIC) that are almost identical, but different from the prediction that stems from the BB bi-Gaussian (Figure 2.1.3, 2.1.4). A feature we for the moment focus on, familiar from the convection tank experiments of Willis and Deardorff (1978, 1981; hereafter WD), is that the locus of the maximum concentration descends until it reaches the ground, causing the maximum ground level concentration to occur much closer to the source than it would in un-skewed turbulence (of otherwise equal properties). For a given source height, the distance x_{\max} to the point of maximum ground level concentration can be estimated by (Misra 1982; Li and Briggs 1987)

$$X_{\max} = \int_{h/Z_i}^{z_s/Z_i} \frac{dz/Z_i}{w_B/w_s} \quad (2.1.18)$$

where X_{\max} is non-dimensional on the translational velocity U and the convective time scale Z_i/w_s . Table 2.1.1 gives X_{\max} , according to the present LS models; the WD water-tank experiments; a simulation by Lamb (1978, 1982) of particle trajectories in the turbulent field generated by Deardorff's (1974) large-eddy simulation; and the CONDORS field experiment, (Briggs 1989). We conclude that (in regard to X_{\max}) the mmi model (and its more economical relative, our alternatively-fitted bi-Gaussian) is superior to the model based on the BB bi-Gaussian. A weakness of the latter pdf is that it implies

$$\frac{\partial w_B}{\partial \langle w^3 \rangle} = - \frac{(\langle w^3 \rangle^2 + 8 \langle w^2 \rangle^3)^{1/2} - \langle w^3 \rangle}{4 \langle w^2 \rangle (\langle w^3 \rangle^2 + 8 \langle w^2 \rangle^3)^{1/2}} < 0$$

for $\langle w^2 \rangle \neq 0$. The magnitude of the mean velocity in the downdrafts decreases with

increasing $\langle w^3 \rangle$, and so takes its maximum value at $\langle w^3 \rangle = 0$. The BB bi-Gaussian model makes x_{max} increase with increasing skewness, contradicting the water-tank simulations. In our alternately-fitted bi-Gaussian, the mean velocity in the thermals and downdrafts is determined by the third order moment only, or by skewness, $\langle w^3 \rangle / \langle w^2 \rangle^{3/2}$, for given velocity variance.

Returning to Figure 2.1.4, overall, the LS models simulate the CWIC distribution in the lower CBL quite well (compare our results with Figure 7 of WD, 1976; Figure 4 of WD, 1978; and Figure 4 of WD, 1981). We note, however, an overprediction of the mean concentration in the upper CBL, particularly near the top boundary (the LB simulation shows the same discrepancy). We satisfied ourselves that this feature of the simulations is not due to the small (< 10%) increase in CBL depth over the period of each tank experiment, nor to detrainment of tracer out of the mixed layer (to address the latter possibility we used partial, rather than perfect reflection at the top boundary). Possibly the velocity statistics we (and others) have adopted poorly represent the actual flow in and near the interfacial layer. That the maximum CWIC line does not impinge on the CBL top (as shown by the WD physical experiments, Lamb's (1982) numerical experiments and the CONDORS field experiments) suggest a mechanism for repelling tracer. Indeed, on applying the LS model to the case $z/Z_i = 0.75$, we get a high CWIC tongue which reaches the CBL top and is reflected back.

2.1.5. Conclusion

Although it is not possible to be conclusive on the basis of comparison with experimental evidence, we suggest on the basis of the foregoing that Lagrangian stochastic models of CBL dispersion should be based on the maximum missing information pdf for vertical velocity, the latter based on the first four Eulerian velocity moments (assumed given). A bi-Gaussian based model is practically as good, when fitted as we have shown here (to reproduce kurtosis). These details improve the prediction of the location of maximum ground level concentration.

Bibliography

- Baerentsen, J.H. and R. Berkowicz, 1984: Monte Carlo simulation of plume dispersion in the convective boundary layer. *Atmos. Environ.* **18**, 701-712.
- Baierlein, R., 1971: *Atoms and Information Theory*. W. H. Freeman and Company, San Francisco, 486 pp.
- Briggs, G.A., 1989: Field measurements of vertical diffusion in convective conditions. *Preprints of 6th Conference on Appl. of Air Pollution Meteorol.*, Jan 30-Feb 3, Anaheim, CA.
- Deardorff, J.W., 1974: Three-dimensional numerical study of the height and mean structure of a heated planetary boundary-layer. *Boundary-Layer Meteorol.* **7**, 81-106.
- Flesch, T.K. and J.D. Wilson, 1992: A two-dimensional trajectory-simulation model for non-Gaussian, inhomogeneous turbulence within plant canopies. *Boundary-Layer Meteorol.* **61**, 349-374.
- Frisch, S.A. and J.A. Businger, 1973: A study of convective elements in the atmospheric surface layer. *Boundary-Layer Meteorol.* **3**, 301-328
- Guiasu, S., 1977: *Information Theory with Applications*. McGraw- Hill, London, 439 pp.
- Hanna, S.R., 1982: Applications in the air pollution modelling. *Atmospheric Turbulence and Air Pollution Modelling*, F.T.M. Nieuwstadt and H. van Dop, (Eds.), D. Reidel Publishing Co., Dordrecht, 275-310.
- Hunt, J.C.R., J.C. Kaimal, and J.E. Gaylor, 1988: Eddy structure in the convective planetary boundary layer - new measurements and new concepts. *Q. J. Roy. Met. Soc.* **114**, 827-858.
- Jaynes, E.T., 1957: Information theory and statistical mechanics. *Phys. Rev.* **106**, 620-630.
- Lamb, R.G., 1978: Numerical simulation of dispersion from an elevated point source in the convective boundary layer. *Atmos. Environ.* **12**, 1297-1304.

- Lamb, R.G., 1982: Diffusion in the convective boundary layer. *Atmospheric Turbulence and Air Pollution Modelling*, F.T.M. Nieuwstadt and H. van Dop, (Eds.), D. Reidel Publishing Co., Dordrecht, 159-229.
- LeMone, M.A., 1990: Some observations of vertical velocity skewness in the convective planetary boundary layer. *J. Atmos. Sci.* **47**, 1163-1169.
- Lenschow, D.H. and P.L. Stephens, 1982: Mean vertical velocity and turbulence intensity inside and outside thermals. *Atmos. Environ.* **16**, 761-764.
- Li, Z. and G.A. Briggs, 1987: Simple pdf models for convective driven vertical diffusion. *Atmos. Environ.* **22**, 55-74.
- Luhar, A.K. and R.E. Britter, 1989: A random walk model for dispersion in inhomogeneous turbulence in a convective boundary layer. *Atmos. Environ.* **23**, 1911-1924.
- Misra, P.K., 1982: Dispersion of nonbuoyant particles inside a convective boundary layer. *Atmos. Environ.* **16**, 239-243.
- Quintarelli, F., 1990: A study of vertical velocity distribution in the planetary boundary layer. *Boundary-Layer Meteorol.* **52**, 209-219.
- Swokowski, E.W., 1979: *Calculus with Analytic Geometry*. 2nd Ed., Prindle, Weber & Schmidt, Boston, 999 pp.
- Thomson, D.J., 1987: Criteria for the selection of stochastic models of particle trajectories in turbulent flows. *J. Fluid Mech.* **180**, 529-556.
- Weil, J.C., 1990: A diagnosis of the asymmetry in top-down and bottom-up diffusion using a Lagrangian stochastic model. *J. Atmos. Sci.* **47**, 501-515.
- Willis, G.E. and J.W. Deardorff, 1976: A laboratory model of diffusion into the convective planetary boundary layer. *Q. J. Roy. Met. Soc.* **102**, 427-445.
- Willis, G.E. and J.W. Deardorff, 1978: A laboratory study of dispersion from an elevated source within a modeled convective planetary boundary layer. *Atmos. Environ.* **12**, 1305-1317.
- Willis, G.E. and J.W. Deardorff, 1981: A laboratory study of dispersion from a source in the middle of the convective planetary boundary layer. *Atmos. Environ.* **15**, 109-

117.

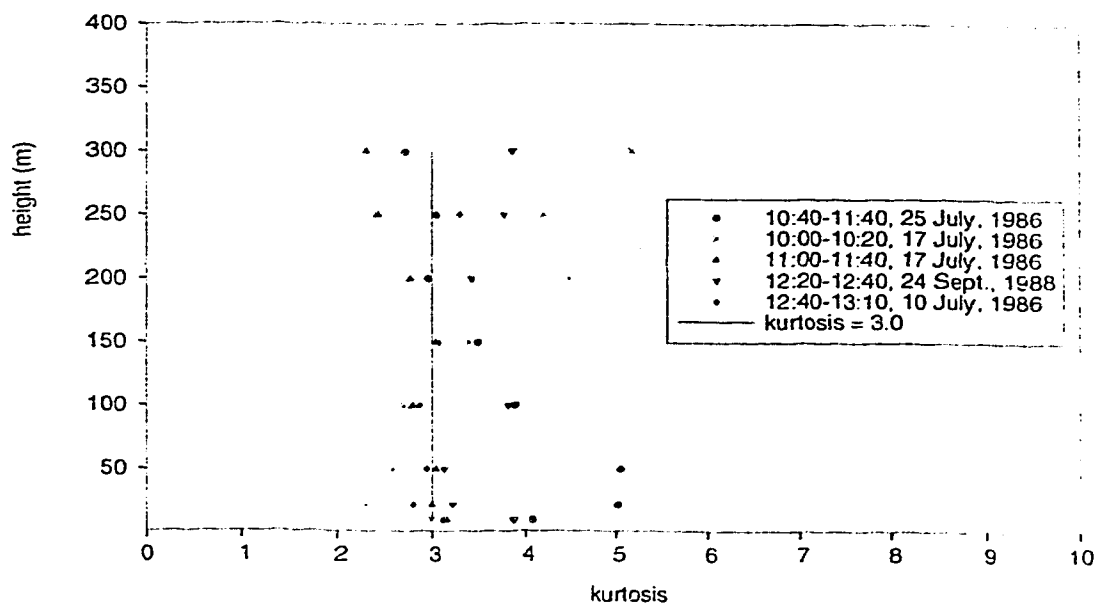


Figure 2.1.1. Kurtosis of the vertical velocity during unstable stratification at the Boulder Atmospheric Observatory tower. The solid line is $K = 3.0$, the kurtosis for Gaussian turbulence.

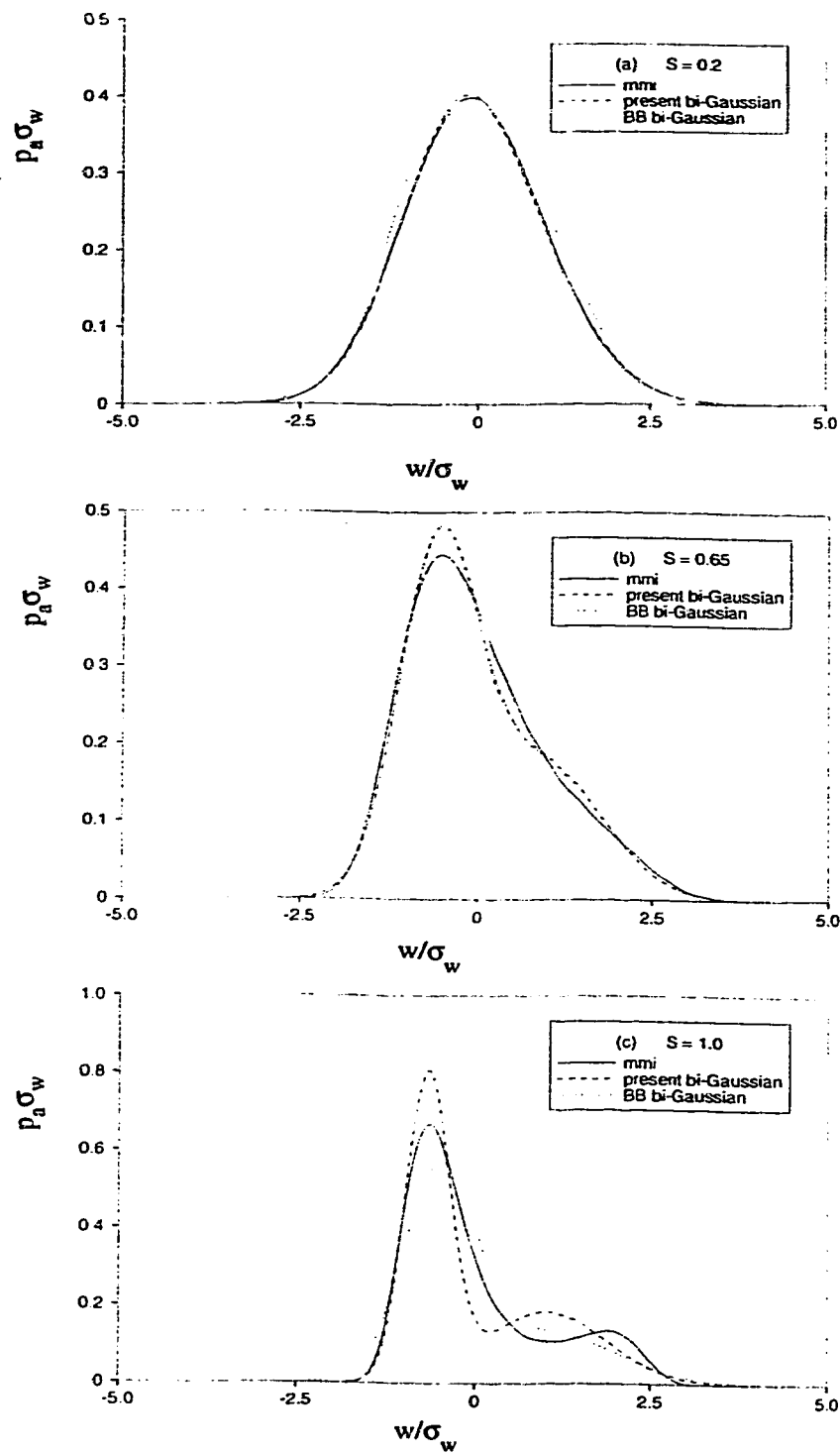


Figure 2.1.2. Comparison of the "correct" pdf which maximizes the missing information with both the present and Baerentsen and Berkowitz bi-Gaussian pdfs for (a) $S = 0.2$; (b) $S = 0.65$, and (c) $S = 1.0$.

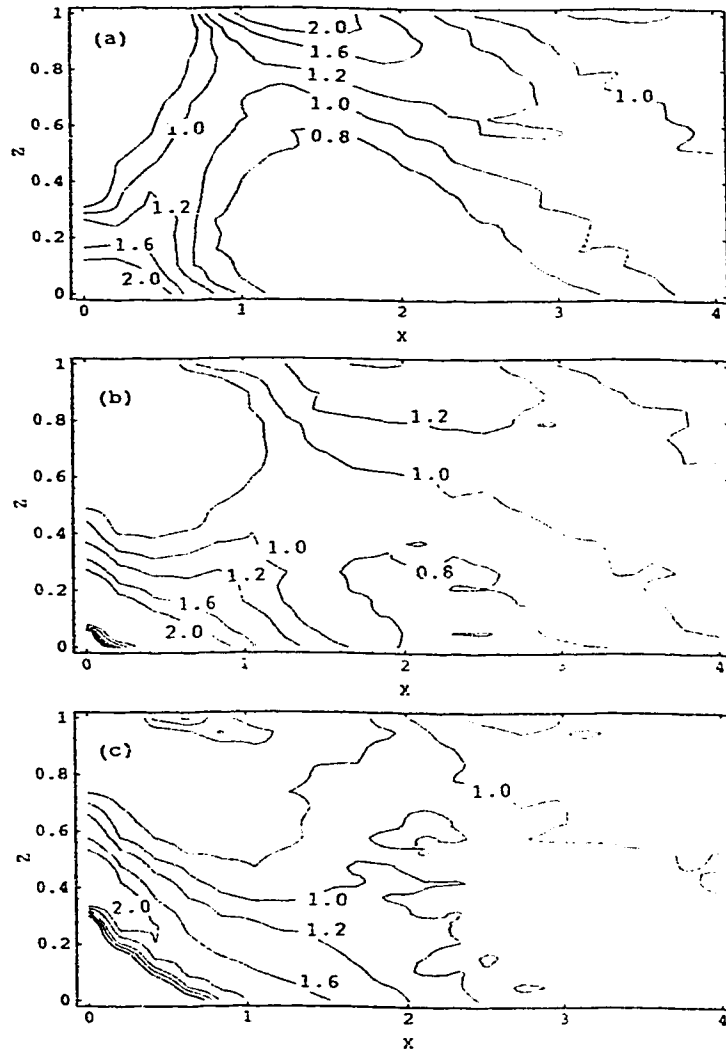


Figure 2.1.3. Prediction of LS model corresponding to the mmf pdf for the CWIC distribution in the CBL for three release heights: (a) $z_s/Z_i=0.067$; (b) $z_s/Z_i=0.24$; and (c) $z_s/Z_i=0.49$.

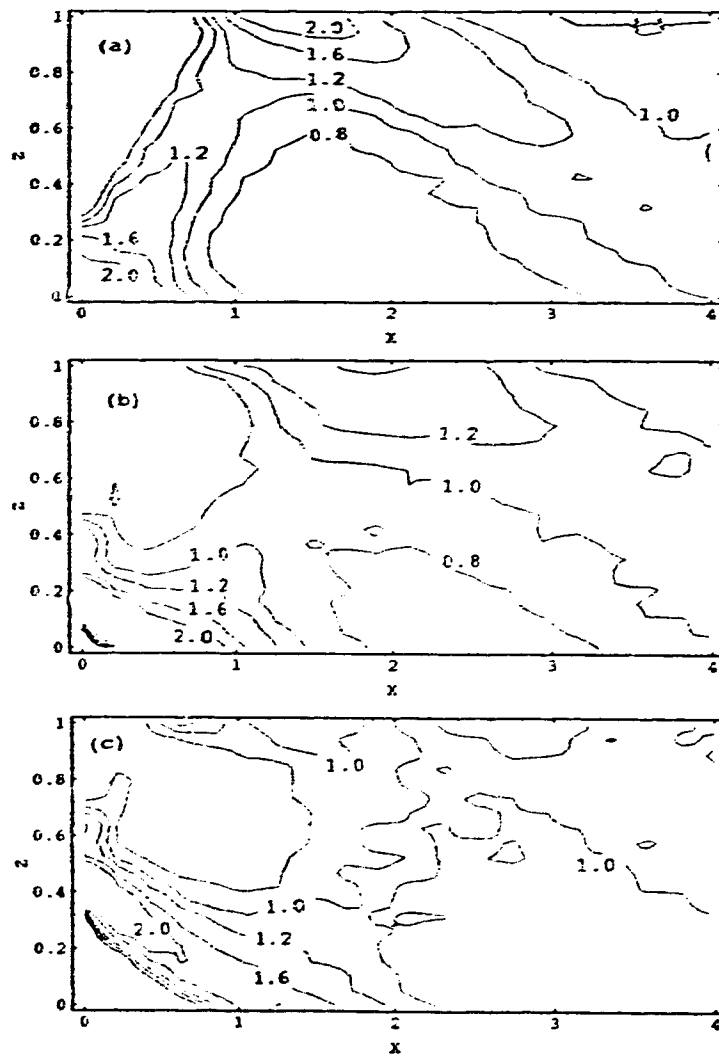


Figure 2.1.4. Prediction of LS model corresponding to the present bi-Gaussian pdf for the CWIC distribution in the CBL for three release heights: (a) $z_r/Z_i=0.067$; (b) $z_r/Z_i=0.24$; and (c) $z_r/Z_i=0.49$.

Table 2.1.1. Location X_{max} of maximum surface concentration according to LS models, and; WD water-tank experiment; Lamb LES/LS simulation; CONDORS field experiment.

z/Z_i	CONVECTION TANK WD	FIELD CONDORS	MODEL			
			LES/LS LAMB*	LS LB	LS MMI**	LS PRESENT BI-GAUSSIAN
0.24	0.4		0.6	0.78	0.6 ± 2	0.68
0.32		0.8-0.9		1.03	0.8 ± 2	0.89
0.49	0.8		1.2	1.54	1.4 ± 2	1.33

*Slightly different release heights were used in Lamb's works: 0.26 corresponding to 0.24 of the WD and 0.50 to 0.49 of the WD.

**For the mmi LS model, the X_{max} is obtained from the calculated CWIC distribution rather than from (2.1.18). However, we infer that the mmi LS model and the LS model derived from the present bi-Gaussian pdf yield the same X_{max} because the mode of velocity in these two pdf's are nearly same.

2.2. ON THE MOMENTS APPROXIMATION METHOD FOR CONSTRUCTING A LAGRANGIAN STOCHASTIC MODEL²

2.2.1. Introduction

In studies of turbulent dispersion it is usual to treat the underlying turbulent flow as "statistically known," the notion normally indicating no more than that means and variances of the turbulent velocity field are specified. This has been completely satisfactory for simple (eg. gradient-diffusion) models of dispersion, which hinge on rudimentary flow knowledge. But modern Lagrangian stochastic (LS) "Random Flight" models, which are used to calculate an ensemble of turbulent trajectories and thus to mimic dispersion, call for and can usefully employ, a deeper statistical knowledge of the flow: and so give sharper definition to what is implied (in the context of dispersion) by calling a flow "known."

Since Thomson's (1987) provision of a selection criterion for LS models (the "well-mixed condition," Section 2.2.2), "known flow" has come to mean that the probability density function (pdf) p_u of the Eulerian velocity field is a mathematically-known function of position. The beauty of Thomson's criterion is that, given complete Eulerian information (p_u), one may derive with reasonable assumptions a consistent though not necessarily unique trajectory model. Further rigorous developments can only pin trajectory models to an even more complete specification of the turbulent flow (eg. two-point, joint pdf's).

Here we focus on the fact that only for *ideal* flows is the velocity pdf p_u completely known. For any *real* flow one has available only partial information on p_u , in the form of a few low-order moments. The LS model for any real flow, therefore, must be built from

² A version of this section has been published. S. Du, J.D. Wilson and E. Yee, 1994, *Boundary-Layer Meteorology* 70, 273-292.

partial information. To overcome this difficulty, Kaplan and Dinar³ (1992, 1993) introduced a "moments approximation," whereby only a finite number of moments of the Eulerian turbulent velocity are needed. The Kaplan-Dinar method relieves the derivation of a trajectory model equation of any fundamental difficulty, but a number of questions remain to be answered:

- (i) Does the moments approximation model satisfy the well-mixed constraint?
- (ii) How many terms in the power series for the conditional mean acceleration of a particle need to be retained, to obtain a satisfactory simulation?
- (iii) How many moments are to be involved?

We will address these questions, and we consider also an alternative approach to building an LS model from partial information on the flow (via the "maximum missing information" pdf corresponding to the given information). We confine our attention to steady-state, one-dimensional problems.

2.2.2. The exact model and the approximate model

The general form of a one-dimensional LS model for the evolution of particle state (z, w) under steady state flow conditions is (Thomson 1987)

$$dw = a(w, z) dt + b(w, z) d\zeta \quad (2.2.1)$$

$$dz = w dt. \quad (2.2.2)$$

Here $a(w, z)$ is the conditional mean particle acceleration, and $b(w, z)d\zeta$ is a random

³ The Kaplan-Dinar model is comprehensive in that it is intended to be applicable to the calculation of multi-particle trajectories (with correct relative velocity statistics) in three dimensional inhomogenous turbulence. We here consider only the basic case of a single particle in one dimensional turbulence.

forcing, $d\zeta$ being a Gaussian random number with mean zero and variance dt .

2.2.2.1. The Well-Mixed Constraint

Corresponding to (2.2.1) and (2.2.2) is a Fokker-Planck equation which governs the evolution of the joint position-velocity pdf of dispersing particles, $p(w,z,t)$:

$$\frac{\partial p}{\partial t} = -\frac{\partial}{\partial z}(wp) - \frac{\partial}{\partial w}(ap) + \frac{1}{2} \frac{\partial^2}{\partial w^2}(b^2 p). \quad (2.2.3)$$

Suppose tracer particles are released at $t = 0$ such that

$$p(w,z,0) \propto \rho_a(z)p_a(w,z),$$

where ρ_a is the fluid density (henceforth assumed constant), and p_a is the Eulerian velocity pdf: then the tracer particles are "well-mixed" with respect to position and velocity. It is natural to expect that they *remain* well mixed, so that for all t ,

$$p(w,z,t) \propto p_a(w,z).$$

It follows that $p_a(w,z)$ should satisfy (2.2.3), i.e.,

$$-\frac{\partial}{\partial z}(wp_a) - \frac{\partial}{\partial w}(ap_a) + \frac{1}{2} \frac{\partial^2}{\partial w^2}(b^2 p_a) = 0. \quad (2.2.4)$$

This is the well-mixed constraint, which restricts the selection of $a(w,z)$ and $b(w,z)$. Evidently the w.m.c. prohibits the spurious growth of order from disorder, and thus (speaking informally) is an entropy-evolution constraint.

Now, $b(w,z)$ can be obtained from the Kolmogorov inertial subrange theory as (Monin and Yaglom 1975)

$$b(w,z) = \sqrt{C_0 \epsilon} \quad (2.2.5)$$

or (in principle equivalently; Thomson 1987) by

$$b(w,z) = \sqrt{\frac{2M_2}{T_L}}, \quad (2.2.6)$$

C_0 is a (supposedly) universal constant, here taken to be 2.0; ϵ is the rate of dissipation of the turbulent kinetic energy; $M_2 (= \sigma_w^2)$ is the variance of the vertical velocity; and T_L is the Lagrangian decorrelation time scale.

The difference between the exact model and the approximate model lies in the specification of $a(w,z)$.

2.2.2.2. The Exact Model

If the Eulerian pdf for the vertical velocity $p_a(w,z)$ is known, $a(w,z)$ can be derived from (2.2.4) in principle as (Thomson 1987)

$$a(w,z) = \frac{\left[\frac{\partial}{\partial w} \left(\frac{1}{2} b^2 p_a \right) + \phi \right]}{p_a} \quad (2.2.7)$$

where ϕ is the solution of

$$\frac{\partial \phi}{\partial w} = - \frac{\partial p_a}{\partial z} \quad (2.2.8)$$

satisfying $\phi \rightarrow 0$ as $|w| \rightarrow \infty$. However, only for particular forms for $p_a(w,z)$ can one solve analytically for ϕ .

2.2.2.3. The Moments Approximation Model

To avoid needing explicitly the Eulerian pdf, Kaplan and Dinar (1992, 1993) approximate $a(w,z)$ as:

$$a(w,z) = C_0(z) + C_1(z)w + C_2(z)w^2 + C_3(z)w^3 + \dots + C_k(z)w^k + \dots \quad (2.2.9)$$

Substituting this expansion into the governing equation for the characteristic function of $p_a(w,z)$

$$\Theta(\theta,z) = \int_{-\infty}^{\infty} p_a(w,z) e^{i\theta w} dw,$$

and making use of eqn (2.2.4), we have

$$\begin{aligned} & -i \frac{\partial^2 \Theta}{\partial z \partial \theta} - i\theta [C_0 \Theta - iC_1 \frac{\partial \Theta}{\partial \theta} - C_2 \frac{\partial^2 \Theta}{\partial \theta^2} + \dots \\ & + (-1)^k i^k C_k \frac{\partial^k \Theta}{\partial \theta^k} + \dots] + \frac{b^2}{2} \theta^2 \Theta = 0 \end{aligned} \quad (2.2.10)$$

(note that no summation is implied by the recurring index k).

Equation (2.2.10) indicates that satisfaction of the w.m.c. is guaranteed provided infinitely many terms in the expansion (2.2.9) are retained. However, the moments approximation method is useful only to the extent that one may truncate eqn (2.2.9) at a small number of terms: so we need to determine how well the w.m.c. remains satisfied upon such truncation.

By repeated differentiation of (2.2.10) with respect to θ , one can obtain (on setting $\theta=0$) a set of simultaneous equations for the coefficients C_i in terms of the moments M_i . Provided the number of terms retained in (2.2.9) is finite, a closed solution for these coefficients in terms of a finite number of specified moments is available. For example if we retain 5 terms (C_0, C_1, C_2, C_3 and C_4) in (2.2.9), we must differentiate (2.2.10) five times, and obtain:

$$\begin{aligned}
C_0 M_0 + C_1 M_1 + C_2 M_2 + C_3 M_3 + C_4 M_4 &= \frac{dM_2}{dz}, \\
C_0 M_1 + C_1 M_2 + C_2 M_3 + C_3 M_4 + C_4 M_5 &= \frac{1}{2} \frac{dM_3}{dz} - \frac{b^2}{2} M_0, \\
C_0 M_2 + C_1 M_3 + C_2 M_4 + C_3 M_5 + C_4 M_6 &= \frac{1}{3} \frac{dM_4}{dz} - b^2 M_1, \\
C_0 M_3 + C_1 M_4 + C_2 M_5 + C_3 M_6 + C_4 M_7 &= \frac{1}{4} \frac{dM_5}{dz} - \frac{3}{2} b^2 M_2, \\
C_0 M_4 + C_1 M_5 + C_2 M_6 + C_3 M_7 + C_4 M_8 &= \frac{1}{5} \frac{dM_6}{dz} - 2b^2 M_3,
\end{aligned} \tag{2.2.11}$$

where M_k is the k -th order moment of the turbulent velocity. In general if the expansion (2.2.9) for $a(w)$ retains terms up to order w^K , then the set of simultaneous equations for the coefficients C_k ($k \leq K$) will involve moments as high as M_{2K} . For the case of $K=1$, we need to assume $dM_3/dz=0$.

Our specification of the C 's is slightly different from that used by Kaplan and Dinar, who made the approximation (from dimensional considerations) that $C_1 = b^2/2M_2$. Therefore the comparisons between "exact" and "approximate" models shown in the following section do not represent necessarily comparisons to the original Kaplan-Dinar model, but rather to a modified version of it.

2.2.3. Comparison of the exact and approximate models

In this section we look at several ideal turbulence systems wherein the velocity pdf (hence all moments) are *known*. Our object is to examine any deterioration of the moments approximation model (relative to the exact model) due to truncation (neglect of high order moments).

2.2.3.1. Gaussian Turbulence

A Gaussian velocity pdf is a satisfactory approximation in many flows (Batchelor 1953), a familiar example being the atmospheric surface layer under neutral stratification. For Gaussian turbulence, the probability density function is

$$p_a(w,z) = \frac{1}{\sqrt{2\pi}M_2^{\frac{1}{2}}} \exp\left(-\frac{w^2}{2M_2}\right), \quad (2.2.12)$$

and the moments are⁴

$$\begin{aligned} M_{2n+1} &= 0, \\ M_{2n} &= (2n-1)!! M_2^n. \end{aligned} \quad (2.2.13)$$

Using (2.2.12), one readily obtains the exact model (Thomson 1987)

$$a(w,z) = -\frac{b^2}{2M_2} w + \frac{1}{2} \left(\frac{w^2}{M_2} + 1 \right) \frac{dM_2}{dz}, \quad (2.2.14)$$

and, by using (2.2.13), exactly the same expression arises following the approximate approach,

$$C_0 = \frac{1}{2} \frac{dM_2}{dz}, \quad C_1 = -\frac{b^2}{2M_2}, \quad C_2 = \frac{1}{2M_2} \frac{dM_2}{dz}, \quad C_3 = 0, \quad C_4 = 0. \quad (2.2.15)$$

The above derivation shows that for Gaussian turbulence, these two methods are consistent with each other, which is not surprising since the pdf is fully defined by the first two moments.

2.2.3.2. Homogeneous Non-Gaussian Turbulence

⁴ $(2n-1)!! = (2n-1)(2n-3)\dots 5.3.1.$

We now examine the flow having pdf⁵

$$p_a(w) = \frac{1}{M_2^{1/2}} \exp \left[- \left[\lambda_0 + \lambda_1 \left(\frac{w}{M_2^{1/2}} \right) + \lambda_2 \left(\frac{w}{M_2^{1/2}} \right)^2 + \lambda_3 \left(\frac{w}{M_2^{1/2}} \right)^3 + \lambda_4 \left(\frac{w}{M_2^{1/2}} \right)^4 \right] \right] \quad (2.2.16)$$

where the λ 's are related to skewness ($S = M_3/M_2^{3/2}$) and kurtosis ($K = M_4/M_2^2$). We will use $S = 0.65$ and $K = 3.0$ (values typical of the convective boundary layer). These constraints, plus normalization, and the specification of zero mean velocity, imply

$$\begin{aligned} \lambda_0 &= 0.9881, \quad \lambda_1 = 0.5941, \quad \lambda_2 = 0.3281, \\ \lambda_3 &= -0.2594, \quad \lambda_4 = 0.0708. \end{aligned} \quad (2.2.17)$$

From eqns (2.2.7, 2.2.8, 2.2.16, 2.2.17) it follows that the exact model is:

$$a(w) = - \frac{b^2}{2M_2^{1/2}} \left[\lambda_1 + 2\lambda_2 \left(\frac{w}{M_2^{1/2}} \right) + 3\lambda_3 \left(\frac{w}{M_2^{1/2}} \right)^2 + 4\lambda_4 \left(\frac{w}{M_2^{1/2}} \right)^3 \right] \quad (2.2.18)$$

i.e., the approximate model (2.2.9) is actually exact provided the C_i are given by⁶

$$\begin{aligned} C_i &= - \frac{b^2}{2} \frac{(i+1)\lambda_{i+1}}{M_2^{(i+1)/2}}, \quad (i=0,1,2,3) \\ C_{i+1} &= 0. \quad (i \geq 4) \end{aligned} \quad (2.2.19)$$

The information (2.2.19) is not available, however, to the hypothetical worker not privileged to know the pdf (2.2.16); who rather is given only a certain number of velocity moments, and wishes to use that restricted information in the approximation (2.2.9).

⁵ Readers may recognize this pdf as being of the form of a maximum missing information pdf. However this pdf is used here simply as a convenient example.

⁶ We are indebted to Dr. N. Dinar for noting this formula.

Let us for convenience set $T_L=30$ [s] and $M_2=1$ [m^2/s^2], The exact model (2.2.18) becomes

$$a(w)=-0.01980-0.02187w+0.02594w^2-0.009447w^3 \quad (2.2.18')$$

Our worker knows some or all of these moments⁷:

$$\begin{aligned} M_0=1, \quad M_1=0, \quad M_2=1, \quad M_3=0.65, \quad M_4=3, \\ M_5=4.64, \quad M_6=15.03, \quad M_7=33.43, \quad M_8=100.27. \end{aligned} \quad (2.2.20)$$

Depending on whether he is given $M_0 - M_4$ or $M_0 - M_6$ or $M_0 - M_8$, he will deduce (in corresponding order) that

$$a(w)=-0.01373-0.04226w+0.01373w^2 \quad (2.2.21a)$$

$$a(w)=-0.01980-0.02187w+0.02594w^2-0.009441w^3 \quad (2.2.21b)$$

$$a(w)=-0.01980-0.02187w+0.02594w^2-0.009441w^3-9.0 \cdot 10^{-8}w^4 \quad (2.2.21c)$$

Small differences between coefficients in 2.2.21(b,c) and in the exact model (2.2.18') are due to roundoff errors.

We have shown that if the worker unknowing of the pdf makes use of only the moments $M_0 - M_4$, he obtains a model (eqn 2.2.21a) quite distinct from the exact model (eqn 2.2.18'). How good or bad is his approximation? Figure 2.2.1 shows that the difference between the exact model and the approximate model is quite large. The deterministic term $a(w)$ normally has the effect of returning the velocity towards its conditional mean value. The approximate model with four or more terms does have that property, but with only three terms it does not. In the latter case, $a(w)$ drives a large positive velocity even larger.

We calculated the spread of particles released at $z_s = 500$ m, into a domain

⁷ These values for $M_5 - M_8$ follow from (2.2.16), although from the viewpoint of our worker unknowing of (2.2.16), they are simply data made available.

bounded by perfect reflection at $z=(0, 1000)$ m, using a time step $0.01T_L$. Figure 2.2.2 compares the calculated standard deviation of the particle position from the exact and the approximate model (2.2.21a) over the range of $(0, 2T_L)$. For a short flight time, the approximate model gives a satisfactory result due to memory of correct release statistics, but for $t > T_L$, it is quite wrong because the particles' flights are governed by an incorrect conditional mean acceleration $a(w)$.

Figure 2.2.3 shows there arises a violation of the w.m.c., with regard to both position and velocity, when the moments approximation model is truncated at $K=2$ (i.e., four moments are used, and we retain terms to order w^2 in $a(w)$). In Figure 2.2.3(a) we show that violation of the w.m.c. in position worsens as the flight time t of the particles increases. For $t=T_L$, the degree of violation is not serious (due to the correct release statistics), but for later time, it becomes unacceptable. Figure 2.2.3(b), on the other hand, indicates that the pdf of the particle velocity, calculated from the moments approximation model, decays with respect to the initial pdf; in particular, at large w the probability density grows with time. This is not surprising in view of the expansion used for $a(w)$: the three term approximation forces large w to be even larger.

Of course, the worker using the approximation (2.2.21a) does not know the correct pdf (2.2.16), so would have no basis for considering the velocity pdf that results from his model (2.2.21a) as "wrong" by comparison with (2.2.16). In fact the moments approximation for $a(w)$, in conjunction with other assumptions made, may (under suitable restrictions) *imply* a pdf. In the present case however (homogeneous, four specified moments, second order polynomial), such a pdf is not implied (see Appendix 2.2). Particles in the present simulation were released with a random velocity from the "exact" pdf (2.2.16), but since the underlying moments approximation model does not imply a pdf, we should not be surprised to see that at later times there is no pdf approaching (2.2.16).

2.2.3.3. Inhomogeneous Non-Gaussian Turbulence

The Eulerian probability density function for vertical velocity in the convective

boundary layer (CBL) is commonly modelled (eg. Baerentsen and Berkowicz 1984) as bi-Gaussian,

$$p_a(w,z) = \frac{A}{\sqrt{2\pi}\sigma_A} \exp\left[-\frac{(w-w_A)^2}{2\sigma_A^2}\right] + \frac{B}{\sqrt{2\pi}\sigma_B} \exp\left[-\frac{(w+w_B)^2}{2\sigma_B^2}\right], \quad (2.2.22)$$

where A(B) is the fractional area occupied by thermals (downdrafts), $w_A(w_B)$ the mean velocity within the thermals (downdrafts) and $\sigma_A(\sigma_B)$ the standard deviation of the fluctuating vertical velocity in thermals (downdrafts). As in Du et al (1994), we choose to relate the parameters of (2.2.22) to the unconditional moments by

$$\begin{aligned} A &= 0.4, & B &= 0.6 \\ w_A &= M_3^{1/3}, & w_B &= \frac{2}{3}M_3^{1/3} \end{aligned} \quad (2.2.23)$$

$$\sigma_A = (M_2 - 0.281M_3^{2/3})^{1/2}, \quad \sigma_B = (M_2 - 0.927M_3^{2/3})^{1/2}$$

We will assume $S=0.65$ and $K=3.0$, typical of values observed in the CBL. In deriving approximate models we will need higher velocity moments. From (2.2.22, 2.2.23) we get

$$\begin{aligned} M_5 &= 4.627M_2^{5/2}, \quad M_6 = 15.662M_2^3, \\ M_7 &= 35.992M_2^{7/2}, \quad M_8 = 116.438M_2^4. \end{aligned} \quad (2.2.24)$$

From (2.2.7, 2.2.8, 2.2.22) we obtain the exact model equations

$$dw = \frac{-\frac{M_2}{T_L}Q + \phi}{p_a(w)} dt + \sqrt{\frac{2M_2}{T_L}} d\zeta, \quad (2.2.25)$$

where

$$\begin{aligned}
\Phi = & -\frac{A}{2} \frac{\partial w_A}{\partial z} \operatorname{erf}\left(\frac{w-w_A}{\sqrt{2}\sigma_A}\right) \\
& + \left[\sigma_A \frac{\partial \sigma_A}{\partial z} + \frac{w(w-w_A)}{\sigma_A} \frac{\partial \sigma_A}{\partial z} + w \frac{\partial w_A}{\partial z} \right] p_A \\
& + \frac{B}{2} \frac{\partial w_B}{\partial z} \operatorname{erf}\left(\frac{w+w_B}{\sqrt{2}\sigma_B}\right) \\
& + \left[\sigma_B \frac{\partial \sigma_B}{\partial z} + \frac{w(w+w_B)}{\sigma_B} \frac{\partial \sigma_B}{\partial z} - w \frac{\partial w_B}{\partial z} \right] p_B
\end{aligned} \tag{2.2.26}$$

$$Q = \frac{(w-w_A) A p_A}{\sigma_A^2} + \frac{(w+w_B) B p_B}{\sigma_B^2} \tag{2.2.27}$$

$$p_A = \frac{1}{\sqrt{2\pi}\sigma_A} \exp\left[-\frac{(w-w_A)^2}{2\sigma_A^2}\right] \tag{2.2.28}$$

$$p_B = \frac{1}{\sqrt{2\pi}\sigma_B} \exp\left[-\frac{(w+w_B)^2}{2\sigma_B^2}\right] \tag{2.2.29}$$

Again, the approximate model equation depends on how many terms in the expansion (2.2.9) are used. If three terms are used,

$$\begin{aligned}
C_0 &= -0.206 \frac{b^2}{M_2^{1/2}} + 0.567 \frac{dM_2}{dz}, \\
C_1 &= \frac{-0.634 b^2 + 0.206 \frac{dM_2}{dz} M_2^{1/2}}{M_2}, \\
C_2 &= \frac{0.206 b^2/M_2^{1/2} + 0.433 \frac{dM_2}{dz}}{M_2}.
\end{aligned} \tag{2.2.30}$$

Using four terms,

$$\begin{aligned}
C_0 &= -\frac{0.279b^2}{M_2^{1/2}} + 0.550 \frac{dM_2}{dz}, \\
C_1 &= \frac{-0.385b^2 + 0.265 \frac{dM_2}{dz} M_2^{1/2}}{M_2}, \\
C_2 &= \frac{\frac{0.353b^2}{M_2^{1/2}} + 0.468 \frac{dM_2}{dz}}{M_2}, \\
C_3 &= \frac{-0.115b^2 - 0.027 \frac{dM_2}{dz} M_2^{1/2}}{M_2^2},
\end{aligned} \tag{2.2.31}$$

while with five terms,

$$\begin{aligned}
C_0 &= \frac{-0.293b^2}{M_2^{1/2}} + 0.579 \frac{dM_2}{dz}, \\
C_1 &= \frac{-0.418b^2 + 0.330 \frac{dM_2}{dz} M_2^{1/2}}{M_2}, \\
C_2 &= \frac{\frac{0.381b^2}{M_2^{1/2}} + 0.412 \frac{dM_2}{dz}}{M_2}, \\
C_3 &= \frac{-0.097b^2 - 0.062 \frac{dM_2}{dz} M_2^{1/2}}{M_2^2}, \\
C_4 &= \frac{\frac{-0.008b^2}{M_2^{1/2}} + 0.016 \frac{dM_2}{dz}}{M_2^2}.
\end{aligned} \tag{2.2.32}$$

We computed the dispersion of trace particles in a flow in which the profile of variance was specified as

$$M_2(z) = w_s^2 \left[0.01 + \left(\frac{z}{Z_i} \right)^{\frac{2}{3}} \left(1 - \frac{z}{Z_i} \right)^{\frac{2}{3}} \right] \tag{2.2.33}$$

where w_s is the scale of vertical velocity, taken to be 1 m/s. This profile (2.2.33) is in qualitative agreement with experimental data in the convective boundary layer (Sawford and Guest 1987; Stull 1988). The Lagrangian decorrelation time scale was set to be

$$T_L(z) = \frac{2.5 M_2 Z_i}{w_s^3}. \tag{2.2.34}$$

Using (2.2.34) is equivalent to taking

$$b = \left(\frac{w_s^3}{1.25 Z_i} \right)^{\frac{1}{2}}. \quad (2.2.35)$$

Simulations were performed for point releases ($z_s=500$ m) and well-mixed releases, with a timestep $0.01T_L$. The height of the boundary layer Z_i was 1000 m.

Figure 2.2.4 shows that the approximate models satisfactorily predict the standard deviation of the dispersing particle position, but not the mean height. The five term approximation is not, however, superior to the four term one.

Figure 2.2.5 shows the mean density distribution (C) at $t=2T_{Lmax}$ (where T_{Lmax} is the Lagrangian time scale at the mid-point of the computational domain) of particles released from a well-mixed initial state ($C=1$). The four term approximation satisfies the w.m.c. (within statistical error), but the three and five term approximations do not (note the accumulation of particles at the middle of the domain and the deficit near the boundaries). This suggests that using more terms does not necessarily improve the approximate model. At first glance, this seems strange. But common sense suggests the expansion for $a(w,z)$ terminating at the term $C_K w^K$ requires to have K odd and $C_K < 0$, otherwise $a(w,z)$ can drive the magnitude of a large velocity even larger. For example if $K=4$, then a positive (negative) C_4 will force a positive (negative) velocity of large magnitude even farther away from its equilibrium value, $w = 0$. In the homogeneous case we studied in the last subsection, this problem is not serious because the coefficient C_4 is extremely small. In strongly inhomogeneous turbulence, C_4 may be numerically large due to the velocity variance gradient term, so that truncating at the $C_4 w^4$ term could be problematical.

The above analysis suggests that when using the moments approximation one should truncate the expansion for $a(w)$ (in powers w^k) at an odd power ($k \leq K$, K odd).

2.2.4. Forming an optional Lagrangian model from partial information on Eulerian velocity statistics

In this sub-section, rather than as earlier assuming a fully-known pdf (whose specification was not however available for the purpose of exploiting the Kaplan-Dinar method), we examine the situation where an LS model is to be built *strictly* from partial information - so that one cannot, even in principle, appeal to an "exact" model as a criterion. Specifically, we will assume only the N lowest-order moments are known, and we compare the following two models

- (i) the modified Kaplan-Dinar moments approximation model;
- (ii) the well-mixed model that corresponds to the "maximum missing information" pdf (n.b., not the true pdf, which is unknown) implied by the given moments.

The model (i) is by now familiar: all information given about the Eulerian velocity is used to determine the coefficients C 's of a truncated expansion for $a(w,z)$. Model (ii) begs explanation.

When one requires to form a pdf on the basis of partial information about a random variable, the scientifically objective choice is that pdf which is "maximally uncommitted with respect to missing information" (Jaynes 1957). This objectivity is achieved by choosing the pdf which maximizes the functional

$$H(p) = - \int_{-\infty}^{\infty} p(w) \ln[p(w)] dw$$

under the given constraints (this inference principle is well-known in statistics, and has already been applied in the context of LS models by Du et al. 1994). Having formed this "mmi" (maximum missing information) pdf, one may then (in principle, though not necessarily easily) derive the corresponding well-mixed LS model.

2.2.4.1. Optimal Trajectory Model From $N=2$ Given Moments

Suppose we are given the mean and variance of the Eulerian velocity. We are not entitled to assume the Eulerian pdf is Gaussian.

The mmi pdf in this case (not the *actual* pdf, which remains unknown) is Gaussian

(Du et al. 1994). Therefore the LS model obtained from the mmi principle and the w.m.c. is simply the model (2.2.14) given earlier (Subsection 2.2.3.1).

If we employ the moments approximation in this case, we are limited to the expansion:

$$a(w,z) = C_0 + C_1 w, \quad (2.2.36)$$

and we obtain

$$C_0 = \frac{dM_2}{dz}, \quad C_1 = -\frac{b^2}{2M_2} \quad (2.2.37)$$

Clearly this model is quite different from (2.2.14) or (2.2.15). We suspect this is not a well-mixed model in the inhomogeneous case. We have been unable to prove this point. But in random flight experiments (using the inhomogeneous turbulences profiles of Subsection 2.2.3), the initial well-mixed distribution was retained much more closely by the mmi model (2.2.14) than by the moments approximation model (2.2.36, 2.2.37), as shown in Figure 2.2.6. This finding must be qualified by stating that, (a) we did not know the correct initial velocity statistics for the moments approximation model; and (b), implementing perfect reflection at the boundaries implied an unavoidable (though arguably minor) violation of the w.m.c. (see Wilson and Flesch 1993) by BOTH models.

In this case, our exploitation of the mmi principle to build an LS model from partial information has yielded a well-mixed (and consequently more-rigorous) model than does the moments approximation (2.2.36).

2.2.4.2. Optimal Trajectory Model From $N=4$ Given Moments

In this case, given the four lowest-order moment constraints, the mmi pdf is (Du et al. 1994)

$$p_a(w,z) = \exp\left(-\sum_{k=0}^4 \lambda_k(z) w^k\right),$$

where the $\lambda_k(z)$'s are determined by the four known moments and the normalization condition. Following Thomson (1987), the corresponding well-mixed LS model is

$$a(w,z) = -\frac{M_2}{T_L} \sum_{k=1}^4 k \lambda_k(z) w^{k-1} + \left[\sum_{k=0}^4 \frac{d\lambda_k(z)}{dz} \int_{-\infty}^w w'^{k+1} p_a(w',z) dw' \right] / p_a(w,z). \quad (2.2.38)$$

We refer to this as the mmi model.

The two methods under consideration use exactly the same information about the Eulerian velocity distribution, but proceed on different routes to obtain the LS model equation. Which is better? To answer this, we simulated dispersion from a continuous point source at height $z_s = 0.24 Z_1$ in the convective boundary layer (of depth Z_1), adopting the velocity statistics $M_2(z)$, $M_3(z)$ and $T_L(z)$ that were previously used for the same purpose by Luhar and Britter (1989), plus a supplementary (and justified; see Du et al. 1994) assumption that $M_4 = 3.0 M_2^2$.

Figure 2.2.7 compares predictions of the two models for the contours of cross-wind integrated concentration (CWIC), and may be compared with the corresponding contours of the convection tank experiment of Willis and Deardorff (1978; their Figure 4). The mmi model seems superior to the modified Kaplan-Dinar model. In Figure 2.2.8 we compare predictions of the alongwind profile of ground-level CWIC. Again, the mmi model gives the better prediction. In particular, at (what should be) suitably large downwind distances ($X \sim 4$), the CWIC predicted by the modified Kaplan-Dinar model is not well mixed.

2.2.5. Conclusion

From a practical viewpoint, the concept of an "exact" Eulerian velocity pdf is absurd (as any experimentalist would confirm), and the Kaplan-Dinar aspiration to build a Lagrangian stochastic model from a realistic, partial knowledge of the turbulence (a few

low-order velocity moments) is appropriate.

However, what is involved here is a statistical inference problem, and the Kaplan-Dinar approach may not be the best one. We have shown that a danger of the Kaplan-Dinar approach is that one may obtain a random flight algorithm that fails the well-mixed condition (does not keep initially well-mixed tracer well-mixed). On the basis of our findings, we suggest that a better alternative to the Kaplan-Dinar approximation is to construct from the known velocity statistics the maximum missing information probability density function; then by the usual procedure (Thomson 1987) derive the corresponding well-mixed trajectory model.

Appendix 2.2. Eulerian velocity pdf implied by the moments approximation

Thomson (1987) has shown that the Eulerian velocity pdf $p_s(w,z)$ must be a solution of the Fokker-Planck equation that corresponds to any suitable model for the evolution of particle velocity (the well-mixed condition referred to earlier). We note that if the expansion (2.2.9) for the model coefficient $a(w,z)$ is substituted into the FP equation, one may obtain an Eulerian pdf that derives consistently from the principal assumptions made (Markovian evolution; model must be well-mixed; coefficient b independent of w ; power series expansion for $a(w,z)$). In the case of homogeneous turbulence, the solution to the FP equation is:

$$p_a(w) = \exp\left[\frac{2}{b^2}\left(C_0 + C_1 w + \frac{C_2}{2} w^2 + \dots + \frac{C_K}{K+1} w^{K+1}\right)\right] \quad (\text{A2.2.1})$$

If K is even, this solution (eqn A2.2.1) is unbounded, and so NOT a pdf.

On the other hand if K is odd, the solution (eqn A2.2.1) is of the form of an mmi (maximum missing information) pdf (for a detailed description of the mmi pdf, the reader is referred to Du et al. 1994). However, determining the coefficients $C_0, C_1 \dots C_K$ of the modified Kaplan-Dinar expansion (and of the above pdf) requires knowledge of $2K$ velocity moments⁸, whereas the pdf (A2.2.1) is exactly the mmi pdf corresponding to a smaller number (K) of given velocity moments. C_0 can be determined by the normalization condition or any one of the given moments.

It is seen, then, that the modified KD model, in effect, may imply a pdf. Presumably the principle of consistency of approximation requires that the particles of a modified KD simulation be released with a random velocity from that pdf.

⁸ The original Kaplan-Dinar approach requires $2K-1$ moments plus an assumption on C_1 in the one dimensional case.

Bibliography

- Baerentsen, J.H. and R. Berkowicz, 1984: Monte Carlo simulation of plume dispersion in the convective boundary layer. *Atmos. Environ.* **18**, 701-712.
- Batchelor, G.K., 1953: *The Theory of Homogeneous Turbulence*. Cambridge University Press, 197pp.
- Du, S., J.D. Wilson and E. Yee, 1994: Constructing a probability density function for vertical velocity in the convective boundary layer, and implied trajectory models. *Atmos. Environ.* **28**, 1211-1217.
- Jaynes, E.T., 1957: Information theory and statistical mechanics. *Phys. Rev.* **106**, 620-630.
- Kaplan, H. and N. Dinar, 1992: A stochastic model for the dispersion of a non-passive scalar in a turbulent field. *Atmos. Environ.* **26A**, 2413-2423.
- Kaplan, H. and N. Dinar, 1993: A three-dimensional model for calculating concentration distribution in inhomogeneous turbulence. *Boundary-Layer Meteorol.* **62**, 217-245.
- Luhar, A.K. and R.E. Britter, 1989: A random walk model for dispersion in inhomogeneous turbulence in a convective boundary layer. *Atmos. Environ.* **23**, 1911-1924.
- Monin, A.S. and A.M. Yaglom, 1975: *Statistical Fluid Mechanics*. Vol. 2, MIT Press. 359 pp.
- Sawford, B.L. and F.M. Guest, 1987: Lagrangian stochastic analysis of flux-gradient relationships in the convective boundary layer. *J. Atmos. Sci.* **44**, 1152-1165.
- Stull, R.B., 1988: *An Introduction to Boundary Layer Meteorology*. Kluwer Academic Publishers, Dordrecht, 666pp.
- Thomson, D.J., 1987: Criteria for the selection of stochastic models of particle trajectories in turbulent flows. *J. Fluid Mech.* **180**, 529-556.
- Weil, J.C., 1990: A diagnosis of the asymmetry in top-down and bottom-up diffusion using a Lagrangian stochastic model. *J. Atmos. Sci.* **47**, 501-515.
- Willis, G.E. and J.W. Deardorff, 1978: A laboratory study of dispersion from an elevated

source within a modeled convective planetary boundary layer. *Atmos. Environ.* **12**, 1305-1311.

Wilson, J.D. and T.K. Flesch, 1993: Flow boundaries in random-flight dispersion models: enforcing the well-mixed condition. *J. Appl. Meteorol.* **32**, 1695-1707.

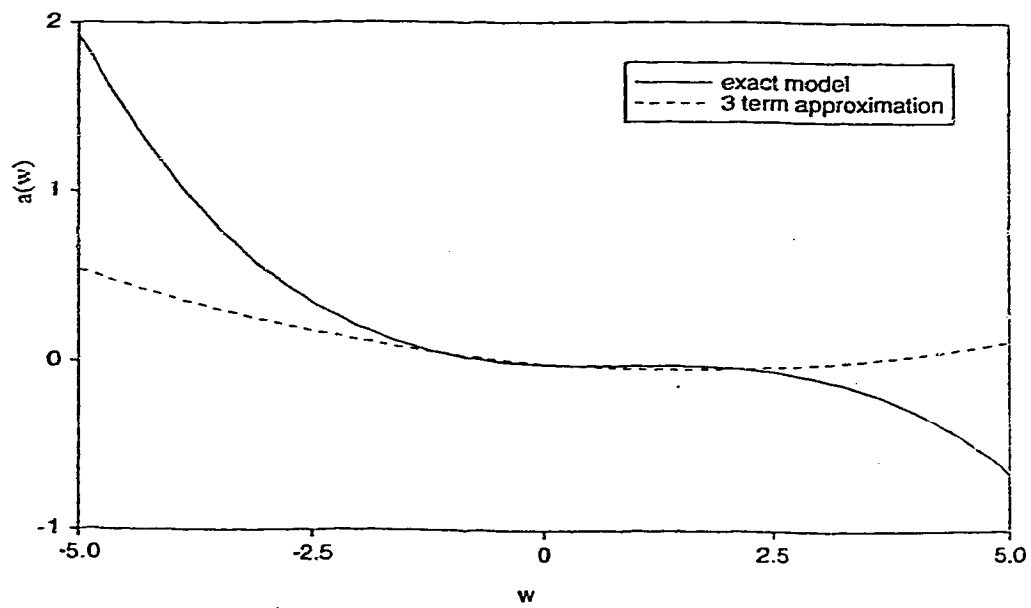


Figure 2.2.1. Comparison of $a(w)$ in the exact model and the three term approximation model. The flow is homogeneous non-Gaussian.

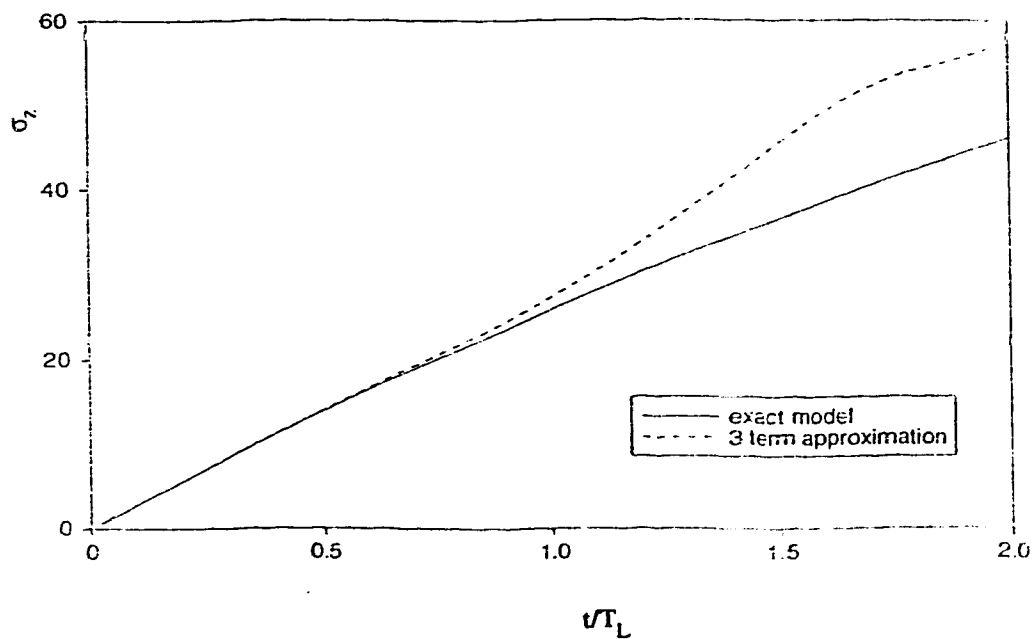


Figure 2.2.2. The predicted standard deviation by both the exact model and the three term approximation model in homogeneous non-Gaussian turbulence. Perfect reflection condition was applied at both top and bottom boundaries. 5,000 particles were released at $z_s=500$ m with initial velocity drawn from the Eulerian velocity distribution. In calculation, $\Delta t=0.01T_L$.

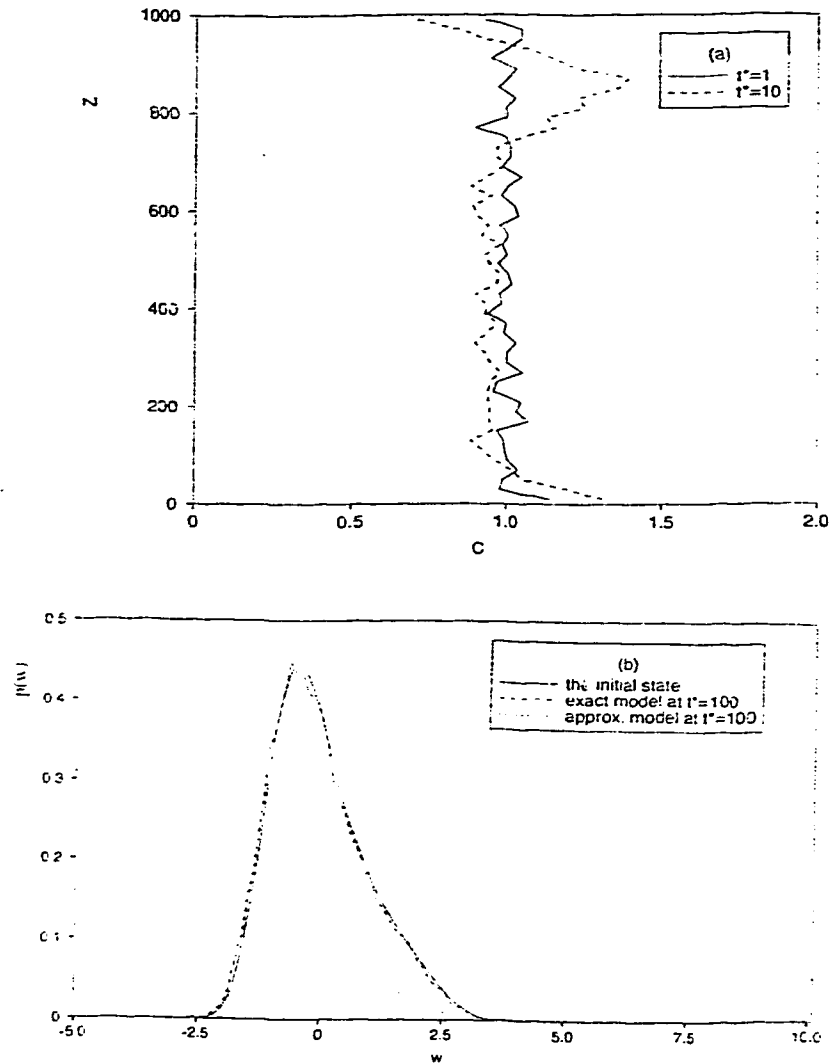


Figure 2.2.3. (a) The evolution of concentration distribution from an initially well-mixed profile ($C=1$) predicted by the three term approximate model. (b) The probability density distribution of vertical velocity at $t^*=t/T_L=100$, calculated from both the exact model and three term approximation model. The solid line is the probability density function at $t=0$. In calculation, 50,000 particles were released with the "well-mixed" initial condition. In calculating the concentration distribution, perfect reflection condition was employed at both boundaries. In calculating the evolution of pdf, no reflection scheme was used.

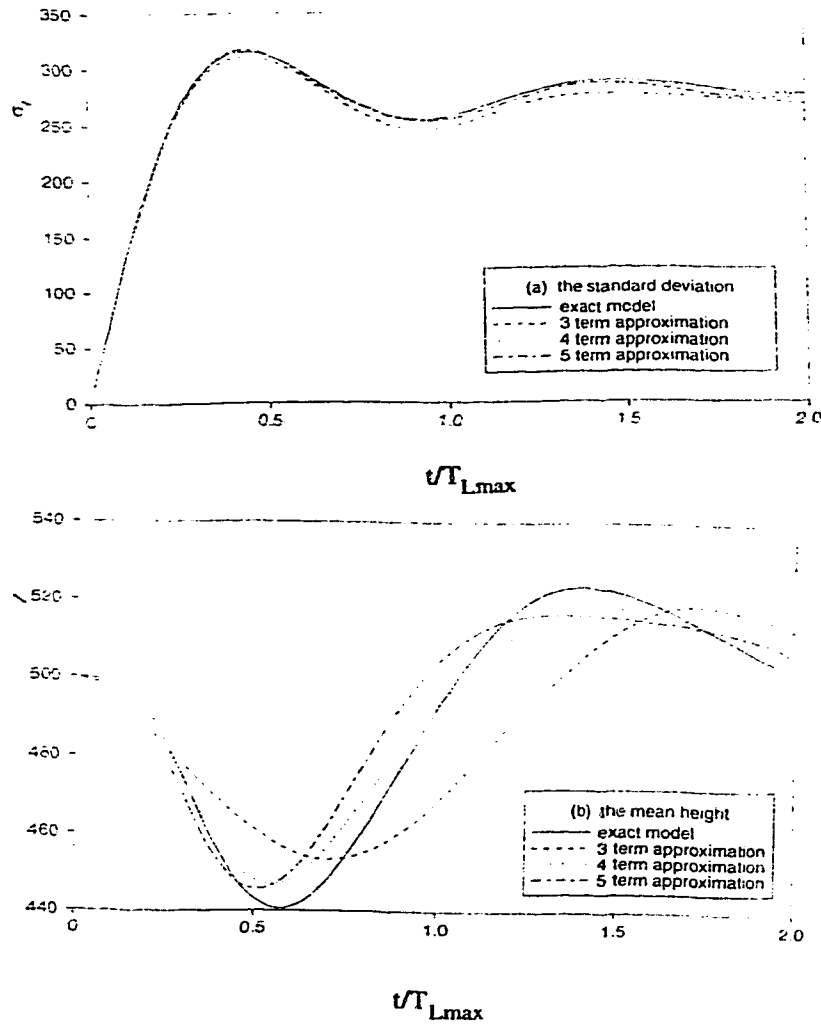


Figure 2.2.4. (a) Comparison of the calculated standard deviation by the exact model and the approximate models in inhomogeneous non-Gaussian turbulence. The source height was $z_s=500$ m. T_{Lmax} is the maximum Lagrangian time scale in the computational domain. (b) Comparison of the calculated mean height of the dispersing particles by the exact model and approximate LS models.

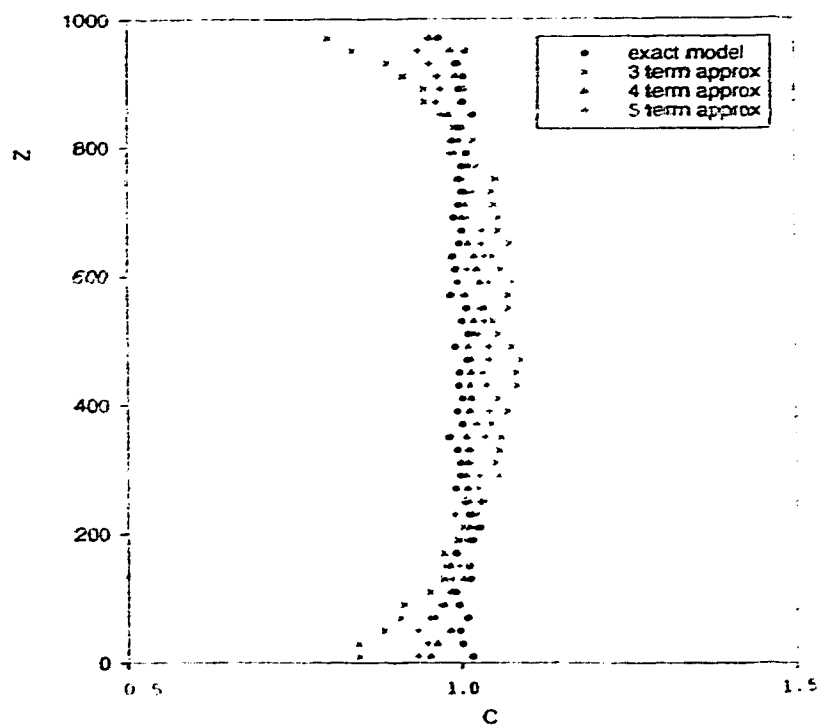


Figure 2.2.5. The evolution of a well-mixed initial concentration profile in the inhomogeneous inhomogeneous non-Gaussian turbulence. The profiles are at $t=2T_{L,max}$. In calculation, 50,000 particles were released.

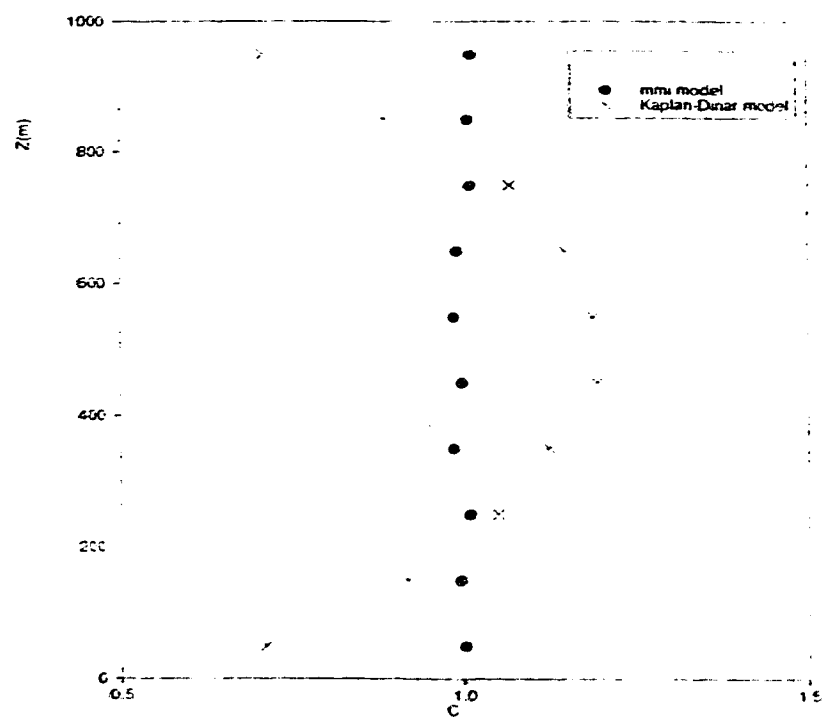


Figure 2.2.6. The evolution of a well-mixed initial concentration profile ($C=1$) in the inhomogeneous turbulence when only two velocity moments are specified. The profiles are at $t=5T_{Lmax}$. In calculation, 50,000 particles were released.

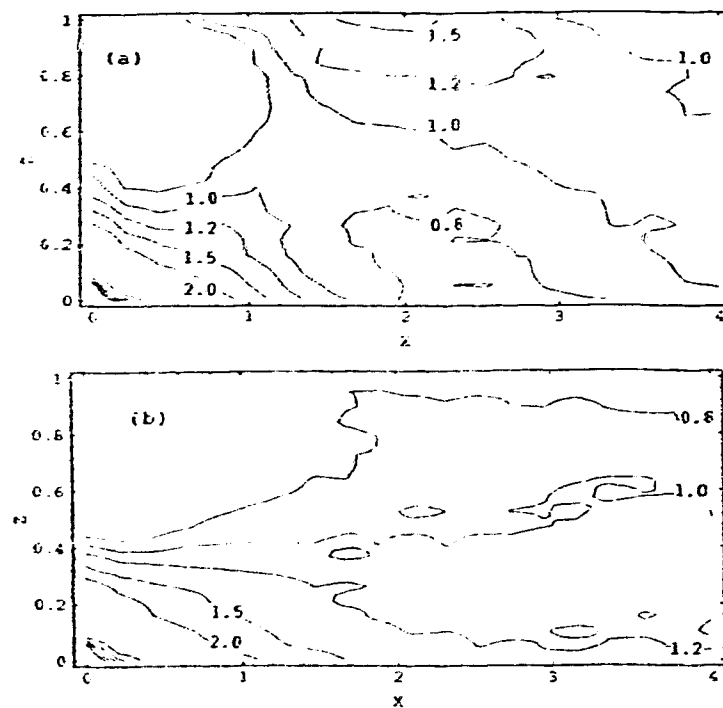


Figure 2.2.7. Comparison of the CWIC contours in the X-Z plane predicted by (a) the mmi model and (b) the modified Kaplan-Dinar model in the convective boundary layer. X is the dimensionless downwind distance defined as $X = xw_s/UZ_1$, and $Z = z/Z_1$.

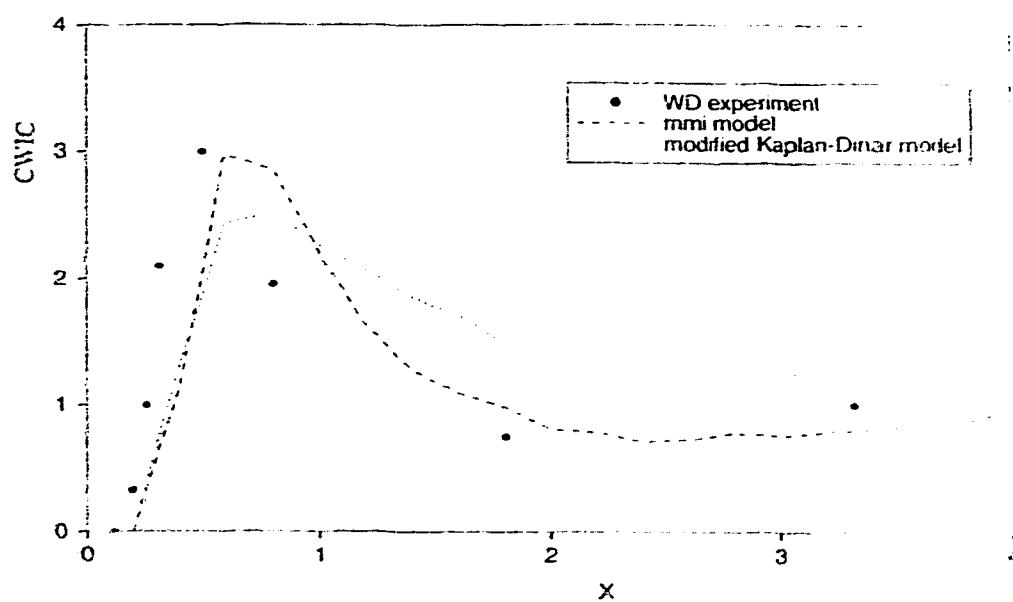


Figure 2.2.8. Comparison of the calculated ground level CWIC from both the mmi model and the modified Kaplan-Dinar model with Willis and Deardorff's water tank experiment. The well-mixed value (which should obtain at large X) is $CWIC = 1$.

2.3. THE EFFECTS OF HIGHER EULERIAN VELOCITY MOMENTS ON THE MEAN CONCENTRATION DISTRIBUTION⁹

2.3.1. Introduction

It is natural to presume (though possibly hard to prove) that the lower the order (n) of a given turbulent velocity moment $\langle w^n \rangle$, the more important its influence on the spread of material from a source (an assumption implicit in most dispersion models). Knowing the first and second moments (mean, variance) of the Eulerian velocity enables us to understand many important features of tracer dispersion. But there are circumstances when knowing those two moments alone is insufficient. For example, in the case of dispersion from sources in the convective boundary layer (CBL), taking account of the third order moment (or skewness) can greatly improve model performance (Baerentsen and Berkowicz 1984; Luhar and Britter 1989; Du et al. 1994).

However, observations of velocity moments of orders higher than four are scarce. Furthermore reported CBL skewness and kurtosis (Sawford and Guest 1987; LeMone 1990; Du et al. 1994; Lenschow et al 1994), when appropriately normalised (mixed-layer scaling), exhibit more variability (from run to run, from experiment to experiment) than does the variance. This is presumably due to the fact that determining higher moments to within the same fractional error as lower moments requires a longer sampling time (Lumley and Panofsky 1964; Lenschow et al. 1994): a given velocity record will usually give better estimates (ie. statistics which are closer, in relative terms, to the corresponding population parameters) of lower order moments than of higher. One wonders, then, how much to trouble oneself, with the provision of high-order statistical information on the

⁹ A version of part of this section has been published. S. Du and J.D. Wilson, 1995, preprint volume for the *11th Symposium on Boundary Layer and Turbulence*, pp 180-183, Amer. Meteorol. Soc.

flow, and the building of dispersion models able to capitalize on such knowledge.

A Lagrangian stochastic (LS) trajectory model is an ideal tool to examine the influence of the Eulerian velocity moments on the pattern of dispersion. Given a set of moments, we can construct a probability density function (where practicable, we prefer to form the "maximum missing information" pdf); then from the specified pdf, by the method laid down by Thomson (1987), we can develop the corresponding LS dispersion model.

With an LS model, we can also examine the small time (or near source) behavior of vertical dispersion, as earlier studied by Hunt (1985), due to continuous point sources in inhomogeneous, skewed turbulence, and the inference made by Hunt that under strongly convective conditions the vertical dispersion may be dominated by the vertical gradient of the third order velocity moment. We will find out, with our model, the range within which Hunt's predictions are good representations of dispersion and, whether his inference is correct.

In this study, we confine ourselves to one dimensional (vertical) dispersion, and to cases where moments up to the fourth order are available. We consider convective conditions only, as almost all reported data on skewness and kurtosis are obtained for that case.

2.3.2. Vertical velocity (w) moments in the Convective Boundary Layer

In a horizontally-homogeneous CBL, $\langle w \rangle = 0$. Many empirical formulae for $\langle w^2 \rangle$ have been advanced, on the basis of field measurements and physical simulations (Lenschow et al. 1980; Sawford and Guest 1987; Sorbjan 1991). Here we adopt the Sawford and Guest empirical formula:

$$\langle w^2 \rangle / w_*^2 = 1.1 (z/Z_i)^{2/3} (1 - z/Z_i)^{2/3} \left[1 - \frac{4(z/Z_i - 0.3)}{(2 + |z/Z_i - 0.3|)^2} \right], \quad (2.3.1)$$

where w_* is the convective velocity scale and Z_i is the CBL height. This formula represents the body of observations, for any z/Z_i , to within about $\pm 50\%$

There is much greater scatter in the case of $\langle w^3 \rangle$. Sorbjan (1991) analyzed the Limagne, Beauce, AMTEX and Minnesota experiments, and found skewness $S = \langle w^3 \rangle / \langle w^2 \rangle^{3/2}$ varied between 0.0 and 1.2 (considering all heights and all experiments), with a mean value 0.5. Sawford and Guest (1987) obtained $S = 0.8$ with a substantial error range, from aircraft measurements (Willis and Deardorff 1974) and water tank experiments (Willis, quoted by Baerentsen and Berkowicz 1984). Although the scatter is large, skewness in the CBL appears to be roughly height-invariant.

Reported results for $\langle w^4 \rangle$, or kurtosis $K = \langle w^4 \rangle / \langle w^2 \rangle^2$, are even fewer. Du et al (1994) obtained $K = 2 \sim 5$ by analyzing BAO data. From the AMTEX and ELDOME experimental data, Lenschow et al. (1994) deduced $K = 3 \sim 5$. Again, the vertical profile of K appears height-invariant.

2.3.3. Eulerian vertical velocity pdf and the corresponding LS model

2.3.3.1 The maximum missing information pdf

To design an LS model satisfying Thomson's (1987) well-mixed criterion, the Eulerian velocity pdf $p_u(w)$ must be known. Invoking the maximum missing information (mmi) principle (Du et al. 1994), we can construct an mmi velocity pdf of the exponential form

$$p_u(w) = \frac{1}{\sigma_w} \exp \left[- \sum_{k=0}^N \lambda_k \left(\frac{w}{\sigma_w} \right)^k \right], \quad (2.3.2)$$

where N is the number of known velocity moments (in this section $N=4$), and $\sigma_w = \langle w^2 \rangle^{1/2}$ is the standard deviation.

Since in the CBL the mean, skewness and kurtosis of the vertical velocity are (at least roughly) height independent, the λ 's in $p_u(w)$ can be taken to be height independent. For given (S, K) the λ 's can be fitted by assuming $\sigma_w = 1 \text{ ms}^{-1}$. In the resulting pdf, all height variation is due to height variation of σ_w .

2.3.3.2. The LS model corresponding to the mmi pdf

According to Thomson's (1987) well-mixed criterion, the coefficients $a(w,z,t)$ and $b(w,z,t)$ of the general Markovian LS model

$$\begin{aligned} dw &= a(w,z,t)dt + b(w,z,t)d\zeta, \\ dz &= wdt, \end{aligned} \quad (2.3.3)$$

must satisfy

$$\mathcal{L}p_a = \frac{\partial p_a}{\partial t} + \frac{\partial}{\partial z}(wp_a) + \frac{\partial}{\partial w}(ap_a) - \frac{1}{2} \frac{\partial^2}{\partial w^2}(b^2 p_a) = 0. \quad (2.3.4)$$

In equations (2.3.3), $d\zeta$ is a Gaussian random number with zero mean and variance dt . Note that

$$\mathcal{L}p(w,z,t) = 0 \quad (2.3.5)$$

is implied by the LS model equations (2.3.3) and is a Fokker-Planck equation governing the evolution of the pdf of the tracer particle's velocity and displacement. In other words, equation (2.3.4) means that the Eulerian pdf $p_a(w,z,t)$ is a solution of equation (2.3.5).

From the Kolmogorov inertial subrange theory (Monin and Yaglom 1975), we expect

$$b(w,z,t) = \sqrt{C_0 \epsilon}. \quad (2.3.6)$$

Here C_0 is a universal constant, which we have taken to be 3.0 (Du et al. 1995); ϵ is the mean rate of dissipation of turbulent kinetic energy. Since we consider one-dimensional dispersion, the other model coefficient $a(w,z,t)$ is uniquely determined by eqn (2.3.4).

Considering stationary turbulence and substituting (2.3.2) into (2.3.4), we obtain (Du et al. 1994)

$$a(w,z) = -\frac{b^2}{2\sigma_w} F + \sigma_w \frac{\partial \sigma_w}{\partial z} \left[\int_{-\infty}^w (1 - F \frac{w}{\sigma_w}) \frac{w}{\sigma_w} p_a \frac{dw}{\sigma_w} \right] / p_a, \quad (2.3.7)$$

where

$$F = \sum_{k=1}^4 k \lambda_k \left(\frac{w}{\sigma_w} \right)^{k-1}. \quad (2.3.8)$$

To implement an LS model, an initial velocity for each trajectory is required. Usually it is assumed that the initial velocity distribution for passive tracer particles is the same as the Eulerian velocity distribution at the source location (otherwise the concentration field obtained is referred to as conditional). An algorithm was developed to produce a random initial velocity for any kind of turbulent field, provided the Eulerian velocity pdf is given. Details are given in Appendix 2.3.

2.3.4. Sensitivity of the mean concentration distribution to the skewness and kurtosis of the vertical velocity

The dissipation rate ϵ was specified by Luhar and Britter's (1989) empirical formula

$$\epsilon = \frac{w_*^3}{Z_i} [1.5 - 1.2 \left(\frac{z}{Z_i} \right)^{1/3}], \quad (2.3.9)$$

which accords quite well with the Ashchurch and Minnesota data.

We calculated the paths of 20,000 particles, with time increment $\Delta t = 0.01(2\langle w^2 \rangle / C_0 \epsilon)$. Perfect reflection was imposed at both boundaries.

Before embarking on numerous calculations with (2.3.7), we examined the special case of Gaussian turbulence ($S=0.0$, $K=3.0$), for which eqn (2.3.7) must in principle reduce to

$$a(w,z) = -\frac{C_0 \epsilon}{2\langle w^2 \rangle} w + \frac{1}{2} \left(\frac{w^2}{\langle w^2 \rangle} + 1 \right) \frac{\partial \langle w^2 \rangle}{\partial z}, \quad (2.3.10)$$

which is the unique 1-d model for this case provided by Thomson (1987). Having been unable to reduce (2.3.7) to (2.3.10) analytically, we resorted to a numerical check: Figure 2.3.1 shows that contours of crosswind-integrated concentration (CWIC) calculated with (2.3.7) and with (2.3.10) are equivalent (bearing in mind the inevitable stochastic error). In Figure 2.3.1 and henceforth, X stands for $tw\sqrt{Z_i}$ (or $xw\sqrt{UZ_i}$), - the dimensionless travel time (or downwind distance) from the source.

2.3.4.1. Sensitivity to the skewness

Holding kurtosis $K=3.0$, we constructed the mmi Eulerian pdf of vertical velocity for skewness $S=0.0\sim 1.0$, Figure 2.3.2(a). The pdf is skewed toward negative velocity for positive skewness and the mode of the velocity becomes more negative with increasing S . When $S>0.6$, the shape of the pdf varies very rapidly with skewness.

In this sub-section, we adopt source height $z_s=0.49Z_i$, consistent with the Willis and Deardorff (1981) water tank simulation. Figure 2.3.3(a) shows the variation of ground-level CWIC with skewness. Maximum ground-level CWIC increases with skewness (see also Figure 2.3.3(b)), but the displacement of that maximum relative to the source, X_{\max} , is almost unchanged. The latter point is surprising at first glance. Earlier studies (eg. Lamb 1982) showed that the slope of the axis of maximum concentration is proportional to the ratio of the mode of w to the alongwind advection velocity U , so that one might expect that X_{\max} would be smaller for more-strongly skewed turbulence than for weakly-skewed turbulence. We offer an explanation for this phenomenon as follows.

The location of maximum ground concentration is mainly determined by two quantities in the downdraught: the average vertical velocity in the downdraught, $\langle w_d \rangle$, and the standard deviation of the velocity fluctuation, σ_d . Intuitively, X_{\max} decreases with increasing $\langle w_d \rangle$ or σ_d . Now, larger S implies larger $\langle w_d \rangle$ (because $\langle w_d \rangle$ is proportional

to the mode of $p_a(w)$; Hunt et al. 1988). Larger S also implies smaller σ_d (refer to Fig 2.3.2; or see Du et al. 1994). Thus a larger S will on the one hand tend to increase X_{max} due to the smaller σ_d , and will on the other hand tend to decrease X_{max} due to the larger $\langle w_d \rangle$, i.e., those two effects are in opposition. We hypothesize that this is why X_{max} is quite insensitive to skewness.

We calculated the mean plume height, $\langle Z \rangle$,

$$\langle Z \rangle = \int_0^{Z_i} C z dz / \int_0^{Z_i} C dz \quad (2.3.11)$$

and the standard deviation of the spread of tracer particles, σ_z ,

$$\sigma_z = \left[\int_0^{Z_i} C (z - \langle Z \rangle)^2 dz / \int_0^{Z_i} C dz \right]^{1/2}. \quad (2.3.12)$$

As shown in Figure 2.3.4, with increasing skewness, $\langle Z \rangle$ decreases rapidly at first to a minimum elevation, begins to rise from that point to the initial height, overshoots to a higher position and then approaches its equilibrium: $\langle Z \rangle / Z_i = 0.5$. The behaviour of σ_z is simpler: in the near source region ($X < 1$) and the region far away from the source ($X > 3$), σ_z is insensitive to the skewness; while in the intermediate range, σ_z increases with the skewness.

Contours of CWIC in the X - Z plane are shown in Figure 2.3.5. For large skewness ($S > 0.8$) the cross-wind integrated plume is divided into downward and the upward branches, both of them becoming narrower with increasing skewness. It is quite obvious that it is the downward plume that is responsible for the high maximum ground level CWIC shown in Fig. 2.3.3. Also worthy of mention is that for stronger (positively) skewed turbulence, the effective zero-concentration area in the near source region becomes bigger, desirable for that region; but the sacrifice is that in the vicinity of the plume centreline touch down point, the CWIC will be larger.

2.3.4.2. Sensitivity to the kurtosis

We now hold $S=0.5$, a plausible magnitude for skewness in the CBL, and we construct the mm Eulerian velocity pdf, as shown in Figure 2.3.1(b).

We carried out a series of numerical calculations with the LS model for kurtosis $K=2.0\sim 6.0$. In Figures 2.3.6, 2.3.7 and 2.3.8 we show the variation, with the magnitude of kurtosis, of ground-level CWIC, mean plume height and standard deviation of the spread of tracer particles, and the contours of CWIC in the X-Z plane. The effect of decreasing kurtosis is qualitatively equivalent to increasing skewness. The spatial distribution of mean concentration is very sensitive to kurtosis when $K \leq 3.0$.

2.3.4.3. Other factors affecting the concentration field

We have not considered all the factors that might affect our prediction of the concentration field, so that the agreement of our predictions with physical simulations (Willis and Deardorff 1981) and field experiment (Briggs 1993) is not expected to be perfect. Among factors bearing on the validity of our model are the boundary condition for the dispersing tracer particles, and the universality of the constant C_0 employed in our model.

Wilson and Flesch (1993) found that no reflection scheme can satisfy the well-mixed condition, when the velocity normal to the reflecting boundary is skewed. In other words, any reflection condition employed in the model will introduce some error in the concentration field. An associated problem is that the structure of the top region of the CBL is very complicated, likely making the concentration prediction in that region even worse.

As to the influence of C_0 , we ran the model with $C_0=2.0, 3.0$ and 4.0 . As shown in Figure (2.3.9), C_0 can indeed make a big difference. It seems that $C_0 = 2.0$ gives best simulation of the Willis and Deardorff (1981) experiment within the framework of the present model; however, we cannot claim that it is generally true, because in the model and the physical experiment there are so many other uncertain factors that can affect the comparison.

2.3.5. Small time behaviour of vertical dispersion

Hunt (1985) proved that at asymptotically small times after release at $z=z_s$ into unbounded turbulence of arbitrary statistical character

$$\frac{d\langle Z \rangle}{dt} = \frac{\partial \langle w^2 \rangle}{\partial z} t, \quad (2.3.13.1)$$

$$\frac{d\langle Z'^2 \rangle}{dt} = 2\langle w^2 \rangle t + \frac{3}{2} \left(\frac{\partial \langle w^3 \rangle}{\partial z} - \frac{1}{3} C_0 \epsilon \right) t^2. \quad (2.3.13.2)$$

where

$$\langle Z'^2 \rangle = \langle (z - z_s)^2 \rangle \quad (2.3.14)$$

(note the deviance from the definition of Z' we used earlier; we here adhere to Hunt's definition, though it is not necessarily a good indicator of the spread, unless $\langle Z \rangle \approx z_s$). Thomson (1987) showed that LS models satisfying his well-mixed condition indeed reproduce this small time behaviour, while earlier models (Thomson 1984; Van Dop et al. 1985) in which the conditional mean acceleration a_i is *linear* in u_i do not.

Hunt (1985) inferred from (2.3.13.2) (see also van Dop et al. 1985; Hunt et al. 1988) that in strong convection (i.e., strongly skewed turbulence), for near-ground releases, the variance of particle spread should reduce to

$$\langle Z'^2 \rangle = \frac{1}{2} \frac{\partial \langle w^3 \rangle}{\partial z} t^3 \quad (2.3.15)$$

because the variance of vertical velocity in the near ground region is small¹⁰.

¹⁰ Dr. D. J. Thomson (UK Meteorological Office) is acknowledged for pointing out that when t is very small the Lagrangian velocity structure function varies quadratically with t , so the $C_0 \epsilon$ term can be neglected. We interpret "very small" as $t \ll t_\eta$, the Kolmogorov

Equation (2.3.13) is rigorously correct for extremely small travel time $t \ll T_L$. In homogeneous, stationary turbulence, T_L is related to the measurable statistics $\langle w^2 \rangle$ and ϵ by $T_L = 2\langle w^2 \rangle / C_0 \epsilon$. But in inhomogeneous (and/or nonstationary) turbulence there is no such simple relationship, and T_L is dependent on releasing time and location. Nevertheless, here for the sake of discussion we evaluate T_L at the source location and release time with $T_L = 2\langle w'^2 \rangle / C_0 \epsilon$.

It would be useful were (2.3.13) valid for a longer travel time, since an analytical prediction has sometimes its advantages. A possible application might be to calculate the mean concentration distribution in the near-source region (see Raupach 1989 for a practical example). With our uniquely correct well-mixed model, we can find out to what travel distance/time (2.3.13) remains approximately valid.

We choose a variance profile

$$\langle w^2 \rangle = w_s^2 \left(1 - \frac{z}{Z_i}\right) \quad (2.3.16)$$

where w_s is a velocity fluctuation scale. We set $z_s = 0.5 Z_i$ to minimize the boundary effect on dispersion in the near source region. We calculated dispersion in skewed turbulence with $S = 0.5$ and $K = 3.0$. As shown in Figure 2.3.10, the Hunt prediction (eqn 2.3.13) represents quite well the mean plume height and the standard deviation of particle spread up to $t \sim 0.5T_L$.

We compared the Hunt formulae, again with ($S = 0.5$, $K = 3.0$), for a very low (near ground) release height ($z_s/Z_i = 0.01$). Although the Hunt prediction is not supposed to remain rigorously correct for this case (because dispersion is affected by the flow boundary), it is our intention here to examine if *practically* it does a good job in predicting dispersion. This example also enables us to test his inference that for short travel time the vertical dispersion from a near ground release is dominated by the vertical gradient of the third moment of velocity. We chose the velocity variance as

micro time scale (Monin and Yaglom 1975, p359).

$$\langle w^2 \rangle = 1.8 w_*^2 \left(\frac{z}{Z_i} \right)^{\frac{2}{3}}, \quad (2.3.17)$$

which gives

$$\frac{d\langle w^3 \rangle}{dz} = 1.8^{3/2} S \frac{w_*^3}{Z_i}, \quad (2.3.18)$$

similar to that used by Hunt et al. (1988). As shown in Figure 2.3.11, up to $t/T_L \sim 1.0$ eqn 2.3.13 accords very well with our LS simulation. It is hard to explain why eqn 2.3.13 prevails for longer travel time (t/T_L) in the latter example, but a possible reason may be the presence of the reflecting boundary.

We quantify the relative importance of inhomogeneity by the ratio $R_{IH} = T_L/T_{IH}$, where $T_{IH} = (d\sigma_w/dz)^{-1}$ is a time scale of inhomogeneity (Wilson et al. 1983). In the two above examples $R_{IH} \sim 0.5$, which corresponds to a fairly strong inhomogeneity in the atmospheric boundary layer and plant canopy layer. So, we suggest that in those turbulent flows the Hunt formula for the dispersion may be valid up to $t \sim 0.5T_L$.

Now, we turn to examine Hunt's inference (eqn 2.3.15).

Figure 2.3.12 compares our model calculation of dispersion in skewed turbulence with Hunt's (2.3.13.2) and the simplification (2.3.15). We see that neither of Hunt's formulae agrees well with our prediction (note that in Figures 2.3.12 we used X as the x -axis, while in Figure 2.3.11 we used t/T_L ; and $X = 1$ implies much longer downwind distance than $t/T_L = 1$ does. The reason we use the former here is that in the literature most experimental diffusion data for the CBL are presented in the form of $\sigma_z \sim f(X)$). In Figure 2.3.12 we also show the model prediction of dispersion in Gaussian turbulence ($S = 0.0$, $K = 3.0$).

Hunt (see also Hunt et al. 1988) considered the experimental data of Briggs (1985) as supporting his inference (see also Briggs 1993). However, we note that both Nieuwstadt (1980) and Deardorff and Willis (1974), from whose work Briggs drew his conclusion, obtained the "3/2" law (i.e., $\sigma_z \propto X^{3/2}$) but offered no explanation why such a

law prevails and whether the effect of velocity variance is negligible. Figure 2.3.12(b) shows that the existence of a "3/2" law does not necessarily imply that the diffusion is dominated by the gradient of the third velocity moment, since in *Gaussian* inhomogeneous turbulence the vertical spread also follows a "3/2" law.

There is a simple explanation for the "3/2" law in strongly inhomogeneous Gaussian turbulence: in calculating particle dispersion, an *effective* velocity variance, rather than the velocity variance at the source height, should be employed. The effective velocity variance is an average of the variance (with the mean concentration as weighting function) over the domain that can be reached by dispersing particles. It is obvious that the effective variance is an increasing function of travel distance (or time) since (in the case we consider) the vertical profile of $\langle w^2 \rangle$ increases monotonically with height, and the majority of the dispersing particles tend to fly to higher elevation after leaving the ground-level source due to the presence of the reflecting boundary. If the effective velocity variance follows a "1/2" law (i.e., $\langle w^2 \rangle_{\text{effective}} \propto X^{1/2}$), the variance of particle spread will then follow a "3/2" law. Our numerical calculations show that for a vertical profile of velocity variance given by (2.3.17), σ_z does follow approximately a "3/2" law.

2.3.6. Conclusions

With a uniquely correct Lagrangian stochastic model, we studied the effects of third and fourth order moments on the spatial distribution of mean concentration in non-Gaussian (positively skewed) turbulence. The main findings are: (1) when the turbulence is strongly skewed ($S > 0.6$), the mean concentration distribution can be very sensitive to the skewness; (2) the maximum ground-level cross-wind integrated concentration increases monotonically with skewness, but the downstream distance for that maximum concentration remains almost unchanged for different values of skewness; (3) the mean concentration distribution is sensitive to kurtosis as $K < 3.0$; and, (4) the effect of decreasing kurtosis is qualitatively equivalent to increasing skewness. These findings suggest that it might be worthwhile to incorporate the third and fourth order moments into

a diffusion model, especially when the velocity skewness is big and the velocity kurtosis is small.

We examined Hunt's (1985) small time predictions of vertical dispersion. Our model calculations show that his predictions well represent the dispersion for travel times up to $t/T_L \sim 0.5$. But his inference that for a ground-level release the rate of dispersion is dominated by the gradient of the third velocity moment is not correct, i.e., a " $d\langle w^3 \rangle/dz$ controlled region" does not exist.

Appendix 2.3. An algorithm to generate random numbers with given pdf

Whenever an Eulerian velocity pdf is available, we can derive a stochastic differential equation for the evolution of a tracer particle's velocity and displacement. For any given turbulent flow (for the present work by "given" we mean that the pdf for velocity, p_u , and the dissipation rate of turbulent kinetic energy, ϵ , are provided), we have a hypothetical homogeneous and stationary flow characterized by p_u and ϵ of the (real) given flow at the source location, z_s and the initial time instant, t_0 . In this hypothetical flow, the evolution of a tracer particle's velocity is simply written as

$$dw = \frac{b^2}{2} \frac{\partial}{\partial w} [\ln p_u(w, z_s, t_0)] dt + b(w, z_s, t_0) d\zeta. \quad (\text{A2.3.1})$$

Integrating eqn (A2.3.1) from $t = 0$ to $t = T_L$ (where $T_L = 2\sigma_w^2/C_0\epsilon$ is the Lagrangian integral time scale in the hypothetical homogeneous and stationary turbulence) with an initial velocity drawn from a Gaussian distribution, we obtain a random velocity w_0 . This w_0 is the desired initial velocity for the given pdf $p_u(w, z_s, t_0)$. Figure A2.3.1 gives an example of this algorithm. In calculation, $dt = 0.01T_L$ was used and 10,000 particles were released.

Bibliography

- Baerentsen, J.H. and R. Berkowicz, 1984: Monte Carlo simulation of plume dispersion in the convective boundary layer. *Atmos. Environ.* **18**, 701-712.
- Briggs, G.A., 1985: Analytical parameterizations of diffusion: The convective boundary layer. *J. Appl. Meteorol.* **24**, 1167-1186.
- Briggs, G.A., 1993: Plume dispersion in the convective boundary layer. Part II: Analysis of CONDORS field experiment data. *J. Appl. Meteorol.* **32**, 1388-1425.
- Caughey, S.J. and S.G. Palmer, 1979: Some aspects of turbulence structure through the depth of the convective boundary layer. *Q. J. R. Meteorol. Soc.* **105**, 811-827.
- Deardorff, J.W. and G.E. Willis, 1974: Computer and laboratory modelling of the vertical diffusion of nonbuoyant particles in the mixed layer. *Advances in Geophysics*, **18B**, H.E. Landsberg and J. van Mieghem, Eds, Academic Press, 187-200.
- Du, S., J.D. Wilson and E. Yee, 1994: Probability density function for velocity in the convective boundary layer, and implied trajectory models. *Atmos. Environ.* **28**, 1211-1217.
- Du, S., B.L. Sawford, J.D. Wilson and D.J. Wilson, 1995: Estimation of the Kolmogorov constant (C_0) for the Lagrangian structure function, using a second-order Lagrangian model of grid turbulence. Submitted to *Physics of Fluids*.
- Hunt, J.C.R., 1985: Turbulent diffusion from sources in complex flows. *Ann. Rev. Fluid Mech.* **17**, 447-485.
- Hunt, J.C.R., J.C. Kaimal and J.E. Gaynor, 1988: Eddy structure in the convective boundary layer--New measurements and new concepts. *Q. J. R. Meteorol. Soc.* **114**, 827-858.
- Lamb, R.G., 1982: Diffusion in the convective boundary layer. *Atmospheric Turbulence and Air Pollution Modelling*, F.T.M. Nieuwstadt and H. van Dop, Eds, Reidel, 159-229.
- LeMone, M.A., 1990: Some observations of vertical velocity skewness in the convective planetary boundary layer. *J. Atmos. Sci.* **47**, 1163-1169.

- Lenschow, D.H., J. Mann and L. Kristensen, 1994: How long is long enough when measuring fluxes and other turbulence statistics? *J. Atmos. Oceanic Tech.* **11**, 661-673.
- Luhar, A.K. and R.E. Britter, 1989: A random walk model for dispersion in inhomogeneous turbulence in a convective boundary layer. *Atmos. Environ.* **23**, 1911-1924.
- Lumley, J.L. and H.A. Panofsky, 1964: *The Structure of Atmospheric Turbulence*. John Wiley & Sons, 239pp.
- Monin, A.S. and A.M. Yaglom, 1975: *Statistical Fluid Mechanics*. Vol. 2, MIT Press.
- Nieuwstadt, F.T.M., 1980: Applications of mixed-layer similarity to the observed dispersion from a ground-level source. *J. Appl. Meteorol.* **19**, 157-162.
- Raupach, M.R., 1989: A practical Lagrangian method for relating scalar concentrations to source distributions in vegetation canopies. *Q. J. R. Meteorol. Soc.* **115**, 609-632.
- Sawford, B.L. and F.M. Guest, 1987: Lagrangian stochastic analysis of flux-gradient relationships in the convective boundary layer. *J. Atmos. Sci.* **44**, 1152-1165.
- Sorbjan, Z., 1991: Evaluation of local similarity functions in the convective boundary layer. *J. Appl. Meteorol.* **30**, 1565-1583.
- Thomson, D.J., 1984: Random walk modelling of diffusion in inhomogeneous turbulence. *Q. J. R. Meteorol. Soc.* **110**, 1107-1120.
- Thomson, D.J., 1987: Criteria for the selection of stochastic models of particle trajectories in turbulent flows. *J. Fluid Mech.* **180**, 529-556.
- Van Dop, H., F.T.M. Nieuwstadt and J.C.R. Hunt, 1985: Random walk models for particle displacements in inhomogeneous unsteady turbulent flows. *Phys. Fluids* **28**, 1639-1653.
- Willis, G.E. and J.W. Deardorff, 1981: A laboratory study of dispersion from a source in the middle of the convective boundary layer. *Atmos. Environ.* **15**, 109-117.
- Wilson, J. D. and T. Flesch, 1993: Flow boundaries in random-flight dispersion models: enforcing the well-mixed condition. *J. Appl. Meteorol.* **32**, 1695-1707.

Wilson, J. D., B.J. Legg and D.J. Thomson, 1983: Calculation of particle trajectories in the presence of a gradient in turbulent-velocity variance. *Boundary-layer Meteorol.* **27**, 163-169.

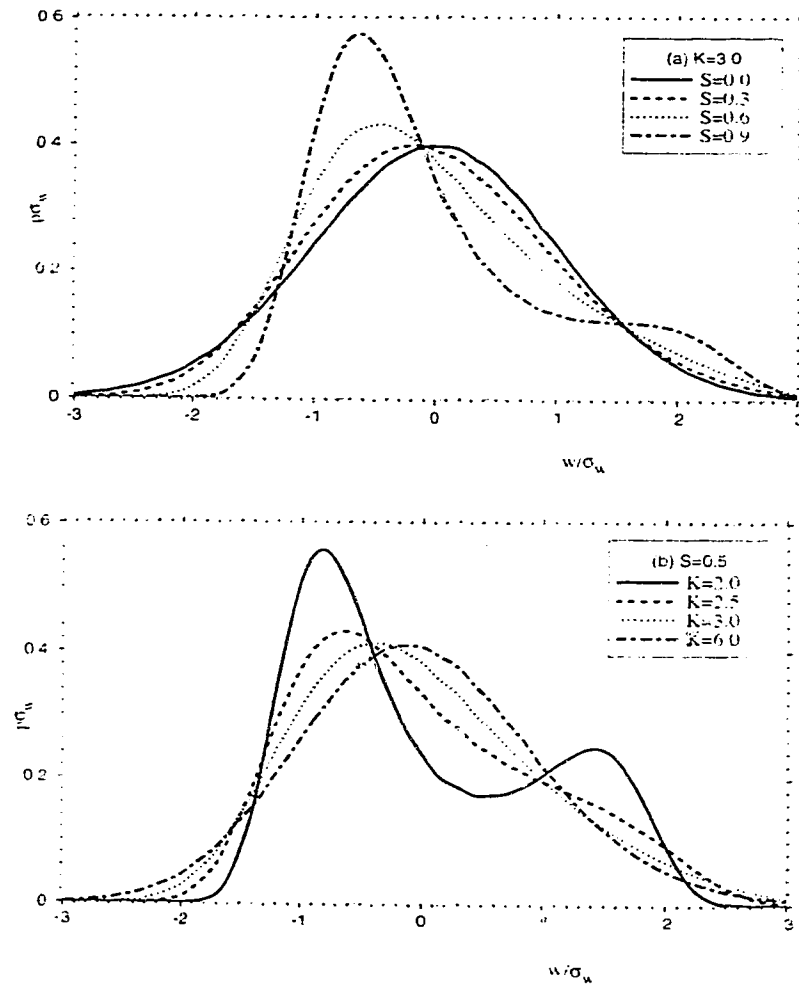


Figure 2.3.1. The variation of the shape of Eulerian pdf of vertical velocity with skewness and kurtosis. (a) For a given kurtosis, $K=3.0$, the variation of pdf with S ; (b) For a given skewness, $S=0.5$, the variation of pdf with K .

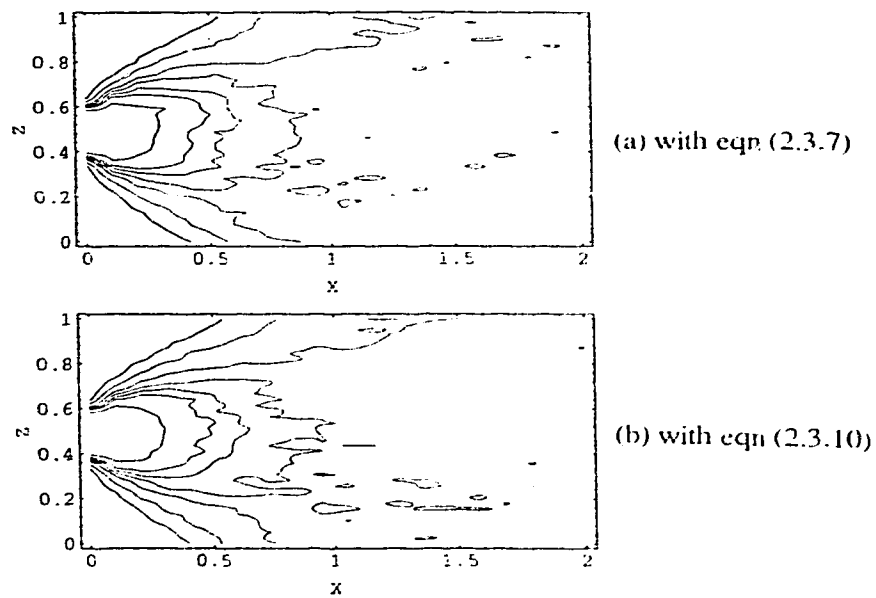


Figure 2.3.2. Test of the present LS model in Gaussian turbulence - the distribution of CWIC in the X-Z plane. Contour levels (from inner to outer) are 2.0, 1.5, 1.3, 1.1, 0.9, 0.6, and 0.3, respectively.

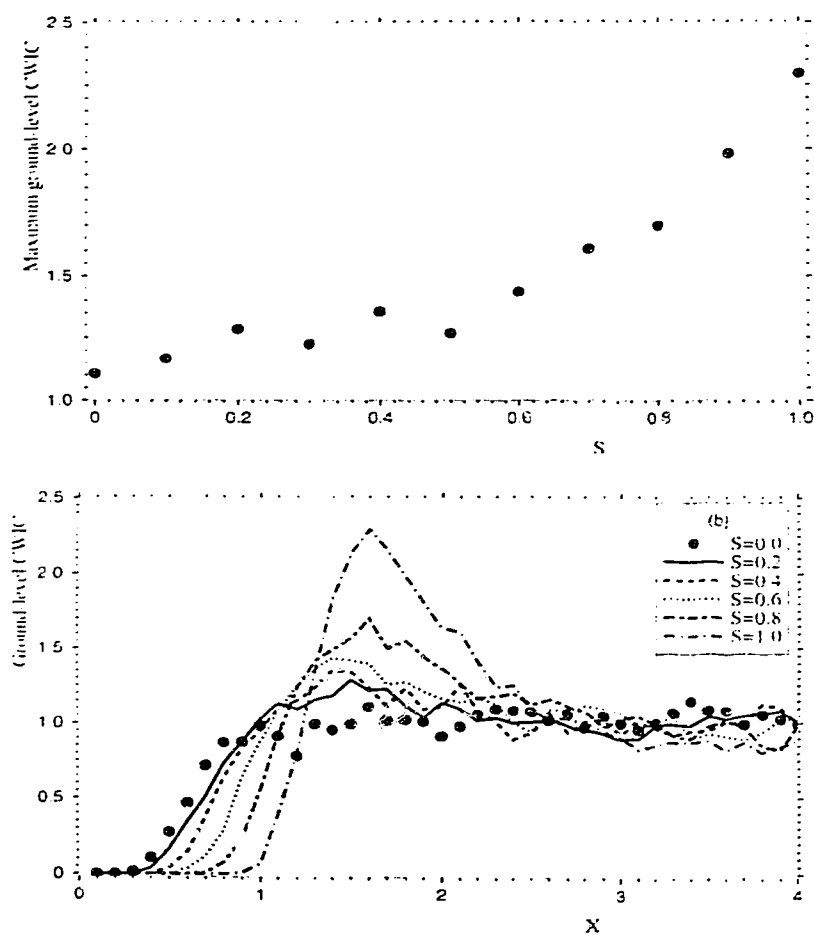


Figure 2.3.3. The variation of the cross-wind integrated concentration (CWIC) with skewness. (a) The variation of the maximum ground level CWIC with skewness; (b) The variation of ground-level CWIC with the non-dimensional downstream distance X for different values of skewness.

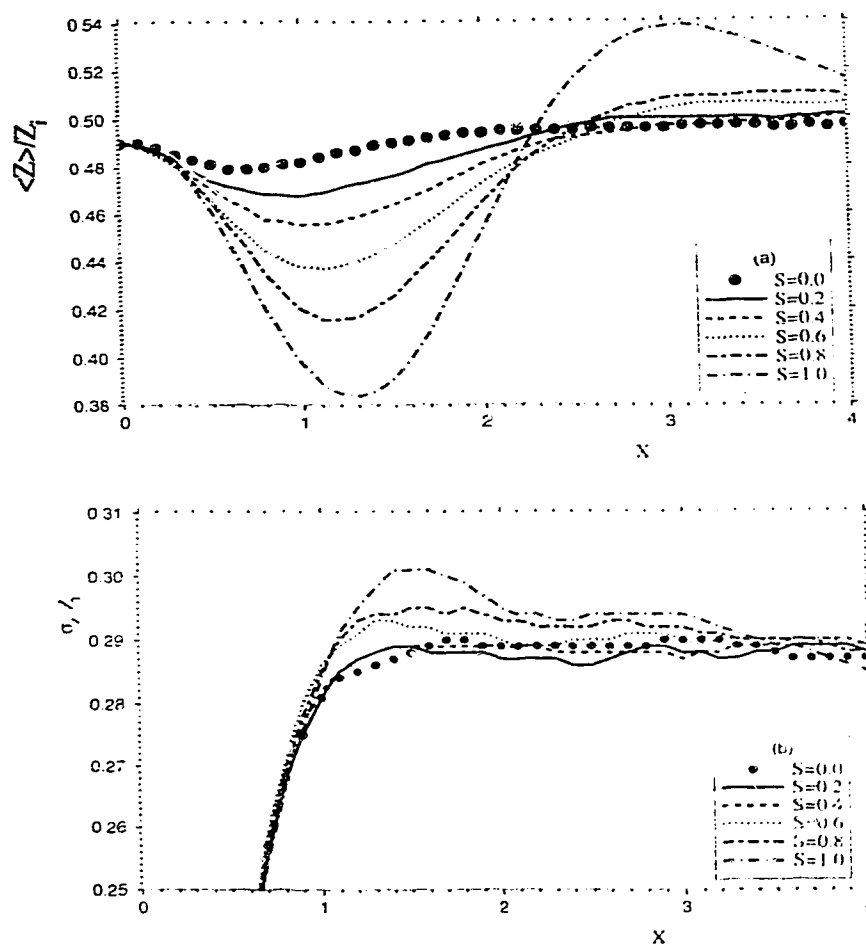
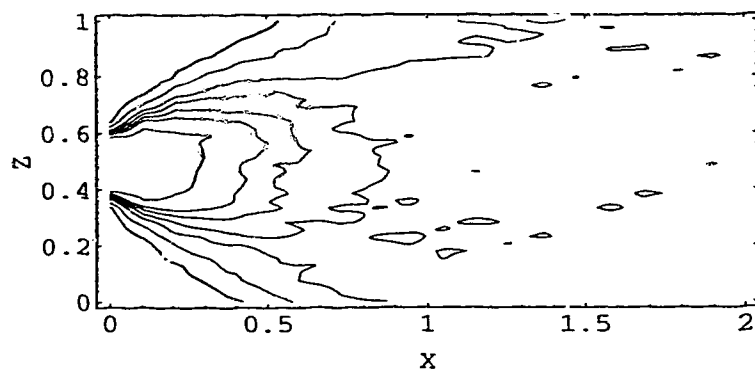
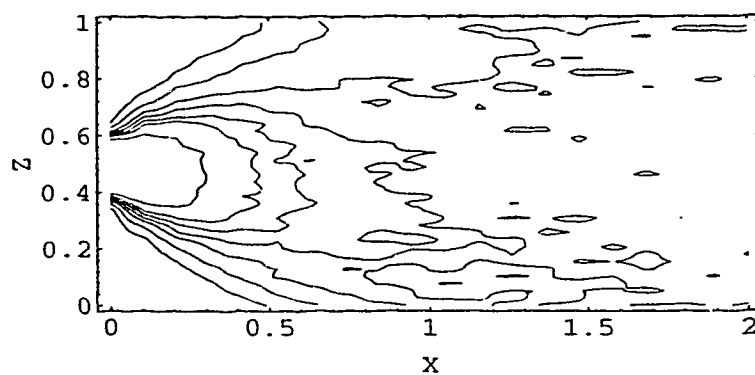


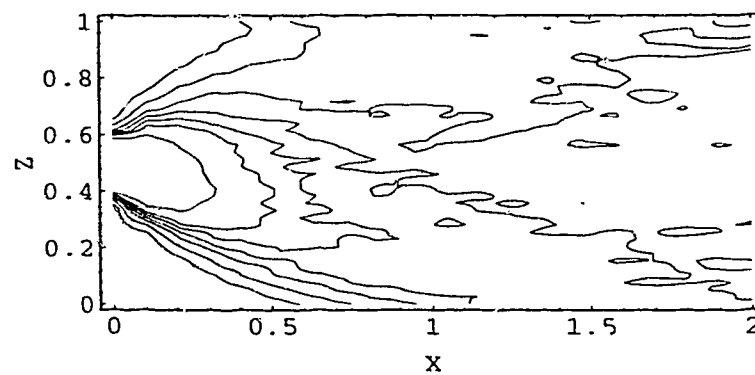
Figure 2.3.4. The variation of (a) the mean plume height and (b) the standard deviation of vertical spread with downstream distance X for different values of skewness.



$S=0.0$



$S=0.2$



$S=0.4$

Figure 2.3.5. CWIC contours in the X-Z plane for different values of skewness (holding $K=3.0$). Contour levels (from inner to outer) are 2.0, 1.5, 1.3, 1.1, 0.9, 0.6, and 0.3, respectively.

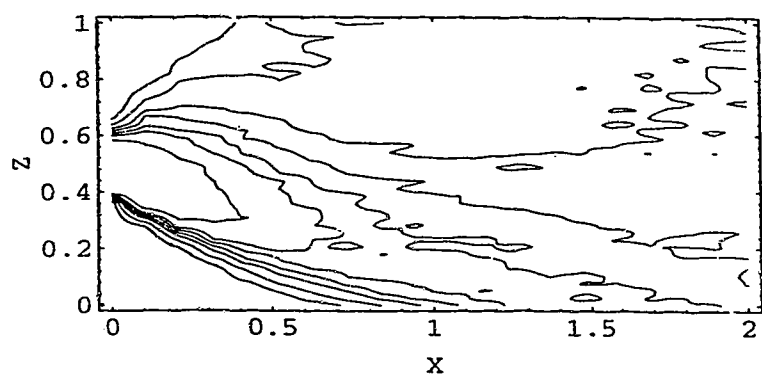
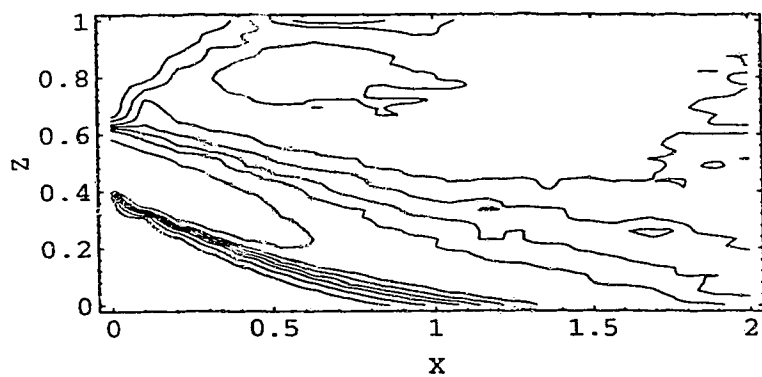
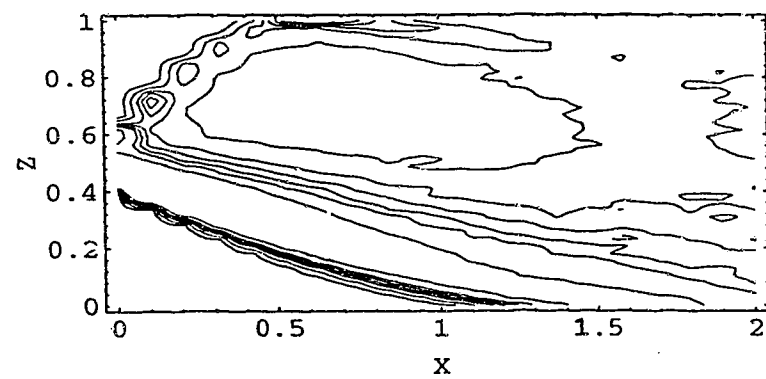
 $S=0.6$  $S=0.8$  $S=1.0$

Figure 2.3.5. Continued.

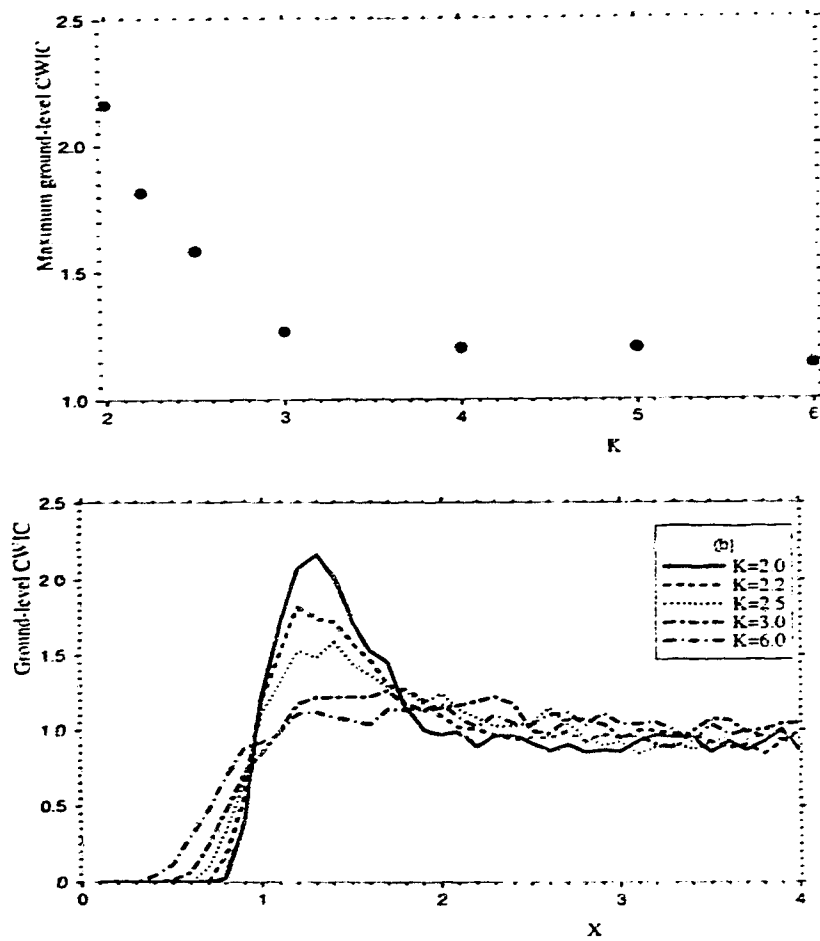


Figure 2.3.6. The variation of the cross-wind integrated concentration (CWIC) with kurtosis. (a) The variation of the maximum ground level CWIC with kurtosis; (b) The variation of ground-level CWIC with the non-dimensional downstream distance X for different values of kurtosis.

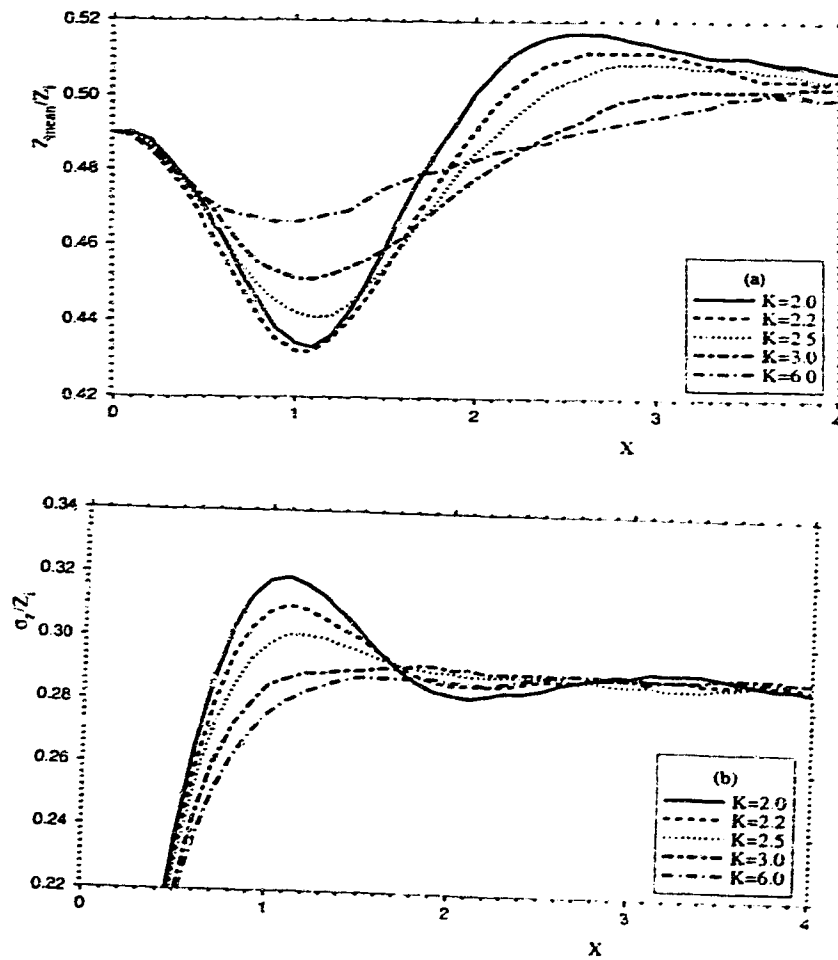
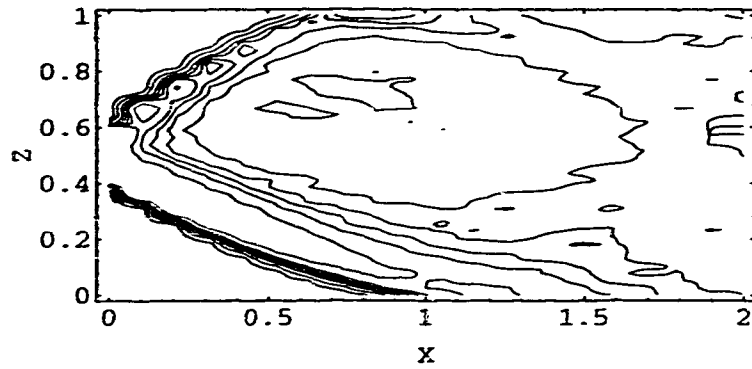
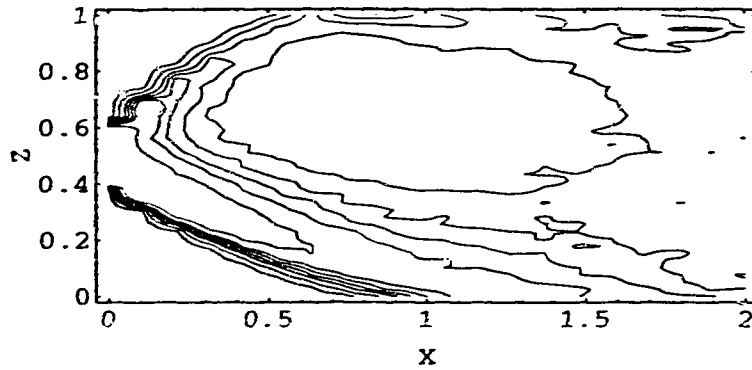


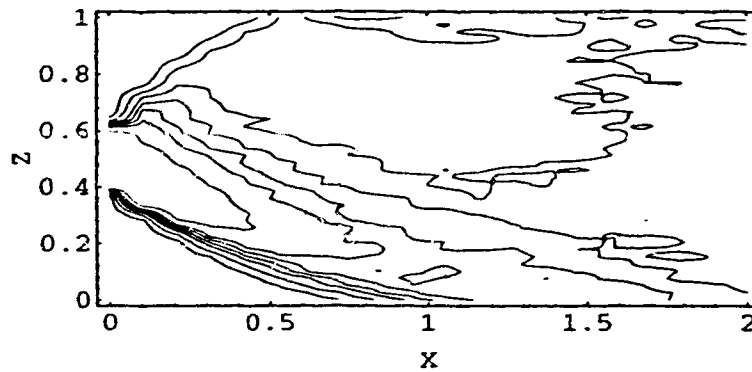
Figure 2.3.7. The variation of (a) the mean plume height and (b) the standard deviation of vertical spread with downstream distance X for different values of kurtosis.



$K=2.0$



$K=2.2$



$K=2.5$

Figure 2.3.8. CWIC contours in X-Z plane for different values of kurtosis (holding $S=0.5$). Contour levels (from inner to outer) are 2.0, 1.5, 1.3, 1.1, 0.9, 0.6, and 0.3, respectively.

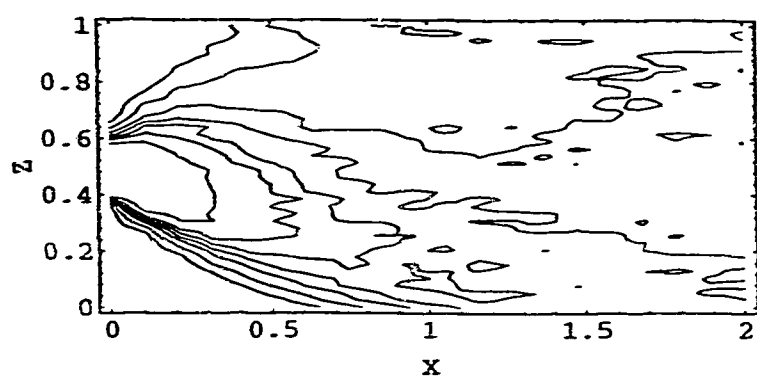
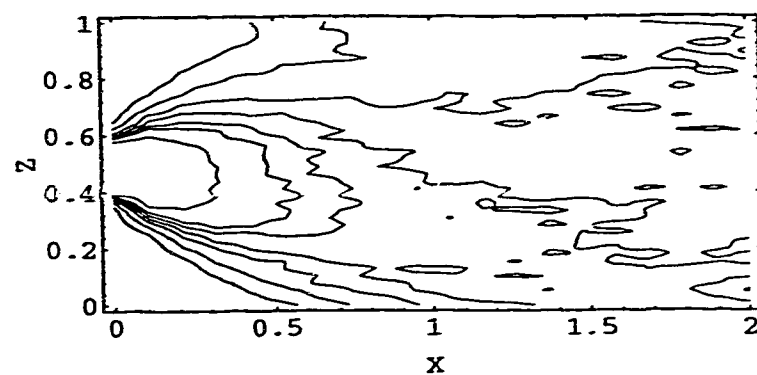
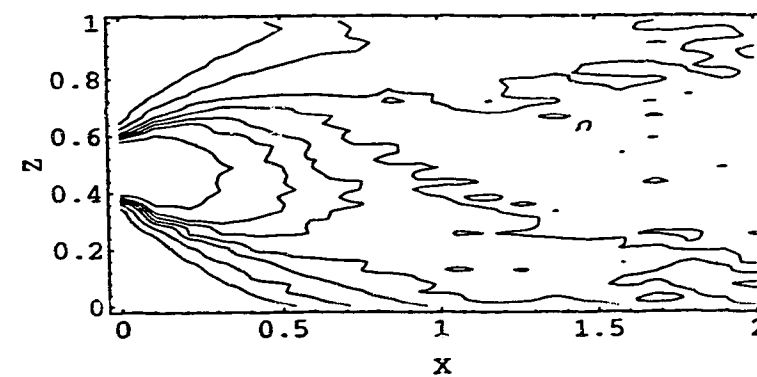
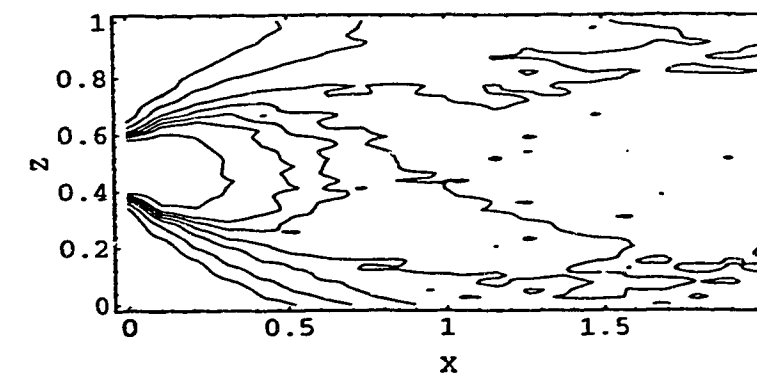
 $K=3.0$  $K=4.0$  $K=5.0$  $K=6.0$

Figure 2.3.8. Continued.

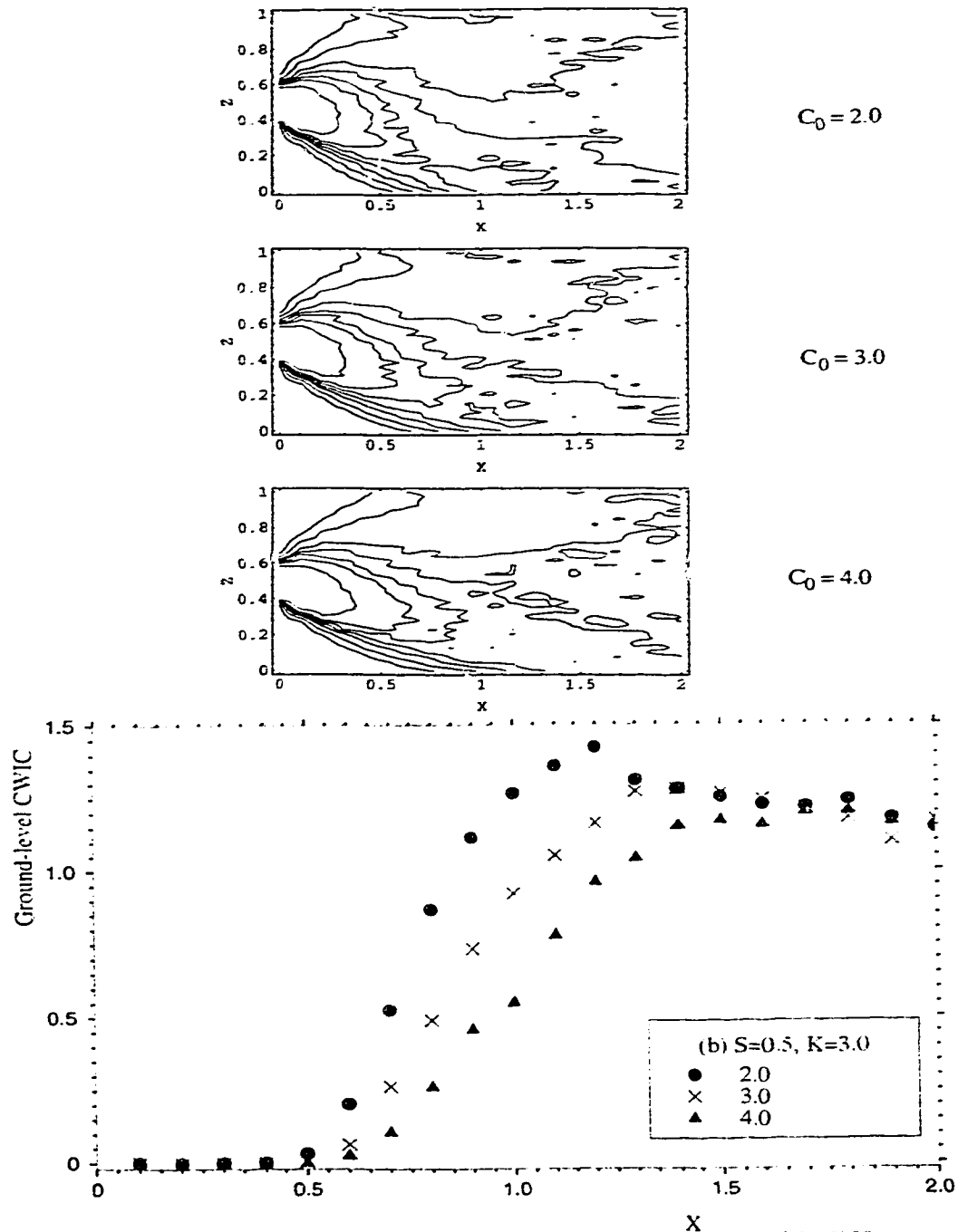


Figure 2.3.9. The variation of the mean concentration distribution with different values of the Kolmogorov constant C_0 . In calculations, $S=0.5$, $K=3.0$. (a) CWIC contours in the X - Z plane, contour levels (from inner to outer) are 2.0, 1.5, 1.3, 1.1, 0.9, 0.6, and 0.3, respectively; (b) variation of ground-level CWIC with downstream distance, different symbols are used for different values of the Kolmogorov constant (2.0, 3.0 and 4.0).

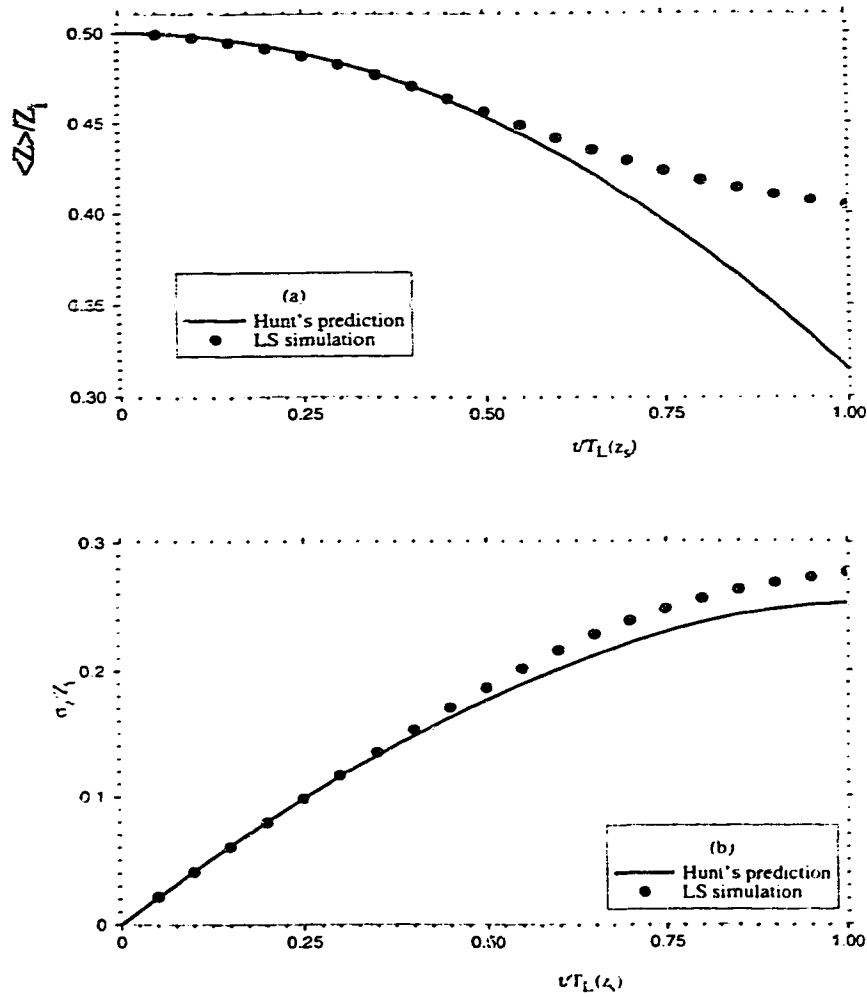


Figure 2.3.10. Comparison of LS simulation with the Hunt prediction (eqn 2.3.13). (a) The mean plume height with travel time from the source; (b) The standard deviation of the particle spread with travel time from the source. The source height is $0.5Z_r$.

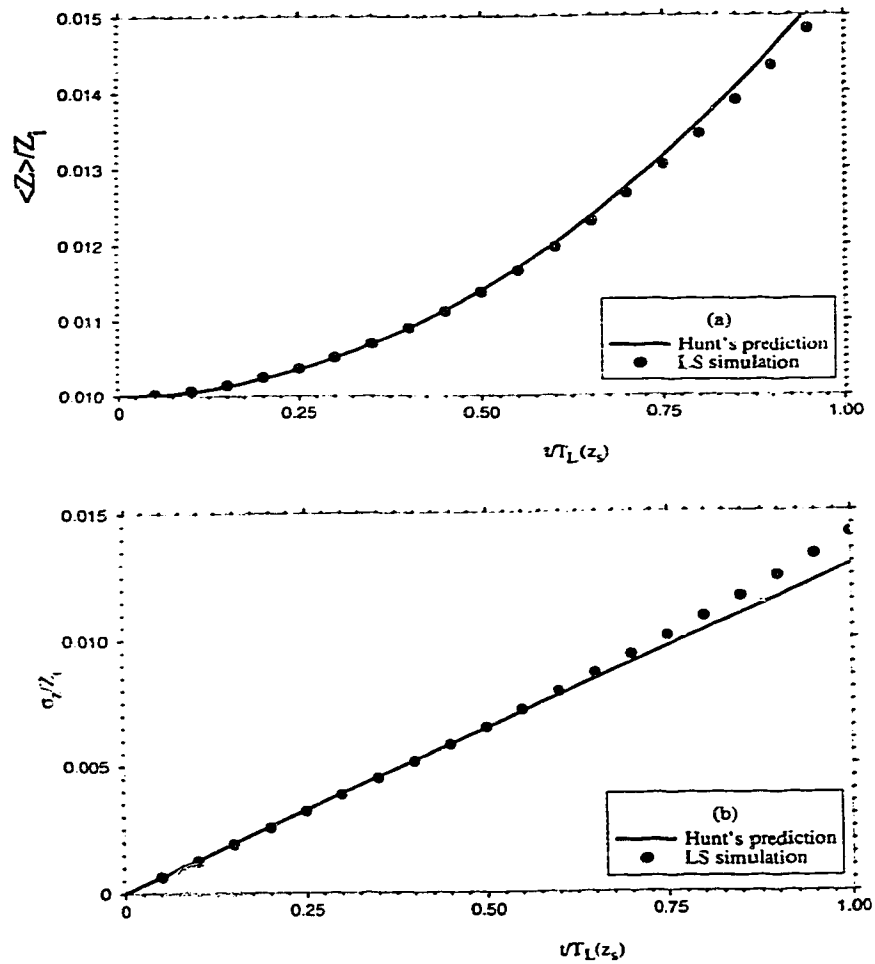


Figure 2.3.11. Comparison of LS simulation with the Hunt prediction (eqn 2.3.13). (a) The mean plume height with travel time from the source; (b) The standard deviation of the particle spread with travel time from the source. The source height $0.01Z_i$.

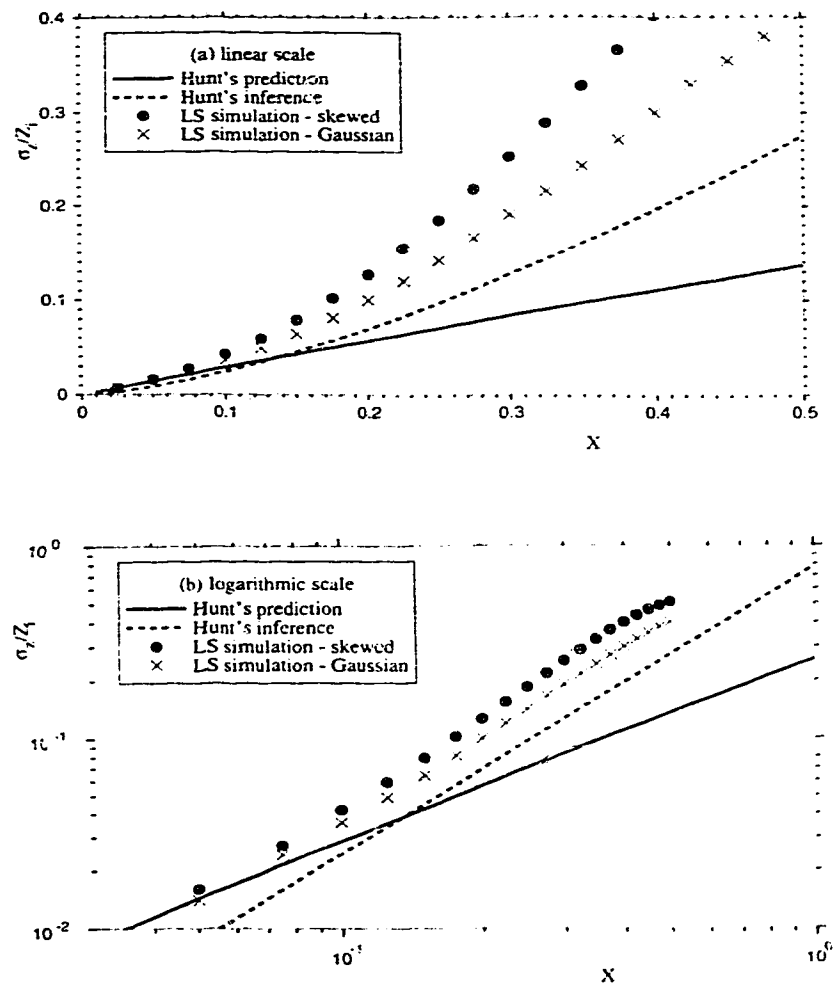


Figure 2.3.12. Test of the Hunt inference (eqn 2.3.14): the standard deviation of the particle spread with travel distance from the source. (a) linear scale, (b) Logarithmic scale.

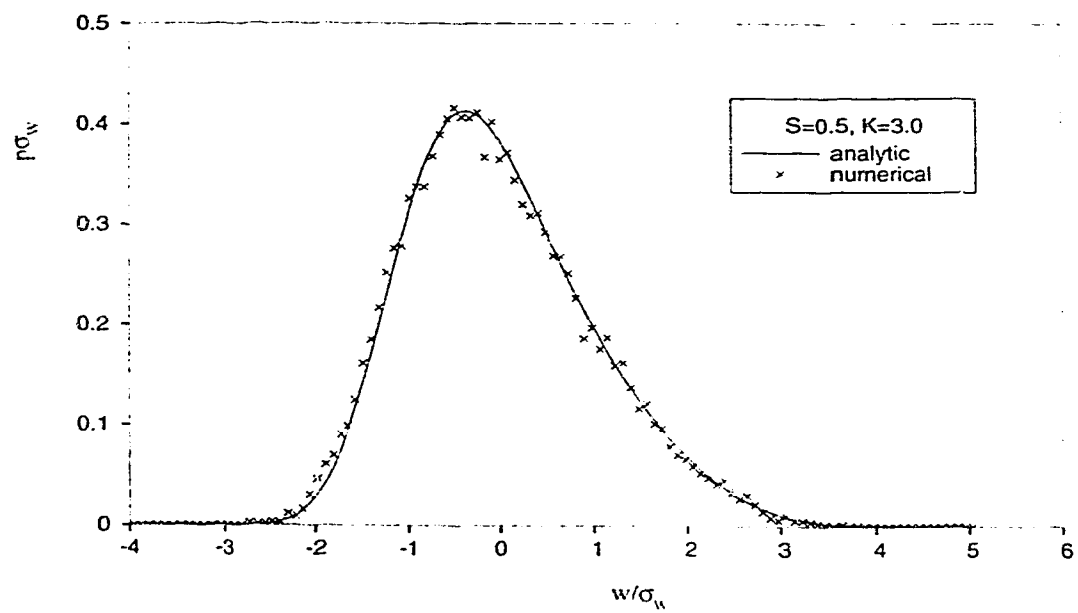


Figure 2.3.A. An example of the distribution of a large set of random numbers generated by the procedure given in the appendix, and the true pdf to which these random numbers are designed.

Chapter 3

ON THE UNIVERSALITY OF THE KOLMOGOROV CONSTANT FOR THE LAGRANGIAN VELOCITY STRUCTURE FUNCTION

Sawford (1991) developed a second-order Lagrangian stochastic model for the ideal case of isotropic, homogeneous and stationary turbulence. In this chapter, that model is extended to (the realisable case of) isotropic, homogeneous but decaying turbulence. The model is used in conjunction with laboratory measurements of dispersion in grid turbulence, to determine the (dimensionless, and hopefully universal) Kolmogorov constant (C_0) for the Lagrangian velocity structure function.

Because C_0 is of great importance in Lagrangian stochastic modelling, in order to encompass a wider range of data we further investigated its value by comparing a first-order LS model with field and laboratory dispersion data at high Reynolds number. We find $C_0 = 3.0 \pm 0.5$.

3.1. Estimation of the Kolmogorov constant (C_0) for the Lagrangian structure function, using a second-order Lagrangian model of grid turbulence¹¹

3.1.1. Introduction

In this paper we are concerned with the numerical value of the universal constant C_0 that appears in Kolmogorov's theoretical small-time estimate

$$D_{ij}(\Delta t) = C_0 \epsilon \delta_{ij} \Delta t \quad (3.1.1)$$

for the Lagrangian velocity structure function

$$D_{ij}(\Delta t) = \langle [U_i^*(t+\Delta t) - U_i^*(t)][U_j^*(t+\Delta t) - U_j^*(t)] \rangle \quad (3.1.2)$$

Here the bracket $\langle \rangle$ denotes the expected value of its contents; U_i^* is the Lagrangian velocity¹²; t and $t+\Delta t$ are arbitrarily separated times; ϵ is the mean rate of dissipation of turbulent kinetic energy; and Δt in eqn (3.1.1) is a time increment satisfying $t_\eta \ll \Delta t \ll T_L$, where t_η is the Kolmogorov inner timescale, and T_L is the integral timescale. Our interest in C_0 stems from the fact that predictions of turbulent dispersion, if obtained using Lagrangian stochastic (LS) models satisfying the criteria provided by Thomson (1987), which include consistency with eqn (3.1.1), will depend upon the value taken for it. That this is so is seen most easily in the case of homogeneous, stationary turbulence; for then (Tennekes 1979) C_0 is related to the Lagrangian timescale by

¹¹ A version of this section has been accepted for publication. S. Du, B.L. Sawford, J.D. Wilson and D.J. Wilson, 1995, *Physics of Fluids*.

¹² We use U^* , $A^* = \partial U^* / \partial t$ for Lagrangian velocity and acceleration; U , $A = dU/dt$ denote the fixed point (Eulerian) velocity and acceleration fields.

$$T_L = \frac{2\sigma_v^2}{C_0 \epsilon} \quad (3.1.3)$$

and the rate of dispersion in homogenous turbulence is $\sigma_y = \sigma_v(2T_L t)^{1/2}$ at $t \gg T_L$ and thus proportional to $C_0^{-1/2}$.

In principle the "true" value of C_0 could be determined from investigations of any turbulent flow, and widely-differing means to do so have been exercised: Lagrangian velocity measurements; Direct Numerical Simulations (DNS); the observed dispersion of tracer particles in a flow. It is perhaps not surprising that a wide range of estimates of C_0 is to be found in the literature (Rodean 1991). Luhar and Britter (1989) and Du et al (1994) obtained (qualitatively) adequate predictions of dispersion from sources in the convective boundary layer (CBL), using well-mixed (Thomson 1987) LS models with $C_0 = 2.0$. Wilson et al. (1981) compared predictions of a well-mixed LS model with the (numerous and definitive) Project Prairie Grass observations (Haugen 1959) of atmospheric surface layer dispersion, and obtained excellent quantitative agreement with (in effect) the specification $C_0 = 3.1$. Hanna (1981) suggested $C_0 = 4.0 \pm 2.0$, on the basis of Lagrangian velocity measurements (neutrally-buoyant balloons) in the CBL. Sawford (1991) suggested $C_0 = 7.0$, by comparing the ratio T_L / t_{η} as obtained from a second-order Lagrangian stochastic model with the value calculated from Yeung and Pope's (1989) DNS of homogeneous isotropic turbulence. And at the upper end of the range suggested, Sawford and Guest (1988) found $5 \leq C_0 \leq 10$ yielded best simulations of dispersion within a physically-modelled neutral boundary layer.

When, as has sometimes been the case, C_0 is inferred from measured tracer dispersion, the value obtained depends on the correctness (or otherwise) of the dispersion model. First order LS models presume the joint evolution of position and velocity (X_i^*, U_i^*) to be Markovian. This is defensible for large Reynolds number turbulence, but at low Reynolds number a better assumption is that position, velocity and acceleration are jointly Markovian (second order LS model). Sawford (1991) suggested that variations in the Reynolds number, across the various dispersion experiments available, may account for

the variability in estimates of C_0 obtained using first-order LS models. By introducing a second-order LS model (in which the Reynolds number is explicitly incorporated and C_0 is *truly* independent of it) for homogeneous, stationary and isotropic turbulence, he showed that in first-order models the *supposedly* universal constant C_0 is *not* universal, but rather depends on the Reynolds number, the effects of which are manifested in first-order models through non-universality across different flows of the "best" value of C_0 .

Our objective here then, is to use a Lagrangian stochastic dispersion model (of known pedigree) to infer the true value of C_0 from measurements of dispersion in the very simplest of turbulent flows. To this end, we will first review the physical basis of Sawford's model. By broadening the well-mixed constraint to encompass acceleration, we will show that the Sawford model is uniquely correct for homogenous, stationary, isotropic turbulence, - only provided it is a satisfactory assumption that for such turbulence the joint probability density function (pdf) for the Eulerian velocity and acceleration is Gaussian (Gaussianity of that pdf was not explicitly assumed by Sawford). Then by extending the model to decaying turbulence, the optimal value of C_0 will be evaluated, by fitting model predictions to laboratory measurements of tracer spread in grid turbulence.

3.1.2. Sawford's second-order model

Consider isotropic, homogeneous and stationary turbulence, and let (Z^+, W^+, A^+) be one component of the position, velocity and acceleration of a tracer particle. Assuming that the collective evolution of (Z^+, W^+, A^+) is Markovian¹³, one has the (otherwise general) model:

$$\begin{aligned} dA^+ &= a(A^+, W^+, Z^+, t)dt + b(A^+, W^+, Z^+, t)d\zeta(t), \\ dW^+ &= A^+ dt, \\ dZ^+ &= W^+ dt, \end{aligned} \tag{3.1.4}$$

¹³ For very high Reynolds number, it is usually assumed that the evolution of velocity and position is jointly Markovian.

where $\zeta(t)$ is a Wiener process. Sawford (1991) assumed within this overall framework a particular form for $a(Z^+, W^+, A^+, t)$, namely:

$$a = -\alpha_1 A^+ - \alpha_2 W^+. \quad (3.1.5)$$

It can be shown that the choice (eqn 3.1.5) *implies* (by virtue of Thomson's 1987 well-mixed condition) a joint Gaussian pdf for A, W . However for our purpose it helps to turn the argument around: we will presently *assume* the Eulerian (A, W) statistics to be Gaussian, and *deduce* the form of $a(Z^+, W^+, A^+, t)$.

The stochastic differential equations (3.1.4) imply a governing equation, the Fokker-Planck equation, for the evolution of the joint probability density function $p(Z^+, W^+, A^+, t)$:

$$\frac{\partial p}{\partial t} = -\frac{\partial}{\partial Z^+}(W^+ p) - \frac{\partial}{\partial W^+}(A^+ p) - \frac{\partial}{\partial A^+}(a p) + \frac{1}{2} \frac{\partial^2}{\partial A^{+2}}(b^2 p) \quad (3.1.6)$$

Now, we extend Thomson's well-mixed constraint by the following proposition: *IF* at time $t=t_0$, p is proportional to p_a , the Eulerian joint pdf of the acceleration, velocity and position, *THEN* at later time $t>t_0$, p must remain proportional to p_a . Mathematically this requires that p_a be a solution of eqn (3.1.6). So, we have:

$$\frac{\partial p_a}{\partial t} = -\frac{\partial}{\partial Z}(W p_a) - \frac{\partial}{\partial W}(A p_a) - \frac{\partial}{\partial A}(a p_a) + \frac{1}{2} \frac{\partial^2}{\partial A^2}(b^2 p_a). \quad (3.1.7)$$

In homogeneous and stationary turbulence this requirement reduces to

$$-\frac{\partial}{\partial W}(A p_a) - \frac{\partial}{\partial A}(a p_a) + \frac{1}{2} \frac{\partial^2}{\partial A^2}(b^2 p_a) = 0. \quad (3.1.8)$$

We now introduce the assumptions upon which, in effect, the Sawford model rests. Firstly we assume the Eulerian velocity pdf to be Gaussian; this is supported by experimental data from homogeneous and isotropic turbulence (Batchelor 1953). Secondly, we assume that the Eulerian acceleration pdf is also Gaussian (the validity of this

assumption is explored in Appendix 3.1). In stationary homogeneous turbulence, velocity and acceleration are uncorrelated, and so in this case we obtain for the Eulerian joint pdf of velocity and acceleration:

$$p_a = \frac{1}{2\pi\sigma_w\sigma_A} \exp\left(-\frac{W^2}{2\sigma_w^2} - \frac{A^2}{2\sigma_A^2}\right), \quad (3.1.9)$$

where σ_w and σ_A are the standard deviations of the velocity and the acceleration, respectively. Substituting into eqn (3.1.8), we obtain

$$a = -\frac{b^2}{2\sigma_A^2} A - \frac{\sigma_A^2}{\sigma_w^2} W. \quad (3.1.10)$$

By requiring his model to yield an asymptotically stationary random process $A^*(t)$, Sawford (1991) from his assumption (eqn 3.1.5 here) found

$$b = \sqrt{2\alpha_1\alpha_2\sigma_w^2}, \quad (3.1.11)$$

where in view of our eqn (3.1.10),

$$\alpha_1 = \frac{b^2}{2\sigma_A^2}, \quad \alpha_2 = \frac{\sigma_A^2}{\sigma_w^2}. \quad (3.1.12)$$

It is obvious that this stationarity property is satisfied by the present (more-general) model. This is not surprising because Thomson's well-mixed constraint encompasses the condition of the asymptotic stationarity of a random process (Thomson 1987).

Eqn (3.1.10) automatically gives the correct velocity structure function in the dissipation range. It is desirable that it also yield the correct correlation function in the inertial subrange. Following Sawford (1991), this is ensured if we specify:

$$b = \sqrt{\frac{2\sigma_w^2}{T_L^3} Re_\tau (1 + Re_\tau^{-\frac{1}{2}})} \quad (3.1.13)$$

where:

$$Re_* = \frac{16 a_0^2}{C_o^4} Re, \quad T_L = \frac{2 \sigma_w^2}{C_o \epsilon},$$

$$Re = \left(\frac{T_E}{t_\eta} \right)^2, \quad T_E = \frac{\sigma_w^2}{\epsilon}$$
(3.1.14)

T_E is an Eulerian timescale, and T_L is a Lagrangian timescale. The dimensionless constant a_0 is defined by (Monin and Yaglom 1975)

$$\sigma_A^2 = \frac{a_0 \epsilon}{t_\eta}. \quad (3.1.15)$$

This is obtained by dimensional analysis in the framework of Kolmogorov's second hypothesis: that in locally-homogeneous and isotropic turbulence, the motion is determined by the forces of viscous friction and inertia (Panchev 1971). For very high Reynolds number, a_0 is universal; but when the Reynolds number is finite, a_0 can be Reynolds-number dependent (Yeung and Pope 1989).

Since b , if specified by eqn (3.1.13), is independent of both W^* and A^* , then a in eqn (3.1.10) will be linear in W^* and A^* . This is the property assumed by Sawford as a precondition of his model for homogeneous, stationary and isotropic turbulence. It follows from our re-examination of that model that since the pdf of acceleration cannot be exactly Gaussian (see Appendix), the Sawford model cannot be exactly correct.

3.1.3. Extension of the Sawford model to decaying turbulence

In any real flow, energy dissipation ensures that the turbulence cannot be both stationary and homogeneous. In this section we extend the Sawford model to homogeneous decaying turbulence, in order to develop a model applicable to decaying grid turbulence.

In non-stationary turbulence, the Eulerian velocity and acceleration are correlated:

$$\rho = \frac{\langle WA \rangle}{\sigma_w \sigma_A} = \frac{1}{\sigma_w \sigma_A} \langle W \frac{dW}{dt} \rangle = \frac{1}{2\sigma_w \sigma_A} \frac{d}{dt} \langle W^2 \rangle \neq 0. \quad (3.1.16)$$

Continuing to assume the Eulerian pdf for velocity and acceleration is a joint Gaussian, we then have:

$$p_a = \frac{1}{2\pi\sigma_w\sigma_A\sqrt{1-\rho^2}} \exp\left[-\frac{\sigma_w^2 A^2 + \sigma_A^2 W^2 - 2\rho\sigma_A\sigma_w WA}{2\sigma_A^2\sigma_w^2(1-\rho^2)}\right] \quad (3.1.17)$$

Equation (3.1.7) yields:

$$\begin{aligned} a = & -\left[\frac{b^2}{2\sigma_A^2(1-\rho^2)} - \rho\frac{\sigma_A}{\sigma_w} - \frac{\sigma_A'}{\sigma_A} + \frac{\rho\rho'}{1-\rho^2}\right]A + \\ & -\left[-\frac{b^2\rho}{2\sigma_A\sigma_w(1-\rho^2)} + \frac{\sigma_A^2}{\sigma_w^2} - \frac{\rho'}{1-\rho^2}\frac{\sigma_A}{\sigma_w}\right]W. \end{aligned} \quad (3.1.18)$$

The symbol (') represents the derivative with respect to time. It is interesting that in this slightly more complicated turbulence the second-order model remains linear in A^* and W^* . Eqn (3.1.18) reduces to the original Sawford model (eqn 3.1.10) for stationary turbulence. Since the statistics of the increment of acceleration A^* are mainly determined by small scale eddies, under the hypothesis of local isotropy b remains as given by eqn (3.1.13), even in decaying turbulence.

3.1.4. The magnitude of C_0

In second-order trajectory models, the constant C_0 is free of the Reynolds-number effects and is therefore genuinely universal. This property makes it possible to determine C_0 by fitting-second-order model predictions to experimental data. In grid turbulence the

collective assumptions of homogeneity, isotropy and Gaussianity (of the velocity pdf) are approximately satisfied. Therefore we will use equations (3.1.4, 3.1.13, 3.1.18) to predict turbulent dispersion in water channel and wind tunnel grid turbulence.

3.1.4.1. Simulation of water channel dispersion

Measurements of the dispersion of a neutrally-buoyant saline tracer released from a point source into decaying homogeneous turbulence (grid turbulence) have been carried out in a water channel at the University of Alberta. A detailed description of the experiment has been given by Wilson et al. (1991), and here we list only the turbulence statistics needed in order to simulate tracer trajectories using the present model:

$$\begin{aligned}\sigma_w &= 0.13U \left(\frac{X+X_0}{M} - 13 \right)^{-\frac{1}{2}}, \\ \sigma_v &= 0.195U \left(\frac{X+X_0}{M} - 6.5 \right)^{-\frac{1}{2}},\end{aligned}\tag{3.1.19}$$

Here $U = 18.75 \text{ cm s}^{-1}$ is the mean alongstream velocity; $M = 7.62 \text{ cm}$ is the center-to-center mesh spacing; X is the downstream distance from the source to the point of interest; and X_0 is the distance from the grid to the source ($X_0 = 147.5 \text{ cm}$).

In decaying homogeneous turbulence, the turbulent kinetic energy budget is approximately a balance between the dissipation rate ϵ and advection by the mean flow, ie.

$$\epsilon \approx -U \frac{\partial k}{\partial X} = -\frac{U}{2} \frac{\partial}{\partial X} \left(\sigma_u^2 + \sigma_v^2 + \sigma_w^2 \right)\tag{3.1.20}$$

(Townsend 1976). Because V was not measured, we assume that $\sigma_v = \sigma_w$.

To specify a_0 we used Pope's (1994) formula

$$a_0 = 3 \left(1 - \frac{22}{Re_\lambda} \right),\tag{3.1.21}$$

where $Re_\lambda = \sigma_w \lambda / \nu$ is the Reynolds number based on the Taylor microscale $\lambda = (15\nu\sigma_w^2/\epsilon)^{1/2}$. This formula is derived from the DNS data of Yeung and Pope (1989).

Figure 3.1.1 compares the measured and predicted standard deviation of vertical spread σ_z , for several assumed values of C_0 . The choice $C_0 = 3.0 \pm 0.5$ gives a good fit of the second-order model to the experimental data.

3.1.4.2. Simulation of wind tunnel dispersion

The rate of dispersion was measured in decaying grid turbulence in a wind tunnel at the Division of Atmospheric Research, CSIRO, Australia. Best-fit formulae for turbulence velocity statistics are:

$$\begin{aligned}\sigma_U &= 0.060U \left(\frac{X+X_0}{X_0} \right)^{-0.74}, \\ \sigma_V &= 0.055U \left(\frac{X+X_0}{X_0} \right)^{-0.71}, \\ \sigma_W &= 0.053U \left(\frac{X+X_0}{X_0} \right)^{-0.69},\end{aligned}\tag{3.1.22}$$

where U ($= 548 \text{ cm s}^{-1}$) is the mean velocity along the wind tunnel, X is the streamwise distance from the source, and $X_0 = 31.0 \text{ cm}$ is the distance from the grid to the source. We estimated the dissipation rate ϵ by the means indicated earlier.

Figure 3.1.2 compares measured and calculated vertical spread of the tracer. As in the case of the water channel data, $C_0 = 3.0 \pm 0.5$ gives a good fit.

3.1.4.3 Estimates of C_0 from infinite Reynolds number flow

The Reynolds number for atmospheric boundary layer turbulence is (effectively) infinite. Rodean (1991) estimated that in the neutral atmospheric surface layer (NSL), the Kolmogorov constant $C_0 \approx 5.7$. The basis for this result (or its equivalent for the

specification of a Lagrangian timescale) is as follows.

Suppose in the NSL we regard the Eulerian velocity statistics as Gaussian (this is quite a good assumption, except within or close to the vegetation, i.e., provided height $z \gg z_0$, where z_0 is the surface roughness length). Thomson (1987) proved that the model

$$dW^* = -\frac{W^*}{T_L(Z)}dt + \frac{1}{2} \frac{\partial \sigma_w^2}{\partial Z} \left(1 + \frac{W^{*2}}{\sigma_w^2} \right) dt + b d\zeta \quad (3.1.23)$$

where

$$b = \sqrt{C_0} \epsilon, \quad T_L(Z) = \frac{2\sigma_w^2}{C_0 \epsilon} \quad (3.1.24)$$

is the uniquely correct 1-dimensional model for Gaussian inhomogeneous turbulence, - that is, it is the "uniquely correct" model within the most rigorous theoretical framework presently available, that of Thomson (1987). This model is easily shown to be equivalent to

$$d\left(\frac{W^*}{\sigma_w} \right) = -\frac{W^*}{\sigma_w} \frac{dt}{T_L} + \frac{\partial \sigma_w}{\partial Z} dt + \sqrt{\frac{2}{T_L}} d\zeta \quad (3.1.25)$$

which is the infinitesimal form of the model compared by Wilson et al. (1981; hereafter WTK) against the Project Prairie Grass field observations of dispersion¹⁴. Now, Durbin (1984) has analysed this model to show that it implies (in the large time limit $t/T_L \rightarrow \infty$) a random displacement (or zero-order) model

$$dZ^* = \sqrt{2 K_s(Z)} d\zeta + \frac{\partial K_s}{\partial Z} dt \quad (3.1.26)$$

where $d\zeta(t)$ is a Wiener process ($d\zeta$ has variance dt), and

¹⁴ The equivalence between the discrete-time implementation of the above equation for $d(w/\sigma_w)$ and the model compared by WTK against field data can be traced through Wilson et al. (1983). Durbin (1983) may independently have suggested this model.

$$K_s = \sigma_w^2 T_L = \frac{2\sigma_w^4}{C_0 \epsilon} \quad (3.1.27)$$

is an effective eddy diffusivity.

Flux-gradient experiments in the horizontally-uniform NSL indicate that the eddy diffusivity is $K_s = \kappa u_* Z$, where u_* is the friction velocity, and the von Kármán constant (κ) is now generally accepted as having the value $\kappa=0.4\pm0.02$ (Dyer and Bradley 1982; Högström 1985). If this (empirical) result is to be matched with Durbin's result (asymptotic eddy diffusion model), we require that

$$C_0 = 2 \left(\frac{\sigma_w}{u_*} \right)^4 \quad (3.1.28)$$

where we have used the fact that in the NSL, $\epsilon \approx u_*^3 / \kappa Z$. Now since $\sigma_w \approx 1.3 u_*$, we have $C_0 \approx 5.7$. This is the value suggested by Rodean, here deduced by a logic which avoids reference to the Lagrangian timescale (the latter being undefined in the case of inhomogeneous turbulence). The equivalent result for a Lagrangian timescale (albeit difficult of interpretation) was arrived at much earlier (eg. Reid 1979).

This is a pleasing theoretical argument. However one does not claim the present generation of LS models to be *ultimately* correct, and may expect Thomson's 1987 criteria eventually to be superseded. The above logic does not *guarantee* that the conformance of (properly selected) LS models with atmospheric observations is optimal, when $C_0=5.7$. In fact, several workers have found otherwise. For example, Wilson et al. (1981) found that a better fit to observed dispersion (Project Prairie Grass) is obtained using (in effect) $C_0 \approx 3.1$ (the WTK model was actually couched in terms of a Lagrangian timescale and WTK wrote $\sigma_w/u_* = 1.25$). Earlier Reid (1979) reached the same conclusion in reference to the Porton field data. Findings corresponding to $C_0 \approx 3.1$ exist (Wilson 1982; Hassid 1983) in the context of *Eulerian* dispersion models, for the magnitude of the turbulent Schmidt number (S_ϵ , the ratio of the eddy diffusivity for mass to the eddy viscosity) giving best agreement with observed (field and wind tunnel) dispersion. $C_0 \approx 3.1$ is close to our

best guess for C_0 on the basis of our examination of laboratory experiments.

3.1.5. First-order Lagrangian stochastic model

Sawford (1991) found that for homogeneous, isotropic and stationary turbulence. Reynolds number effects in first-order models can be incorporated by replacing the universal constant C_0 with

$$C_0^{effective} = C_0(1 + Re_*^{-1/2})^{-1}. \quad (3.1.29)$$

Now we ask: is this correction to the first-order model useful in homogeneous, isotropic but decaying turbulence?

For such a flow, the one dimensional first-order model is (Thomson 1987):

$$dW^* = -\left(\frac{C_0 \epsilon}{2\sigma_w^2} - \frac{\sigma'_w}{\sigma_w}\right)W^* dt + \sqrt{C_0 \epsilon} d\zeta, \quad (3.1.30)$$

$$dZ^* = W^* dt.$$

By replacing C_0 in eqn (3.1.30) by $C_0^{effective}$ as given by eqn (3.1.29), and carrying out a simulation with the revised first-order model, we found that eqn (3.1.29) works well, especially for the wind tunnel experiment (Figure 3.1.3). For comparison, we also show the prediction with $C_0^{effective} = 3.0$.

Figure 3.1.4 shows the Reynolds number in the range of interest of the wind tunnel and water channel experiments. This helps to explain why the correction (eqn 3.1.29) is more significant for the wind tunnel experiment. In the water channel, the Lagrangian Reynolds number Re_* is sufficiently high that the Reynolds-number correction to the first-order model is not large. But in the wind tunnel experiment Re_* is lower, so $C_0^{effective}$ is significantly different from its asymptote.

3.1.6. Conclusions

The Sawford (1991) model has been shown to be implied by a generalized well-mixed constraint, for (hypothetical) homogeneous, isotropic, stationary turbulence, for which the Eulerian joint pdf for the velocity and acceleration is Gaussian.

We have extended that model to cover decaying grid turbulence. By comparing measured and modelled dispersion, the universal Kolmogorov constant C_0 is estimated to be 3.0 ± 0.5 , substantially different from the result, $C_0 = 7.0$, obtained by Sawford by comparing modelled dispersion statistics with direct numerical simulation data (Yeung and Pope 1989).

When the Reynolds-number-effect is incorporated into the first-order model via the supposedly universal constant C_0 , ie., by replacing C_0 with a variable $C_0^{\text{effective}}$ (eqn 3.1.29), the first-order model also gives a very good prediction, suggesting that Sawford's revision of the first-order model for finite-Reynolds-number flow is satisfactory. This is useful, because first-order models are simpler than second-order, and require less Eulerian statistical information on the flow.

APPENDIX 3.1. The pdf for fixed-point acceleration

The spatial derivative of velocity is not Gaussian (Batchelor 1953), and recent studies of isotropic turbulence show that, even if the single-point velocity pdf is identically Gaussian, the distribution of the pressure fluctuation is negatively skewed (Holzer and Siggia 1993; Pumir 1994). While it is not clear how these non-Gaussian properties impact the Eulerian acceleration pdf, we believe the latter is non-Gaussian on this and the following evidence.

Recall that we signify Lagrangian quantities by superscript (+). The Eulerian acceleration field

$$A(X_0, t_0) = \lim_{t \rightarrow t_0} \frac{U(X_0, t) - U(X_0, t_0)}{t - t_0} = \lim_{\tau \rightarrow 0} \frac{\Delta_\tau U}{\tau} \quad (\text{A3.1.1})$$

is defined by the difference of Lagrangian velocity over an infinitesimal time interval

(Monin and Yaglom 1975, p368, eqn 21.47). Here $U^+(X_0, t)$ is velocity at time t of that fluid element which, at time t_0 , was at location X_0 . We can therefore infer the distribution for Eulerian acceleration if we know the distribution of the Lagrangian velocity difference, taken over a very short time interval. According to Figure (15) of Yeung and Pope (1989), derived from Direct Numerical Simulation of isotropic turbulence, the distribution of Lagrangian velocity difference $\Delta_\tau U^+$ (where U^+ is one component of U^+) is symmetric about $\Delta_\tau U^+ = 0$ for any time interval τ , and deviates from the Gaussian distribution as τ gets smaller. When τ is extremely small ($\tau \sim t_\eta$), the distribution appears to be exponential.

Because the Eulerian acceleration is given by the Lagrangian velocity difference $\Delta_\tau U^+$ over an extremely small interval τ , we may assume on the evidence of Yeung and Pope that the pdf for Eulerian acceleration is exponential and is symmetric about $A=0$. We derived a second-order model from the exponential pdf, and compared its prediction for tracer spread with the prediction of the model presented in section 3.1.2. No substantial difference was found: out to $t/T_L=10$, the maximum difference was less than 5% in σ_z , and had no effect on the choice of $C_0 = 3.0 \pm 0.5$. So we propose, a Gaussian pdf for Eulerian acceleration is an acceptable approximation, at least for the purpose of predicting the mean concentration distribution.

Bibliography

- Batchelor, G.K., 1953: *The Theory of Homogeneous Turbulence*, Cambridge University Press, 197pp.
- Du, S., J.D. Wilson and E. Yee, 1994: Probability density function for velocity in the convective boundary layer, and implied trajectory models, *Atmos. Environ.* **28**, 1211-1217.
- Durbin, P.A., 1983: *Stochastic differential equations and turbulent dispersion*. NASA reference publication No. 1103.
- Durbin, P.A., 1984: Comments on papers by Wilson et al. (1981) and Legg and Raupach (1982), *Boundary-Layer Meteorol.* **29**, 409-411.

- Dyer, A.J. and E.F. Bradley, 1982: An alternative analysis of flux-gradient relationships at the 1976 ITCE, *Boundary-Layer Meteorol.* **22**, 3-19.
- Hanna, S.R., 1981: Lagrangian and Eulerian time-scale relations in the day-time boundary layer. *J. Appl. Meteorol.* **20**, 242-249.
- Hassid, S., 1983: Turbulent Schmidt number for diffusion models in the neutral boundary layer, *Atmos. Environ.* **17**, 523-527.
- Haugen, D.A., 1959: *Project Prairie Grass, a Field Program in Diffusion (Volume III)*, *Geophysical Research Papers No.59*, Air Force Cambridge Research Centre-TR-59-235(III).
- Högström, U., 1985: Von Kármán constant in atmospheric boundary layer flow: Revaluated. *J. Atmos. Sci.* **42**, 263-270.
- Holzer, M. and E.D. Siggia, 1993: Skewed, exponential pressure distribution from Gaussian velocities. *Phys. Fluids A* **5**, 2525-2532.
- Luhar, A.K. and R.E. Britter, 1989: A random walk model for dispersion in inhomogeneous turbulence in a convective boundary layer, *Atmos. Environ.* **23**, 1911-1924.
- Monin, A.S. and A.M. Yaglom, 1975: *Statistical Fluid Mechanics*, Vol. 2, MIT Press.
- Panchev, S., 1971: *Random Functions and Turbulence*, Pergamon.
- Pope, S.B., 1994: Lagrangian pdf methods for turbulent flows, *Annual Review of Fluid Mechanics*, **26**, 23-63.
- Pumir, A., 1994: A numerical study of pressure fluctuations in 3D, incompressible, isotropic turbulence. *Phys. Fluids* **6**, 2071-2083.
- Reid, J.D., 1979: Markov chain simulations of vertical dispersion in the neutral surface layer for surface and elevated releases, *Boundary-Layer Meteorol.* **16**, 3-22
- Rodean, H.C., 1991: The universal constant for the Lagrangian structure function, *Phys. Fluids A* **3**, 1479-1480.
- Sawford, B.L., 1991: Reynolds number effects in Lagrangian stochastic models of turbulent dispersion. *Phys. Fluids A* **3**, 1577-1586.
- Sawford, B.L., 1993: Recent developments in the Lagrangian stochastic theory of

- turbulent dispersion, *Boundary-Layer Meteorol.* **62**, 197-215.
- Sawford, B.L. and F.M. Guest, 1988: Uniqueness and Universality of Lagrangian stochastic models of turbulent dispersion, *Preprints of 8th Symp. Turb. Diff.*, AMS, San Diego, CA, 96-99.
- Tennekes, H., 1979: The exponential Lagrangian correlation function and turbulent diffusion in the inertial subrange. *Atmos. Environ.* **13**, 1565-1567
- Thomson, D.J., 1987: Criteria for the selection of stochastic models of particle trajectories in turbulent flows, *J. Fluid Mech.* **180**, 529-556.
- Townsend, A.A., 1976: *The Structure of Turbulent Shear Flow*, Cambridge University Press, Cambridge.
- Wilson, D.J., B.W. Zelt and W.E. Pittman, 1991: *Statistics of turbulent fluctuations of scalars in a water channel*, Technical Report for Canadian Defence Research Establishment, Suffield, 60pp.
- Wilson, J.D., 1982: An approximate analytical solution to the diffusion equation for short range dispersion from a continuous ground-level source, *Boundary-Layer Meteorol.* **23**, 85-103.
- Wilson, J.D., B.J. Legg and D.J. Thomson, 1983: Calculation of particle trajectories in the presence of a gradient in turbulent-velocity variance. *Boundary-Layer Meteorol.* **27**, 163-169.
- Wilson, J.D., G.W. Thurtell and G.E. Kidd, 1981: Numerical simulation of particle trajectories in inhomogeneous turbulence, III: comparison of predictions with experimental data for the atmospheric surface layer, *Boundary-Layer Meteorol.* **21**, 443-463.
- Yeung, P.K. and S.B. Pope, 1989: Lagrangian statistics from direct numerical simulation of isotropic turbulence, *J. Fluid Mech.* **207**, 531-586.

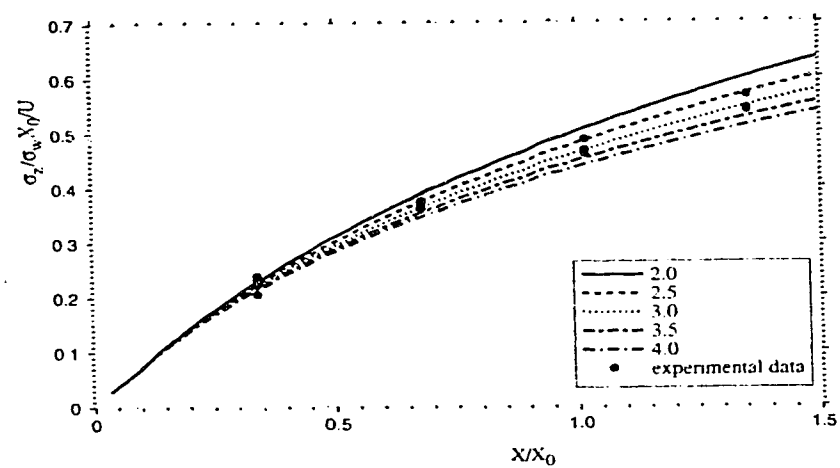


Figure 3.1.1. Vertical dispersion from a tracer source in a water channel experiment, compared with simulations using a second-order LS model with different values of C_0 . Curves for Kolmogorov's constant C_0 from 2.0 to 4.0.

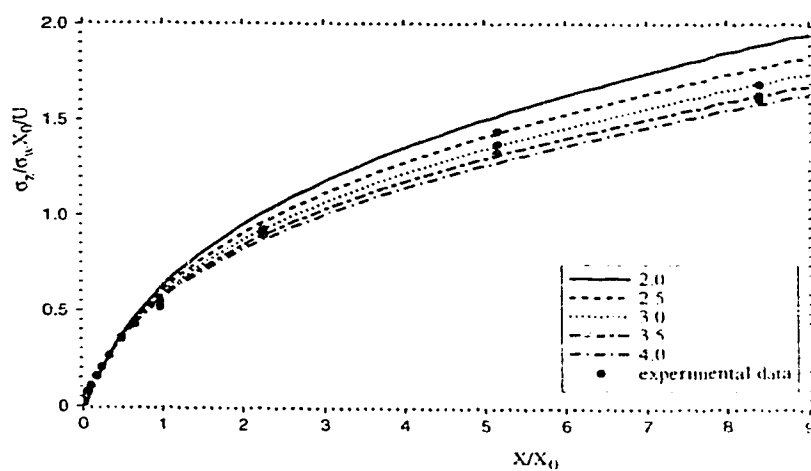


Figure 3.1.2. Vertical dispersion from a tracer source in a wind tunnel experiment, compared with simulations using a second-order LS model with different values of C_0 . Curves for Kolmogorov's constant C_0 from 2.0 to 4.0.

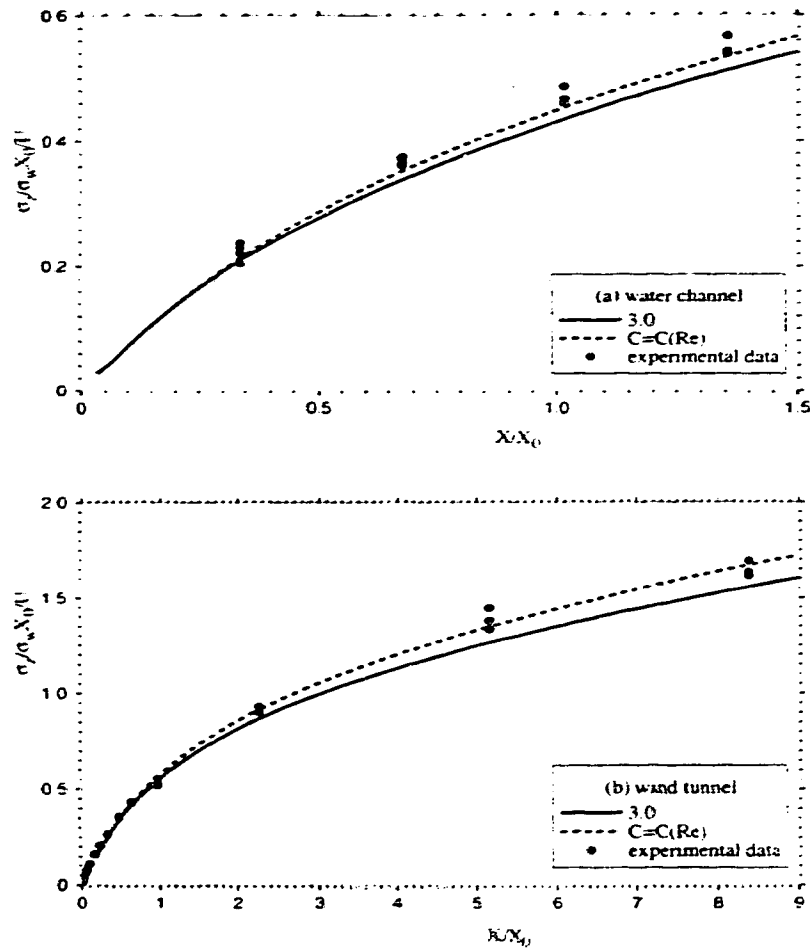


Figure 3.1.3. Vertical dispersion from a tracer source compared with simulations using a first-order model (with and without Reynolds number correction): (a) water channel, (b) wind tunnel. Curves for different effective Kolmogorov's constant $C_0^{effective}$.

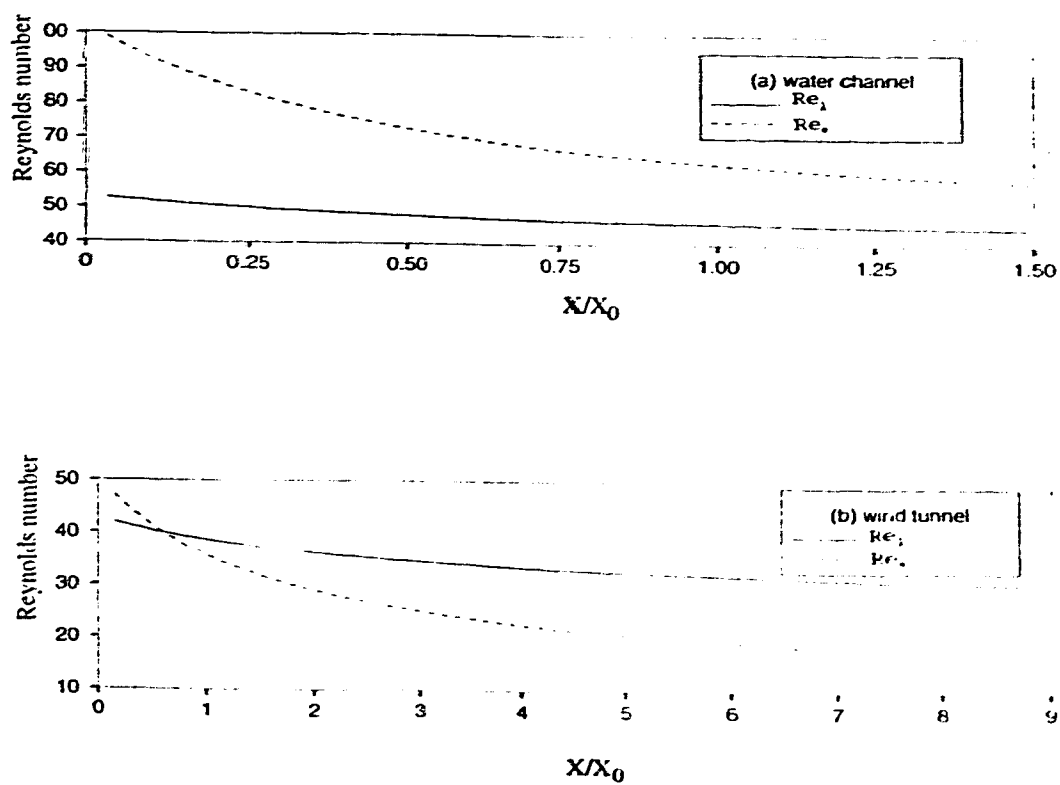


Figure 3.1.4. Reynolds number versus alongstream distance in the experimental grid turbulence: (a) water channel, (b) wind tunnel.

3.2. Universality of the Kolmogorov constant for the Lagrangian velocity structure function across different kinds of turbulence

3.2.1. Introduction

In Lagrangian stochastic (LS) simulations of turbulent dispersion, the value of Kolmogorov's (universal?) constant (C_0) for the Lagrangian velocity structure function in the inertial subrange, or the trivially related coefficient (henceforth denoted β) of the local decorrelation time scale, T_L , is of great importance. Since C_0 is determined by turbulence statistics in the inertial subrange, it is *supposed* to be universal; ie., it should take the same value for any turbulent flow, provided only that the Reynolds number is sufficiently large (so as to ensure an inertial subrange is present).

In homogeneous, stationary and isotropic turbulence, T_L is the Lagrangian integral time scale and is related to C_0 by (Tennekes 1979)

$$\begin{aligned} T_L &= \beta \frac{L_E}{\sigma_v} \\ &= \frac{2\sigma_v^2}{C_0 \epsilon}, \end{aligned} \tag{3.2.1}$$

where σ_v is the standard deviation of the turbulent velocity, ϵ is the mean rate of dissipation of the turbulent kinetic energy, and L_E is the Eulerian integral length scale, equal to $0.8\sigma_v^3/\epsilon$ according to Townsend (1976). Accepting Townsend's estimate for L_E , it follows from (3.2.1) that the constants β and C_0 are related by $\beta C_0 = 2.5$ in this ideal flow.

In the atmospheric boundary layer, the flow is so complicated that it is very difficult to relate the Lagrangian integral time scale to local Eulerian turbulent statistics. Historically a time scale is defined using the first line of eqn (3.2.1), but this time scale can not be identified as the *Lagrangian integral time scale*. Rather, it is a *local decorrelation time scale* (Durbin 1983; Sawford 1985). In recent work on LS simulation of inhomogeneous turbulence, T_L is used only symbolically.

In the neutral surface layer, the dissipation rate is well represented by

$$\epsilon = \frac{u_*^3}{\kappa z}, \quad (3.2.2)$$

where u_* is the friction velocity, κ (≈ 0.4) is the von Kármán constant, and z is the height above ground. It follows from (3.2.1, 3.2.2) that

$$T_L = b_2 \frac{z}{\sigma_w}, \quad (3.2.3)$$

since $\sigma_w = b_1 u_*$ ($b_1 \sim 1.3$); from (3.2.1, 3.2.2) we also have

$$T_L = \left(\frac{2b_1^3 \kappa}{C_0} \right) \frac{z}{\sigma_w}, \quad (3.2.4)$$

so b_2 in (3.2.3) is related to C_0 by

$$b_2 C_0 = 2b_1^3 \kappa. \quad (3.2.5)$$

There has been a controversy in recent years about the value of C_0 . Sawford (1985) drew attention to the issue in his review paper, summarizing the values of b_2 used in several LS models of diffusion within the neutral boundary layer. There were two "popular" values for b_2 at that time: 0.3 ($C_0 \sim 5$) and 0.5 ($C_0 \sim 3$). The former was supported by Ley (1982) and Legg (1983), while the latter was preferred by Reid (1979), Wilson et al (1981b) and Davis (1983). Three years later, Sawford and Guest (1988) reported an even bigger range for the possible values of C_0 : in wind tunnel grid turbulence $C_0 \approx 2.1$, and in a wind tunnel boundary layer flow, from which Legg (1983) obtained $C_0 \approx 5$, $C_0 = 5 \sim 10$ (disagreement between values obtained by Sawford and Guest and by Legg may relate to the Legg model not having the well-mixed property).

The present study will evaluate the value of C_0 by comparing LS simulations with experimental data gathered from grid turbulence (wind tunnel and water channel), laboratory boundary layer turbulence (Legg 1983; Raupach and Legg 1983) and

atmospheric surface layer turbulence (Project Prairie Grass). We will also identify problems with earlier studies.

3.2.2. C_0 in Grid Turbulence

In grid-generated turbulence, wherein the Reynolds number ($Re=UM/v$; U the mean velocity, M the mesh spacing, v the kinematic viscosity) is generally not very large, the dissipation range and the energy-containing range (of eddy size/wavenumber) are not widely separated. Therefore a first-order LS model may be inapplicable, unless the travel time of tracer from the source is substantially greater than the integral time scale, T_L .

Sawford (1991) designed a second-order LS model for the *ideal (but unrealisable)* case of homogeneous, isotropic and stationary turbulence. With his model, Sawford found that for Reynolds numbers typical of grid turbulence the Reynolds-number-dependence cannot be neglected. He also found that in order to render a first-order model applicable to low Reynolds-number flow, a modified Kolmogorov constant $C_0^{\text{effective}}$, which is dependent on the Reynolds number and differs from the true of Kolmogorov constant (C_0), should be employed.

Du et al. (1995) extended Sawford's model to an experimentally *realizable* but still very simple flow: grid turbulence. Comparing predictions of this model with wind and water channel measurements of dispersion (for details, see Section 3.1), Du et al. found best-fit when $C_0=2.5\sim 3.5$. A smaller value $C_0^{\text{effective}}$ can render the (actually, inapplicable) first order model prediction in better accordance with experimental data than the choice $C_0=2.5\sim 3.5$. This explains why an earlier study by Anand and Pope (1985) found predictions with a first order model, using $C_0=2.1$, fit well with several wind tunnel grid turbulence experiments.

3.2.3. C_0 from a Wind Tunnel Boundary Layer

A diffusion experiment reported by Raupach and Legg (1983) and Legg (1983) is

of particular interest, because with the support of data gathered in this experiment Legg (1983) obtained $C_0 \approx 5$ and Sawford and Guest (1988) obtained $C_0 = 5-10$, estimates differing substantially from those summarised above (and given in more detail in Section 3.1) for grid turbulence.

For our LS simulations we specified turbulence statistics drawn from Legg (1983) and Raupach and Legg (1983):

$$\begin{aligned}
 U &= \frac{u_{*mean}}{\kappa} \ln\left(\frac{z-d_0}{z_0}\right), \\
 \sigma_w &= \begin{cases} [0.68-23.0(z-0.1)^2](1-x/13.6), & \text{for } (z \leq 0.1m) \\ 0.68(1-x/13.6), & \text{for } (z > 0.1m) \end{cases} \\
 \langle uw \rangle &= \begin{cases} -0.28(1-x/8.5), & \text{for } (z \leq 0.066m) \\ -[0.28-0.475(z-0.066)](1-x/8.5), & \text{for } (z > 0.066m) \end{cases} \\
 \epsilon &= 0.9 \frac{u_*^3}{\kappa z},
 \end{aligned} \tag{3.2.6}$$

where units are MKS; von Kármán's constant $\kappa=0.37$ (in this experiment); zero-plane displacement $d_0=6 \times 10^{-3}$ m; the roughness length $z_0=1.8 \times 10^{-4}$ m; and the average friction velocity used in the mean wind profile, $u_{*mean}=0.5 \text{ ms}^{-1}$. The line source lay at a height $h=0.06$ m above the zero plane displacement.

Since below $z \sim 0.2$ m the turbulence was approximately Gaussian, it is appropriate to use the unique, well-mixed, one-dimensional¹⁵ (vertical), first-order¹⁶ LS model (Thomson 1987):

¹⁵ We compared the first-order model and a two-dimensional (x-z) version of Thomson's model for Gaussian turbulence. Differences between the two models' predictions for diffusion were quite small up to travel distance $x=2$ m (beyond which distance no diffusion measurements were made).

¹⁶ We also compared the 1D first-order model and the 1D second-order model (outlined in section 3.1.2) in an equivalent homogeneous turbulence (i.e., whole-domain-averaged turbulence statistics replaced the real statistics): no appreciable difference was observed.

$$dw = \left[-\frac{C_0 \epsilon}{2\sigma_w} w + \frac{1}{2} \left(1 + \frac{w^2}{\sigma_w^2} \right) \frac{\partial \sigma_w^2}{\partial z} \right] dt + \sqrt{C_0 \epsilon} d\zeta, \quad (3.2.7)$$

$$dz = w dt.$$

We used (3.2.7) to calculate vertical diffusion, with different values of C_0 . As shown in Figure 3.2.1, $C_0 = 3.0 \pm 0.5$ gives better prediction than does $C_0 = 5.0$, for the vertical plume width $\sigma_z(x)$ in the downstream range $x \leq 1.2$ m. $C_0 = 5.0$ gives superior prediction for $x > 1.2$ m; and $C_0 = 10.0$ does a poor job over the whole range.

Figure 3.2.2 gives predicted vertical profiles of the mean concentration, for differing C_0 . Comparing with the measured mean concentration profiles (Figure 5(a), Raupach and Legg, 1983), we see $C_0 \sim 3$ gives best fit to the measured profile, particularly for the lower part of the boundary layer. This is further supported by Figure 3.2.3, a comparison of predicted ground-level concentration with the experimental data.

It is clear that overall $C_0 \sim 3$ makes the model prediction best fit the experimental data; but one may still wonder why $C_0 \sim 3$ performs poorly (in predicting σ_z) when $x > 1.2$ m. Recall the vertical velocity in the upper part of the wind tunnel boundary layer is not Gaussian, but positively skewed: this will certainly affect vertical diffusion in that region. Positively skewed vertical velocity will push the tracer downward (Lamb 1982; and Section 2.3), so σ_z will be smaller than it would be in Gaussian turbulence (note that spread is confined by the lower boundary). Since bigger C_0 implies smaller σ_z , this perhaps explains why a bigger (effective) C_0 is spuriously deduced for far downstream distance.

Legg's model does not satisfy the (subsequently provided) model design criterion, the well-mixed constraint (Thomson 1987), which is arguably reason enough to prefer the present derivation of the value of C_0 implied by these experiments. On the other hand, the Sawford and Guest (1988) model is indeed well-mixed; but these authors overestimated the standard deviation of the vertical velocity (σ_w). Because bigger C_0 implies weaker diffusion (see Figure 3.2.1), and bearing in mind that in unbounded homogeneous turbulence the far-field spread is related to C_0 by $\sigma_z = 2 \sigma_w^2 (t/C_0 \epsilon)^{1/2}$, we reason that an

overestimate of σ_w will necessitate an overestimate of C_0 , to result in a good prediction for tracer spread.

3.2.4. C_0 in the Neutral Atmospheric Surface Layer: Project Prairie Grass (PPG)

Project Prairie Grass

Project Prairie Grass (PPG; Barad, 1958) is an extensive field diffusion experiment carried out during the summer of 1956, over a flat plain near O'Neill, Nebraska. In the experiment, 70 runs of 10-minute average concentration data were collected along five azimuthal arcs of detectors at downstream distances (from the continuous point source) of $x = 50\text{m}$, 100m , 200m , 400m and 800m . On the 100m arc only, six towers measured *vertical* profiles of the mean concentration.

A point source at height $z_s = 0.46\text{m}$ was used in all runs, and in each run sulphur dioxide was released steadily; the source strength differed from run to run. Meteorological variables to be used to determine wind and turbulence statistics and atmospheric stratification were measured simultaneously.

In this sub-section we simulate vertical dispersion in the PPG experiment for runs performed under neutral stratification. In the neutral surface layer (NSL), turbulent velocity statistics are height-invariant, so the 1-d well-mixed model for Gaussian turbulence reduces to:

$$dw = -\frac{C_0 \epsilon}{2\sigma_w} w dt + \sqrt{C_0 \epsilon} d\zeta, \quad (3.2.8)$$

$$dz = w dt.$$

where $\epsilon = u_*^3 / \kappa z$, and $\kappa = 0.4$. We carried out model simulations for six individual PPG runs. Figure 3.2.4 compares measured and simulated vertical profiles of cross-wind integrated concentration (CWIC). In calculations, perfect reflection was employed at the bottom boundary because it guarantees that (3.2.8), which is derived for unbounded flows, remains well-mixed for the present bounded turbulence (Wilson and Flesch 1993), and

there is no evidence that absorption of SO_2 by the grassy surface caused significant loss of tracer material up to 100m downstream (Barad 1958, p77). Best agreement between our LS simulations and the field measurement is achieved when $C_0 = 3.0 \pm 0.5$, which is completely consistent with the conclusion of Wilson et al. (1981).

3.2.5. Criterion to Determine C_0 in the Neutral Atmospheric Boundary Layer

In principle, C_0 should be evaluated from measurements of the difference of Lagrangian velocity over a short travel time Δt , satisfying $t_\eta \ll \Delta t \ll T_L$, where t_η is the Kolmogorov micro time scale and T_L is the time scale of the energy-containing eddies. However, carrying out such an experiment is extremely difficult, so that we have to turn to other alternatives. Inferring C_0 from diffusion measurements, as in the present study, is only one of these alternatives. A disadvantage of the present method is that the rate of diffusion is not sensitive to C_0 for travel time $t \ll T_L$ (ie, in the inertial range); only when $t \sim T_L$ or even $t > T_L$, can we see the consequence of assuming different values for C_0 .

We realize that with different methods for evaluating C_0 we may arrive at different values for C_0 , though C_0 is supposedly universal. Nevertheless, we believe for the purpose of simulating diffusion with an LS model, $C_0 = 3.0 \pm 0.5$ is the best choice for any turbulent flow.

Now we review the criterion used by Sawford (1985) and many others for selecting an optimal value of C_0 . Recall that in the neutral atmospheric surface layer the standard deviation of vertical velocity, $\sigma_w = b_1 u_*$, is height-independent, while the dissipation rate of turbulent kinetic energy $\epsilon = u_*^3 / \kappa z$ (which indicates that the atmospheric surface layer is not vertically-homogeneous). If we apply to surface layer dispersion G.I. Taylor's analytical formula (recognising however that this formula is exact only in truly stationary and homogeneous turbulence), then for large travel time (quantified by Sawford as $t \gg z_*/u_*$) or far downstream distance the standard deviation of the vertical spread of tracer about the release height is

$$\sigma_z = \sigma_w \sqrt{2T_L t} . \quad (3.2.9)$$

On the other hand, for large travel time the diffusion equation is applicable. By matching the Langevin equation and the diffusion equation, the diffusivity is then related to σ_z by (Csanady 1973)

$$K_s = \frac{1}{2} \frac{d\sigma_z^2}{dt} = \sigma_w^2 T_L . \quad (3.2.10)$$

Note that (3.2.10) is exact only in the *ideal* of homogeneous and stationary turbulence. By assuming that (3.2.10) holds in the neutral atmospheric surface layer (which is not really homogeneous since ϵ is height-dependent, and in (3.2.10) T_L is supposed to be a constant but in the neutral surface layer it is not), and by invoking the Reynolds analogy (ie., by assuming the eddy diffusivity K_s is equal to the turbulent viscosity $K_m = \kappa u_* z$, which assumption, according to Dyer and Bradley 1982, is supported by field experiments in the neutral surface layer) it follows that

$$T_L = \frac{\kappa u_* z}{\sigma_w^2} = \left(\frac{\kappa}{b_1}\right) \left(\frac{z}{\sigma_w}\right). \quad (3.2.11)$$

Thus the coefficient b_2 in eqn (3.2.3) is constrained by

$$b_1 b_2 = \kappa. \quad (3.2.12)$$

Sawford (1985), after obtaining the foregoing criterion, proposed that in the surface layer, $b_2 = \kappa/b_1 \approx 0.3$ (ie, $C_0 \approx 5$). We conclude this section by noting the inconsistencies of this derivation.

3.2.6. Conclusions

We have shown a universal value for Kolmogorov's constant C_0 applies, across decaying grid turbulence, wind tunnel boundary layer flow, and the atmospheric boundary

layer flow. The universal numerical value is $C_0=3.0\pm0.5$.

We are confident about this value for C_0 only in the context of diffusion calculations. For other applications, $C_0=3.0\pm0.5$ may not be the best choice and should be used cautiously. To completely settle the question of the universality of C_0 , other methods should be explored (eg., comparison of modelled and measured Lagrangian spectra).

Bibliography

- Anand, M.S. and S.B. Pope, 1985: Diffusion behind a line source in grid turbulence. *Turbulent Shear Flows 4*, Durst F. et al eds. Springer Verlag, 46-61.
- Barad, M.L., 1958: *Project Prairie Grass: a Field Program in Diffusion. Geophysical Research Papers No. 59 (II) TR-58-235 (II)*, Air Force Cambridge Research Centre, USA
- Csanady, G.T., 1973: *Turbulent Diffusion in the Environment*. D. Reidel Publishing Company.
- Du, S., B.L. Sawford, J.D. Wilson and D.J. Wilson, 1995: Estimation of the Kolmogorov constant (C_0) for the Lagrangian structure function, using a second-order Lagrangian model of grid turbulence. Submitted to *Physics of Fluids*.
- Lamb, R.G., 1982: Diffusion in the convective boundary layer. *Atmospheric Turbulence and Air Pollution Modelling*. F.T.M. Nieuwstadt and H. van Dop eds., D. Redidel, 159-229.
- Legg, B.J., 1983: Turbulent dispersion from an elevated line source: Markov chain simulations of concentration and flux profiles. *Quart. J. Roy. Meteorol. Soc.* **109**, 645-660.
- Ley, A.J., 1982: A random walk simulation of two-dimensional turbulent diffusion in the neutral surface layer. *Atmos. Environ.* **16**, 2799-2808.
- Pope, S.B., 1994: Lagrangian pdf methods for turbulent flows. *Annual Review of Fluid Mechanics*, Vol. **26**, 23-63.
- Raupach, M.R. and B.J. Legg, 1983: Turbulent dispersion from an elevated line source:

- measurement of wind-concentration moments and budgets. *J. Fluid Mech.* **136**, 111-137.
- Reid, J.D., 1979: Markov chain simulations of vertical dispersion in the neutral surface boundary layer. *Boundary-Layer Meteorol.* **16**, 3-22.
- Sawford, B.L., 1985: Lagrangian stochastic simulation of concentration mean and fluctuation fields. *J. Appl. Meteorol.* **24**, 1152-1166.
- Sawford, B.L., 1991: Reynolds number effects in Lagrangian stochastic models of turbulent dispersion. *Phys. Fluids A3*, 1577-1586.
- Sawford, B.L. and F.M. Guest, 1988: Uniqueness and universality of Lagrangian stochastic models of turbulent dispersion. *8th Symposium on Turbulence and Diffusion*, American Meteorol. Soc. pp96-99.
- Thomson, D.J., 1987: Criteria for the selection of stochastic models of particle trajectories in turbulent flows. *J. Fluid Mech.* **180**, 529-556
- Townsend, A.A., 1976: *The Structure of Turbulent Shear Flow*, Cambridge University Press, Cambridge.
- Wilson, J.D. and T.K. Flesch, 1993: Flow boundaries in random-flight dispersion modes: enforcing the well-mixed condition. *J. Appl. Meteorol.* **32**, 1695-1707.
- Wilson, J.D., G.W. Thurtell and G.E. Kidd, 1981a: Numerical simulation of particle trajectories in inhomogeneous turbulence, II: Systems with variable turbulent velocity scale. *Boundary-Layer Meteorol.* **21**, 423-441.
- Wilson, J.D., G.W. Thurtell and G.E. Kidd, 1981b: Numerical simulation of particle trajectories in inhomogeneous turbulence, III: Comparison of predictions with experimental data for the atmospheric surface layer. *Boundary-Layer Meteorol.* **21**, 443-463.

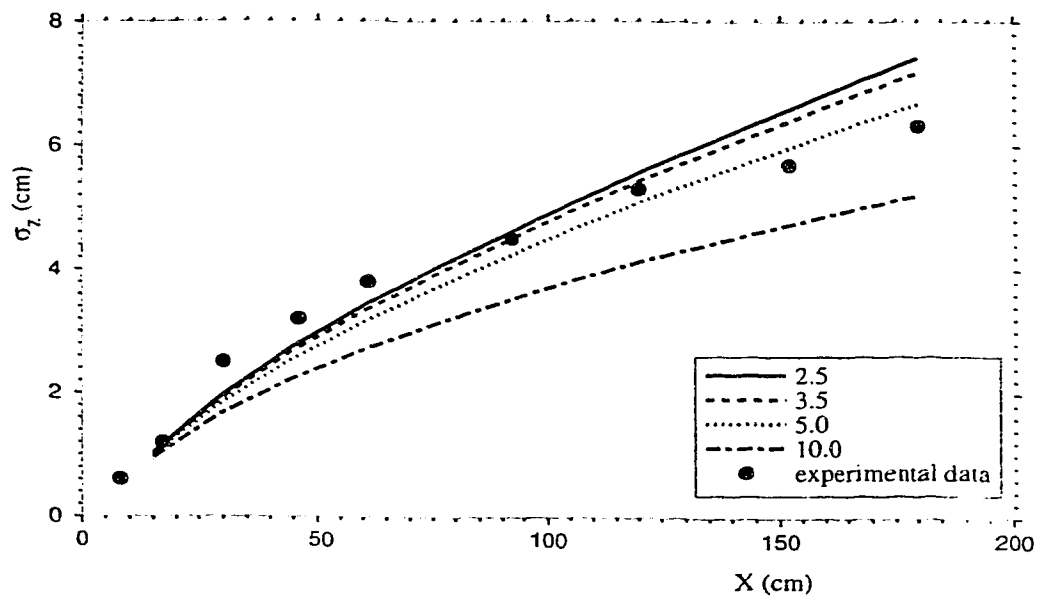


Figure 3.2.1. Measured and simulated vertical spread of tracers, σ_z , for source height $h=6$ cm in a boundary layer with downstream distance x for wind tunnel data of Raupach and Legg (1983). Curves for the Kolmogorov constant C_0 from 2.5 to 10.0.

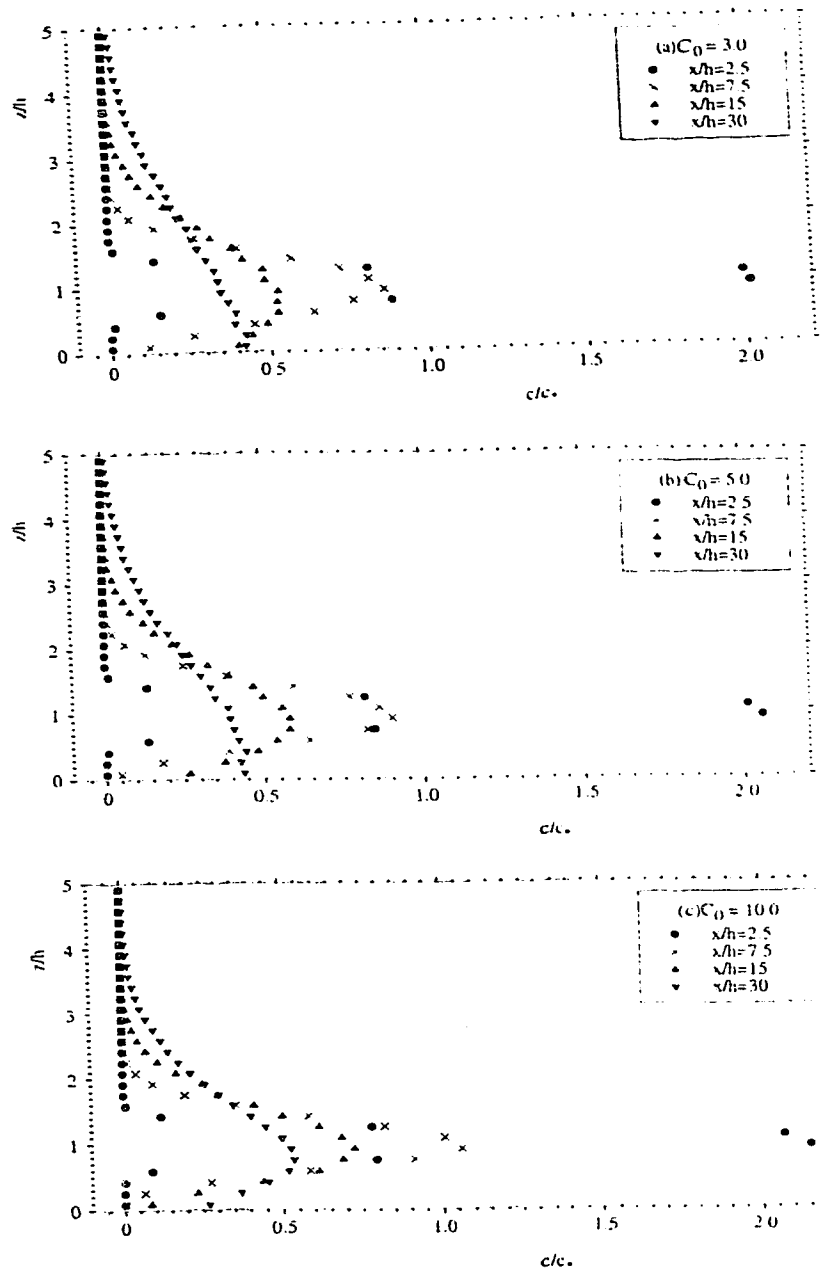


Figure 3.2.2. Simulated vertical profiles of mean concentration with different values of C_0 in a wind tunnel boundary layer flow due to a line source of height $h = 6$ cm. c_s is defined by $c_s = Q/hU(h)$, where Q is the source strength per unit length.

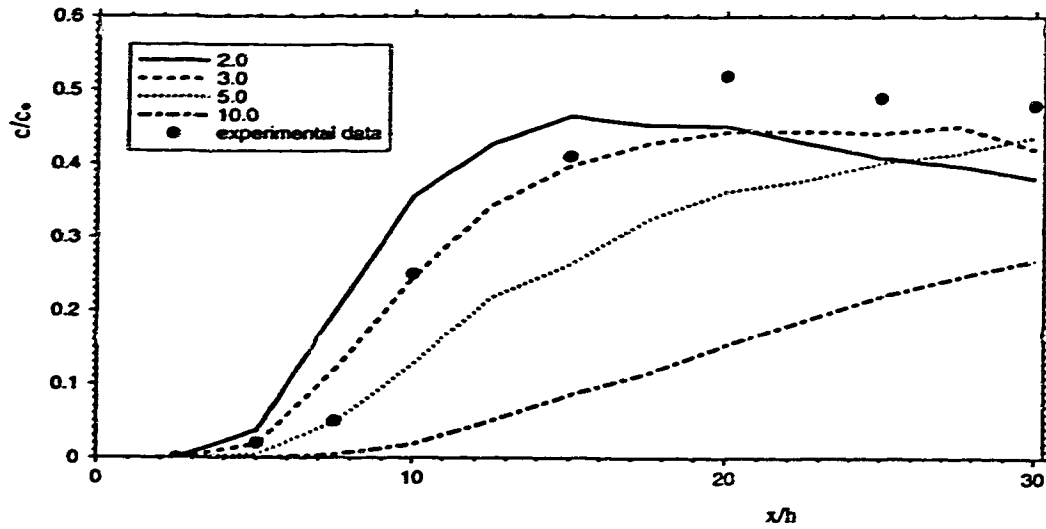


Figure 3.2.3. Measured and simulated ground-level mean concentration in the wind tunnel boundary layer flow (Raupach and Legg 1983) due to a line source of height $h = 6$ cm. c_s is defined by $c_s = Q/hU(h)$, where Q is the source strength perunit length. Curves for the Kolmogorov constant C_0 from 2.0 to 10.0.

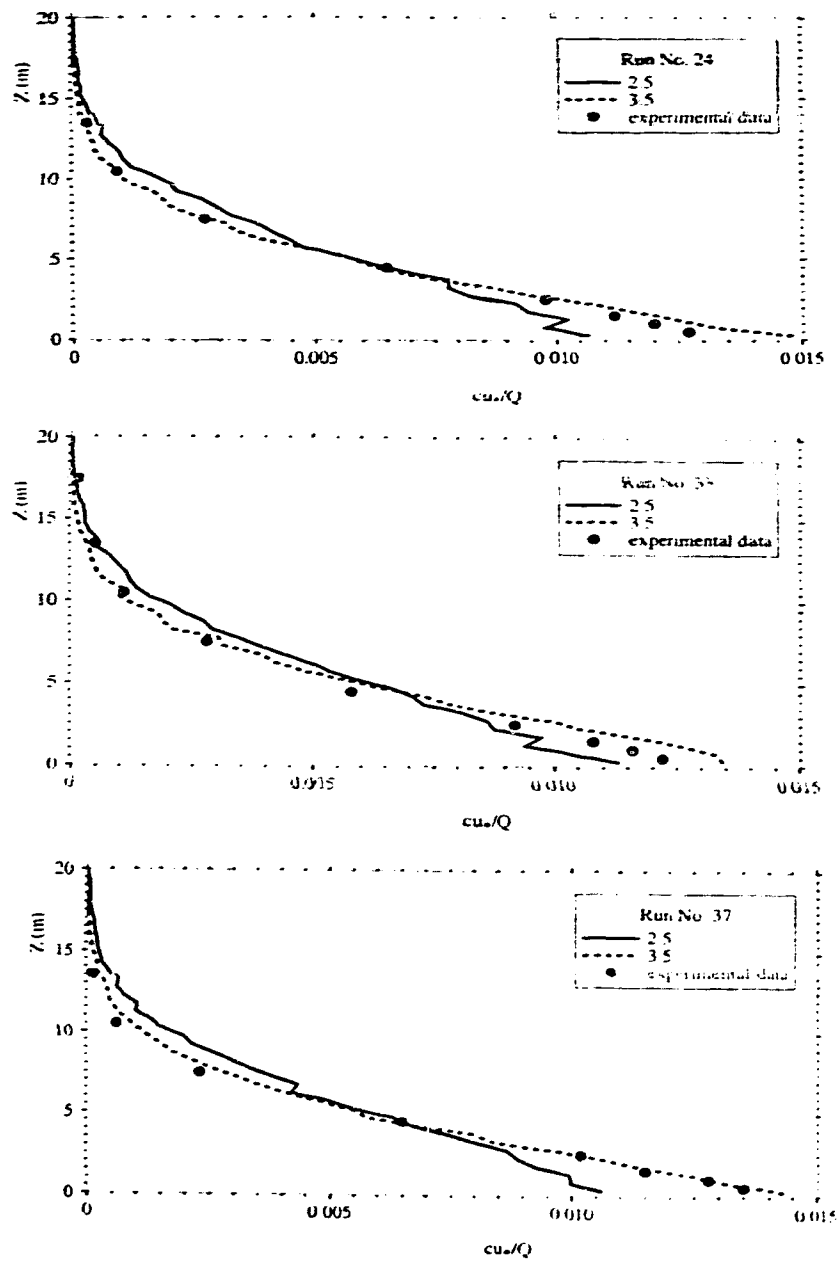


Figure 3.2.4. Measured and simulated vertical profiles of cross-wind integrated concentration for 6 neutral-stratification runs of the Project Prairie Grass. Curves for different values of the Kolmogorov constant 2.5 and 3.5, respectively.

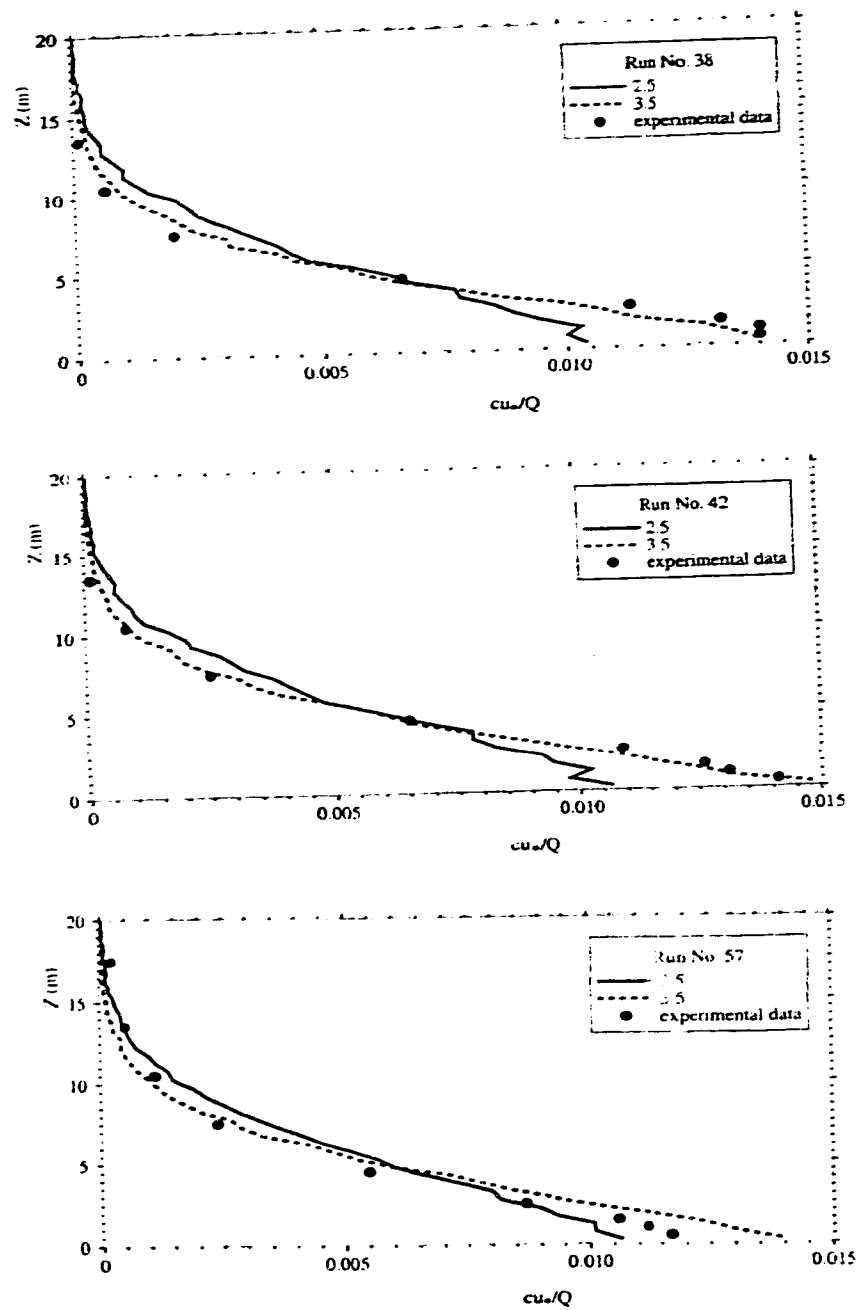


Figure 3.2.4. Continued.

Chapter 4

OTHER APPLICATIONS OF STOCHASTIC METHODS

In this chapter two other applications of the stochastic techniques are presented.

The first is a study of turbulence effects on the collision of cloud droplets. Earlier LS models used for the droplet collision problem were of zeroth-order. This is fundamentally wrong: the droplet-separation of interest is much less the turbulence integral length scale. A first-order, two-particle model is employed to study the effect of turbulence and to examine earlier models.

The other subject in this chapter is an *Eulerian* problem: the temporal evolution of concentration at a given spatial point. By assuming the evolution of concentration is a Markov process, a (model) time series of concentration can be generated, and many useful statistics of the concentration time series can be calculated. In section 2 the rate of upcrossing over certain ("threshold") concentration levels is predicted; and accords quite well with field measurements obtained in the Dugway experiment.

4.1. MODELLING THE EFFECT OF TURBULENCE ON THE COLLISION OF CLOUD DROPLETS¹⁷

4.1.1. Introduction

It has been recognized for a long time that turbulence can influence collisions of cloud droplets, possibly spurring the growth of cloud droplet size between the ranges where (initially) effects of condensation and then (finally) gravitational coalescence dominate (Rogers and Yau 1989). Over the last two decades, a number of theoretical investigations have been done on this subject, and in some of them the Lagrangian Stochastic (LS; ie., trajectory, or "Random Flight") simulation has been employed (eg. de Almeida 1976, 1979a, 1979b; Reuter et al. 1988).

Quantitatively the effect of turbulence can be expressed in the stochastic collection equation (SCE) for the evolution of the cloud droplet number density distribution function, $N(V,t)$, [units, # m⁻³]. This function is defined such that $N(V,t)dV$ is the average number density [# m⁻³] at time t , of cloud droplets of a size lying within droplet volume interval $(V, V+dV)$. The SCE is:

$$\begin{aligned} \frac{\partial}{\partial t} N(V,t) = & \frac{1}{2} \int_0^V N(V-v,t) N(v,t) K(V-v,v) dv \\ & - N(V,t) \int_0^\infty N(v,t) K(V,v) dv, \end{aligned} \quad (4.1.1)$$

where $K(V,v)$ is the collection kernel [m³ s⁻¹] which describes the rate of change of the probability that a droplet of volume V merges with a droplet of volume v , provided both are present in unit concentration. Given $K(V,v)$, which is to some extent influenced by

¹⁷ A version of this section has been accepted for publication. S. Du and J.D. Wilson, 1995, *Journal of the Atmospheric Sciences*.

turbulence, the SCE determines the evolution of an initial distribution of droplet volume $N(V, t_0)$.

A trajectory simulation is the natural way to study the movement of small particles in turbulent flows, for example in order to calculate the collection kernel. However to the author's knowledge, in LS models applied to date for cloud droplet collisions, the correlation of cloud droplet velocity between consecutive instants was not accounted for: i.e., the random *displacement* of a cloud droplet was assumed to be Markovian. This is incorrect when calculating a cloud droplet trajectory over a time period shorter than the integral time scale of the background turbulent field, because the displacement of a particle can be taken as Markovian only when the travel time of interest is much longer than the integral time scale of the droplet velocity (Sawford 1991). Another problem associated with some earlier LS simulations of cloud droplet collisions was the use of independent, single-particle trajectories (single particle models). This in principle is not acceptable, because the movements of nearby cloud droplets are highly correlated (in space).

For reasons that will be given in Section 4.1.3, in this work we study collisions between large droplets (by large we mean that the radius (r) of droplets $r \geq 50 \mu\text{m}$). For simplicity, we take the coalescence efficiency to be unity (cloud droplets merge upon collision), and hydrodynamic effects when drops are in close proximity are neglected. Although "large-large" collisions are much less frequent than "large-small" or "small-small" collisions, their contribution may be important because overtaking a single large drop ($\sim 50 \mu\text{m}$) is equivalent to collecting many (~ 100) small ($\sim 10 \mu\text{m}$) cloud droplets. On occasion, the majority of cloud droplets may be quite large as a result of flow dilution at the upper parts of the cloud (Kogan 1993).

4.1.2. Relevant scales in the cloud droplet collision problem

Before considering the class of Lagrangian stochastic model that might be appropriate in studying cloud droplet collisions, we need to establish some critical timescales of the problem. In doing so, we recognise that turbulence statistics differ in

different kinds of clouds, and even within *one* cloud there is spatial variability.

In mature cumulus clouds, typical values for the standard deviation of the vertical velocity fluctuation and the rate of dissipation of turbulent kinetic energy (TKE) are $\sigma_w = 2.0 \text{ ms}^{-1}$, $\epsilon = 0.02 \text{ m}^2 \text{ s}^{-3}$ (Weil et al. 1993). Extreme values in the literature are $\epsilon = 0.0003 \text{ m}^2 \text{ s}^{-3}$ for small cumuli (Ackerson 1967), and $\epsilon = 0.25 \text{ m}^2 \text{ s}^{-3}$ in very strong cumulus congestus (Panchev 1971). Assuming for the kinematic viscosity of cloud air $\nu = 1.2 \times 10^{-5} \text{ m}^2 \text{ s}^{-1}$, the corresponding range in the Kolmogorov time scale $t_\eta = (\nu/\epsilon)^{1/2}$, which characterises the smallest eddies in the flow, is about $10^{-2} \leq t_\eta \leq 10^{-1} \text{ s}$. The corresponding Kolmogorov length scale $\eta = (\nu^3/\epsilon)^{1/4}$ is in the range of $10^{-4} \leq \eta \leq 10^{-3} \text{ m}$.

The Kolmogorov (inner) scale describes the minimum lengths over which changes (in velocity) occur in the airflow. These are to be contrasted with the Lagrangian integral (outer) scales, which measure typical spatial and temporal persistence of the turbulent velocity. In stationary, homogeneous turbulence, the Lagrangian integral timescale can be determined from the velocity variance (σ_v^2) and the TKE dissipation rate (ϵ) as (Tennekes 1979)

$$T_L = \frac{2\sigma_v^2}{C_0\epsilon}, \quad (4.1.2)$$

where C_0 is a (supposedly) universal constant ($C_0 = 3.0$, according to Du et al. 1995). Adopting $\sigma_v \sim 1 \text{ ms}^{-1}$, then $T_L = 10 \sim 10^3 \text{ s}$ and the Lagrangian integral length scale is $L = \sigma_v T_L = 10 \sim 10^3 \text{ m}$. It is our proposition that in some regions of real clouds, there exists a wide separation in scale between dissipation range and energy-containing range of scales, i.e., $t_\eta \ll T_L$ and $\eta \ll L$. The truth of this bears on the validity of the model we later construct for droplet paths.

Now we want to establish a timescale t_c characterising the collision interval, which will limit the permissible time step Δt upon which we discretize droplet trajectories. Firstly, consider non-precipitating cumulus, wherein the liquid water content is of order 1 gm^{-3} and the mean radius of the cloud droplet is about $5 \mu\text{m}$ (Pruppacher and Klett 1978, pp 14-16). It follows from simple geometry that, assuming a uniform spatial distribution of droplets,

the mean separation (d) between neighbouring cloud droplets is about 10^{-3} m, i.e., $d \ll L$. It seems d/η could be of the order of unity in small cumuli, and about one order larger in deep convective clouds.

For the purpose of discussion, assume (temporarily) that the separation d satisfies the condition $\eta \ll d \ll L$. Using dimensional arguments, $\delta d / \delta t \sim (\epsilon d)^{1/3}$. It follows that for two cloud droplets separated by d , a collision takes place at intervals of order $t_c \sim (d^2/\epsilon)^{1/3} \sim 10^{-2} - 10^{-1}$ s. This is about the same order as the Kolmogorov time scale. If d were of the same order as η , it is very unlikely that the collision time interval t_c could be larger than the Kolmogorov time scale. Hence for the small droplets, the discretization time step Δt is necessarily small w.r.t. t_η , and droplet *acceleration* is an auto-correlated time series.

In contrast, for large cloud droplets of radius $r \geq 50 \mu\text{m}$, it is estimated that the separation between neighbouring drops is of order 10^{-2} m: so if the turbulence in the cloud is strong ($\epsilon \sim 0.1 \text{ m}^2\text{s}^{-3}$), the collision interval is about $t_c \sim 10^{-1}$ s. This is an order of magnitude larger than the Kolmogorov time scale ($\sim 10^{-2}$), yet much smaller than the Lagrangian time scale (~ 10 s), i.e., t_c is well within the inertial subrange. In this case it is appropriate to consider droplet velocity and position to (jointly) constitute a Markov process.

4.1.3. First-order two-particle LS model for the collisions between large droplets

4.1.3.1. Model order

Sawford (1991) summarized the hierarchy of LS models in a study of Reynolds number effects in LS models of turbulent dispersion. According to Sawford, the appropriate order of LS model to be used is determined by the ratios t/t_η and t/T_L , where t is the time interval of interest. We will assume the cloud can be regarded as homogeneous, isotropic and stationary: probably a satisfactory assumption, since the relative movement of initially-nearby cloud droplets is caused by the smallest scale eddies of the field, having approximately this simple statistical structure.

If $t \gg T_L$, a "zeroth-order" LS model

$$dx^i = \sqrt{2 K_s} d\zeta^i \quad (4.1.3)$$

is sufficient to study the displacement of tracer elements (random walk in position). In (4.1.3) and hereafter, $d\zeta^i$ is the increment of a Wiener process (i.e., $d\zeta$ is a Gaussian random number with zero mean and variance dt). The superscript i is the direction index; and K_s is the eddy diffusivity, $K_s = \alpha_v^2 T_L$. This very simple model is acceptable because both acceleration and velocity are uncorrelated over discretization intervals Δt satisfying $T_L \ll \Delta t$. However this model is inapplicable to our cloud droplet problem: we have argued (Section 4.1.2) that the collision interval (thus t , the duration of simulations) is $t_c \ll T_L$.

At the other extreme, if t_c/t_η is small or order 1, the only permissible choice is a "second order" model, in which the acceleration, velocity and displacement of the moving tracer particle are taken to be collectively Markovian, and the acceleration is modelled as an auto-correlated stochastic process. From Section 4.1.2, we conclude that for a general study of cloud droplet collisions, one indeed requires a second-order model. This is a difficulty, because such models are not well-developed.

However for collisions between large cloud droplets, and provided the turbulence in the cloud is strong, the required duration of a simulation of the droplet trajectory (estimated in Section 4.1.2 as " t_c ") satisfies $t/t_\eta \gg 1$, and t/T_L finite. In this case a "first-order" LS model is appropriate (Thomson 1987): we can choose a time step Δt in the range $t_\eta \ll \Delta t \ll T_L$ to resolve the evolution in velocity and position over time period t (Lagrangian acceleration correlation vanishes over timesteps $\Delta t \gg t_\eta$). The uniquely correct LS model (for a *single non-buoyant tracer particle* in homogeneous, isotropic turbulence) is (Borgas and Sawford 1994):

$$\begin{aligned} du^i &= -\frac{u^i}{T_L} dt + \sigma_v \sqrt{\frac{2}{T_L}} d\zeta^i, \\ dx^i &= u^i dt. \end{aligned} \quad (4.1.4)$$

4.1.3.2. Need for a 2-particle model

If the separation of two cloud droplets is not much larger than the integral length scale, their movements are spatially-correlated, because the movements of the fluid elements embedding them are correlated. Turbulent fluctuations at one point can be viewed as the superposition at that point of an ensemble of eddies having different scales and orientations (Townsend 1976). Relative motion (due to turbulent fluctuations in the cloud) of a pair of particles is caused by eddies of sizes smaller than, or of the same order as, the separation. Larger-scale eddies only cause a coordinated displacement of both droplets together. So we conclude, in studying collision problems, it is not appropriate to use a single particle model, in which the motion of any particle is assumed independent of all others, and the relative motion of a pair of particles is attributed to *all* eddies of various scales. An example of single-particle model is the work by Reuter et al. (1988), who chose a constant diffusivity, rather than a diffusivity which is dependent on the separation according to Richardson's law, to study relative movement between two air elements.

4.1.3.3. A heuristic model for trajectories of large droplets

We consider two large cloud droplets of radii r_1 and r_2 moving in a turbulent flow. Since the three components of the relative velocity of air elements that carry the droplets are not independent (being constrained by the incompressibility condition), a three dimensional, two-particle model must be employed. If we assume a small enough droplet Reynolds number $Re=r\delta U/\nu$ (where δU is the velocity of the droplet relative to the surrounding air, and r is r_1 or r_2), then the air-droplet drag is linear in relative velocity, and we may write a first-order model:

$$\begin{aligned}
\frac{dv_1^i}{dt} &= \frac{1}{\tau_{a1}}(u_1^i - v_1^i) - g\delta^{3i}, \\
\frac{dx_1^i}{dt} &= v_1^i, \\
\frac{dv_2^i}{dt} &= \frac{1}{\tau_{a2}}(u_2^i - v_2^i) - g\delta^{3i}, \\
\frac{dx_2^i}{dt} &= v_2^i,
\end{aligned} \tag{4.1.5}$$

where the superscript (i) is the direction index; the subscript (1 or 2) is the droplet label; v is the droplet velocity; u is the velocity of the air surrounding the droplet; x is the droplet position; g is the gravitational acceleration; and τ_a is the droplet aerodynamic response time (time constant for response to a step change in the velocity of the surrounding air). For large cloud droplets, the following empirical formula for τ_a is appropriate (Pruppacher and Klett 1978, p324; Rogers and Yau 1989, p126):

$$\tau_a = \frac{8000r}{g}, \tag{4.1.6}$$

where r is the radius of the droplet.

Kaplan and Dinar (1988) have given a *heuristic* two particle model for the evolution of the velocity of a pair of fluid elements in stationary, homogeneous, isotropic turbulence:

$$\begin{aligned}
u_1^i(t+\Delta t) &= R_L(\Delta t)u_1^i(t) + \sqrt{1-R_L^2(\Delta t)}\theta_1^i(t), \\
u_2^i(t+\Delta t) &= R_L(\Delta t)u_2^i(t) + \sqrt{1-R_L^2(\Delta t)}\theta_2^i(t), \\
u_1^i(0) &= \theta_1^i(0), \\
u_2^i(0) &= \theta_2^i(0),
\end{aligned} \tag{4.1.7}$$

where $R_L(\Delta t) = \exp(-\Delta t/T_L)$ is the Lagrangian temporal correlation coefficient, and θ is a random field that is spatially correlated, but temporally uncorrelated from t to $t+\Delta t$. By assuming the spatial correlation between the components of $\theta(t)$ is equal to the spatial Eulerian velocity correlation of the turbulent field, and using the conditions of continuity and isotropy, Kaplan and Dinar developed an algorithm to calculate the random field $\theta(t)$. The θ field is strongly dependent upon the separation of the two moving particles: only when the separation is much larger than the Eulerian length scale do θ_1 and θ_2 become uncorrelated. For a detailed description of the construction of the θ -field, please refer to the original paper.

We used the Kaplan-Dinar model to calculate the driving fluid element velocity (i.e., velocity of the fluid element surrounding the cloud droplet). Since the driving fluid velocity time series is not a Lagrangian series (i.e., at different instants the droplet is surrounded by different air elements), we reduced the Lagrangian time scale T_L in the manner suggested by Sawford and Guest (1991)

$$T_{L_g}^{1,2} = T_L \left[1 + \left(\frac{2\beta v^t}{\sigma_v} \right)^2 \right]^{-\frac{1}{2}},$$

$$T_{L_g}^3 = T_L \left[1 + \left(\frac{\beta v^t}{\sigma_v} \right)^2 \right]^{-\frac{1}{2}}. \quad (4.1.8)$$

This accounts (heuristically) for the "crossing trajectory" effect (Csanady 1963), i.e., the fact that the cloud droplet is not accompanied and driven by the same air parcel at different times. In (4.1.8), v^t is the terminal velocity of the cloud drop in still air, related to τ_a by $v^t = \tau_a g$. β relates Lagrangian and Eulerian length scales (defined as $\beta = \sigma_v T_L / L_f$, L_f is the Eulerian integral length scale in the vertical direction), and following Sawford and Guest we set $\beta = 1.5$. Equation (4.1.8) is simply an interpolation between the integral time scales for a passive tracer, and for a particle of very large terminal velocity relative to the ambient fluid. For a passive tracer, $v^t = 0$, and the time scale reduces to T_L ; for particles of large velocity relative to the surrounding air, the time scale becomes L_f/v^t (L_f is Eulerian length

scale of the turbulence). L_E takes values L_f for the direction parallel to the external force and $L_f/2$ for the direction perpendicular to the external force.

4.1.4. The collision probability and the collection kernel

The movement of a cloud droplet can be divided into two parts: movement *with* the ambient air and, movement *relative to* the ambient air (Saffman and Turner 1956). For a very small cloud droplet, the former dominates, i.e., the turbulent motion of the air controls the movement of the droplet; while for a very large droplet, movement is mainly of the latter type, because in this case the turbulent fluctuation of the cloud air hardly affects the droplet's movement.

When only movement relative to the ambient air is present, the collection kernel in the SCE has the following simple form (Rogers and Yau 1989, p130):

$$K(V,v) = \pi(R+r)^2 |u(R) - u(r)| E(R,r), \quad (4.1.9)$$

where $E(R,r)$ is the collection efficiency, the product of collision efficiency and coalescence efficiency, the droplet radii R and r are trivially related to V and v by $V = (4/3)\pi R^3$ and $v = (4/3)\pi r^3$. We here set $E=1$, which assumes that as two cloud droplets approach, one droplet's trajectory is not affected by the presence of the other droplet, and that those two droplets coalesce upon collision.

When movement *with* the ambient air is involved (smaller droplets), the collection kernel becomes far more complicated. For this case, whether or not two cloud droplets can collide depends on the turbulent field in the cloud, in addition to their (initial) relative positions. From the model outlined in the last sub-section, we can calculate the trajectories of a pair of cloud droplets for any given initial separation. When the separation (between the centres of the two droplets) is equal to or less than the summation of the two drops' radii, they collide, otherwise they do not.

$K(V,v)$ is related to the probability $p(R,r,x_1,x_2,T)$ that a pair of droplets of radii r and R , having arbitrary initial separation $(x_1 - x_2)$, will collide within time interval T .

According to Reuter et al. (1988),

$$K(V,v) = \frac{2\pi}{T} \int_{\Sigma} p(R,r,\mathbf{x}_1,\mathbf{x}_2,T) D_H dD_H dD_Z. \quad (4.1.10)$$

Here D_H is the initial horizontal distance between the centres of the two droplets (the projection of $|\mathbf{x}_1 - \mathbf{x}_2|$ onto the horizontal plane); dD_H and dD_Z are the horizontal and vertical length increments, respectively; and Σ is the initial-separation-domain over which $p(R,r,\mathbf{x}_1,\mathbf{x}_2,T)$ is non-zero. Note that the property of symmetry about the vertical axis has been used.

To calculate $p(R,r,\mathbf{x}_1,\mathbf{x}_2,T)$ numerically, we calculated an ensemble (N members) of trails, in each of which we released a pair of cloud droplets (droplet 1 has radius R and is located at \mathbf{x}_1 at $t=0$; droplet 2 is of radius r and is located at \mathbf{x}_2 at $t=0$), and followed their trajectories to examine whether or not they would collide within time $t \leq T$ (with time increment $\Delta t = 0.01T$). If the two droplets collide n times in N realizations, then

$$\lim_{N \rightarrow \infty} p(R,r,\mathbf{x}_1,\mathbf{x}_2,T) = \frac{n}{N}$$

We used our thus-determined collision probability to estimate the function

$$K_r(V,v,D_H) = \frac{2\pi}{T} \int_{-\infty}^{\infty} p(R,r,\mathbf{x}_1,\mathbf{x}_2,T) D_H dD_Z \quad (4.1.11)$$

in terms of which $K(V,v)$ follows by integration w.r.t. D_H .

4.1.5. Results

In addition to the first-order two-particle model defined above (and hereafter referred to as model 1), we examined two simplifications of it: a zeroth-order two-particle model (referred to as model 2; temporal correlation along the driving air parcel trajectory is ignored); and a zeroth-order single-particle model (referred to as model 3; spatial

correlation across the two driving parcels is also ignored). These latter trajectory models are fully defined in the appendix. For each initial separation 5,000 pairs of droplets were released. The total flight time for each pair of droplets was 0.1 s.

4.1.5.1 Large droplets, strongly turbulent cloud ($\sigma_v=2\text{ms}^{-1}$, $\epsilon=0.1\text{m}^2\text{s}^{-3}$)

First we considered droplets of distinct radii $50\mu\text{m}$ and $100\mu\text{m}$. Our results (Figure 4.1.1) for the collection kernel from model 1 and model 2 are probably not significantly different, and as shown in Table 4.1.1, the enhancement of K (over purely gravitationally-driven coalescence) due to turbulence was quite small (order 20%). The predictions from model 3 were markedly different. Relative to model 1 (which is certainly more rigorous than models 2,3), model 3 underestimates collision probability when the droplet separation is small, but overestimates when the droplets are far apart. Explanation is easy: recall that model 3 assumes that the two cloud droplets move independently, and their relative velocity is simply the difference of two independent velocities. Thus when two droplets are initially close to each other, if they do not promptly collide, they fly apart rapidly (with the erroneously overestimated relative velocity): the collision probability for later time becomes very small and as a result, the calculated collision probability for two close droplets is reduced. On the other hand, if the initial separation is large (but still much smaller than the integral length scale), the falsely exaggerated relative velocity gives the droplets more opportunity to collide; and thus model 3 overestimates the collision probability for far separated droplets. In their comment on the paper by Reuter et al. (1988), Cooper and Baumgardner (1989) argued that model 3 overestimated the turbulence effect. Our calculations confirm this, but model 3 does not overestimate the collision probability everywhere: for small horizontal separation model 3 *underestimates* the collision probability.

As we noted, in this example, turbulence has minor influence on the frequency of collisions between cloud droplets: the relative velocity due to turbulence is much smaller than that which would be caused by gravity alone. But in the case of the collision of two

droplets of equal size, the collection kernel due to gravitational collision is zero: so turbulence accounts entirely for collisions (*absolute* movement of each cloud droplet is still strongly affected by gravity). The result of a simulation for the case of large droplets of equal size $r=50\mu\text{m}$, is given in Figure 4.1.2. Model 2 generated a $K_p(R,r,D_H)$ that is smaller than that from model 1, in the range $0.015\text{ cm} \leq D_H \leq 0.10\text{ cm}$. For the full collection kernel K , model 1 yielded $K = 0.94 \times 10^{-9}\text{ m}^3\text{s}^{-1}$; whereas model 2 gave $K = 0.77 \times 10^{-9}$; model 2 underestimates the collection kernel by about 20%.

4.1.5.2. Large droplets, weakly turbulent cloud ($\sigma_v=0.5\text{ ms}^{-1}$, $\epsilon=0.01\text{ m}^2\text{s}^{-3}$)

It is less defensible to apply the present first-order LS model (model 1) in weak turbulence, so the following result will bear re-examination when better models are developed. As shown in Figure 4.1.3 and Table 4.1.2, whether for droplets of different radii ($50\mu\text{m}$ and $100\mu\text{m}$) or of equal radii ($50\mu\text{m}$), model 1 and model 2 gave (within numerical error) equal results for the collection kernel.

4.1.5.3 Small droplets, strongly turbulent cloud ($\sigma_v=2\text{ ms}^{-1}$, $\epsilon=0.1\text{ m}^2\text{s}^{-3}$)

In the case of small droplets ($5\mu\text{m}$, $10\mu\text{m}$), at small (large) horizontal separation, model 2 underestimated (overestimated) the collection kernel. Overall, model 2 substantially overestimated the impact of the turbulence: the collection kernels and enhancement factors (over gravity-driven collection) were,

$$\text{model 1} \quad K=9.2 \times 10^{-11}\text{ m}^3\text{s}^{-1}, \quad \text{e.f.} = 3.3$$

$$\text{model 2:} \quad K=1.4 \times 10^{-10}\text{ m}^3\text{s}^{-1}, \quad \text{e.f.} = 4.8$$

Although model 1 is invalid when separations d between droplets are very small (so that $d \gg \eta$ does not hold), our comparison nevertheless suggests model 2 gives a bad prediction of the collection kernel for small droplets.

4.1.6. Conclusion

By considering the scales of motion in a cumulus cloud, in comparison to typical cloud droplet separations, we have suggested that to study the evolution of a full droplet spectrum, one will require a second-order, multi-particle trajectory model. Rigorous models of that type are not yet available, and needed turbulence statistics (at the level of fluid element acceleration) are unknown, - one must parameterize the spectral region between the dissipation and inertial subranges.

However for large droplets in a very turbulent cloud, a first-order model will suffice. Using such a model, we have shown the need to account for both the temporal and spatial velocity correlations existing in the cloud, over time and space scales relevant to droplet collisions.

APPENDIX 4.1. Three droplet trajectory models

Equations (4.1.5) of Section (4.1.3) were used to calculate the trajectories of droplets 1,2 in all three models, but the means to calculate U , the velocity of the air element surrounding the droplet, differs across the three models we have studied.

Model 1 is the *first-order two-particle* model of Section (4.1.3.3). When the temporal correlation of the driving fluid element velocity between consecutive instants is neglected, model 1 reduces to:

Model 2: *zeroth-order two-particle* model. Spatial correlation between the two driving-parcel's velocities is taken into account, but the temporal correlation of each air parcel's velocity is not. The trajectory equations for the air parcels containing droplets 1,2 are:

$$\begin{aligned} u_1^i(t) &= \theta_1^i(t), \\ u_2^i(t) &= \theta_2^i(t), \end{aligned} \tag{A4.1.1}$$

where θ_1 and θ_2 are two spatially correlated random numbers, given by the Kaplan-Dinar method. When spatial velocity correlation between the two moving air parcels is neglected, model 2 reduces to:

Model 3: *zeroth-order single-particle* model. Neither spatial correlation between the two parcel's velocities nor temporal correlation of each air parcel's velocity, are accounted. The trajectory equations are:

$$\begin{aligned} u_1^i(t) &= \zeta_1^i(t), \\ u_2^i(t) &= \zeta_2^i(t), \end{aligned} \tag{A4.1.2}$$

where ζ_1 and ζ_2 are independent random numbers, each with a zero mean and variance σ_v^2 .

Bibliography

- Ackerman, B., 1967: The nature of the meteorological fluctuations in clouds. *J. Appl. Meteor.* **6**, 61-71.
- Borgas, M.S. and B.L. Sawford, 1994: A family of stochastic models for two-particle dispersion in isotropic, homogeneous and stationary turbulence. *J. Fluid Mech.* **279**, 69-99.
- Cooper, W.A. and D. Baumgardner, 1989: Comments on "The collection kernel for two falling cloud drops subjected to random perturbations in a turbulent air flow: a stochastic model." *J. Atmos. Sci.* **46**, 1165-1167.
- Csanady, G.T., 1963: Turbulent diffusion of heavy particles in the atmosphere. *J. Atmos. Sci.* **20**, 201-208.
- de Almeida, F.C., 1976: The collisional problem of cloud droplets moving in a turbulent environment. Part 1: A method of solution. *J. Atmos. Sci.* **33**, 1571-1578.
- de Almeida, F.C., 1979a: The collisional problem of cloud droplets moving in a turbulent environment. Part 2: Turbulent collision efficiencies. *J. Atmos. Sci.* **36**, 1564-1576.
- de Almeida, F.C., 1979b: The effect of small-scale turbulent motions on the growth of a cloud droplet spectrum. *J. Atmos. Sci.* **36**, 1557-1563.
- Du, S., B.L. Sawford, J.D. Wilson and D.J. Wilson, 1995: Estimation of the Kolmogorov constant (C_0) for the Lagrangian structure function, using a second-order Lagrangian model of grid turbulence. Submitted to *Physics of Fluids*.
- Kaplan, H. and N. Dinar, 1988: A three-dimensional stochastic model for concentration fluctuation statistics in isotropic homogeneous turbulence. *J. Comput. Phys.* **79**, 317-335.
- Kogan, Y.L., 1993: Drop size separation in numerically simulated convective clouds and its effect on warm rain formation. *J. Atmos. Sci.* **50**, 1238-1253.
- Panchev, S., 1971: *Random Functions and Turbulence*. Pergamon, 444 pp.
- Pruppacher, H.R. and J.D. Klett, 1978: *Microphysics of Clouds and Precipitation*, D. Reidel, 714pp.

- Rogers, R.R. and M.K. Yau, 1989: *A Short Course in Cloud Physics*, 3rd edition, Pergamon Press, 293pp.
- Reuter, G.W., R. de Villiers and Y. Yavin, 1988: The collection kernel for two falling cloud drops subjected to random perturbations in a turbulent air flow: A stochastic model. *J. Atmos. Sci.* **45**, 765-773.
- Saffman, P.G. and J.S. Turner, 1956: On the collision of drops in turbulent clouds. *J. Fluid Mech.* **1**, 16-30.
- Sawford, B.L., 1991: Reynolds number effects in Lagrangian stochastic models of turbulent dispersion. *Phys. Fluids A* **3**, 1577-1586.
- Sawford, B.L. and F.M. Guest, 1991: Lagrangian statistical simulation of the turbulent motion of heavy particles. *Bound. Layer Meteor.* **54**, 147-166.
- Tennekes, H., 1979: The exponential Lagrangian correlation function and turbulent diffusion in the inertial subrange. *Atmos. Environ.* **13**, 1565-1567.
- Thomson, D.J., 1987: Criteria for the selection of stochastic models of particle trajectories in turbulent flows. *J. Fluid Mech.* **180**, 529-556.
- Townsend, A.A., 1976: *The Structure of Turbulent Shear Flow*, 2nd ed., Cambridge University Press, 429 pp.
- Weil, J.C., R.P. Lawson and A.R. Rodi, 1993: Relative dispersion of ice crystals in seeded cumuli, *J. Appl. Meteorol.* **32**, 1055-1073.

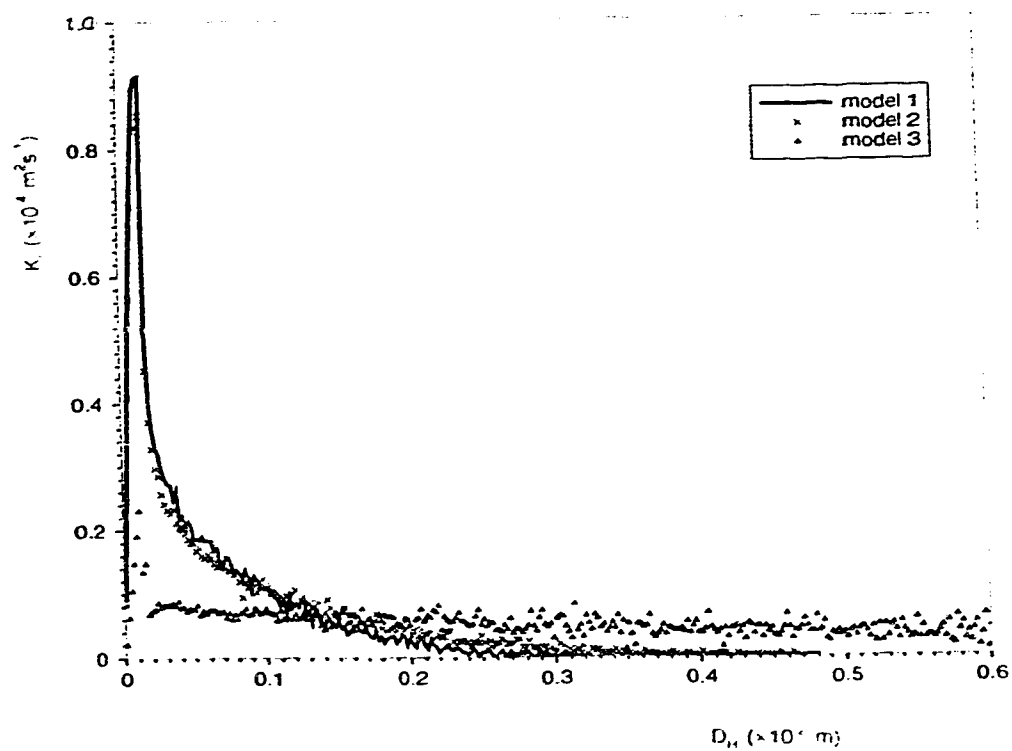


Figure 4.1.1. Distribution of the collection kernel according to models 1, 2, 3 for droplets of radii 50 μm , 100 μm in strong turbulence ($\sigma_v=2.0 ms^{-1}$; $\epsilon=0.1 m^2s^{-3}$).

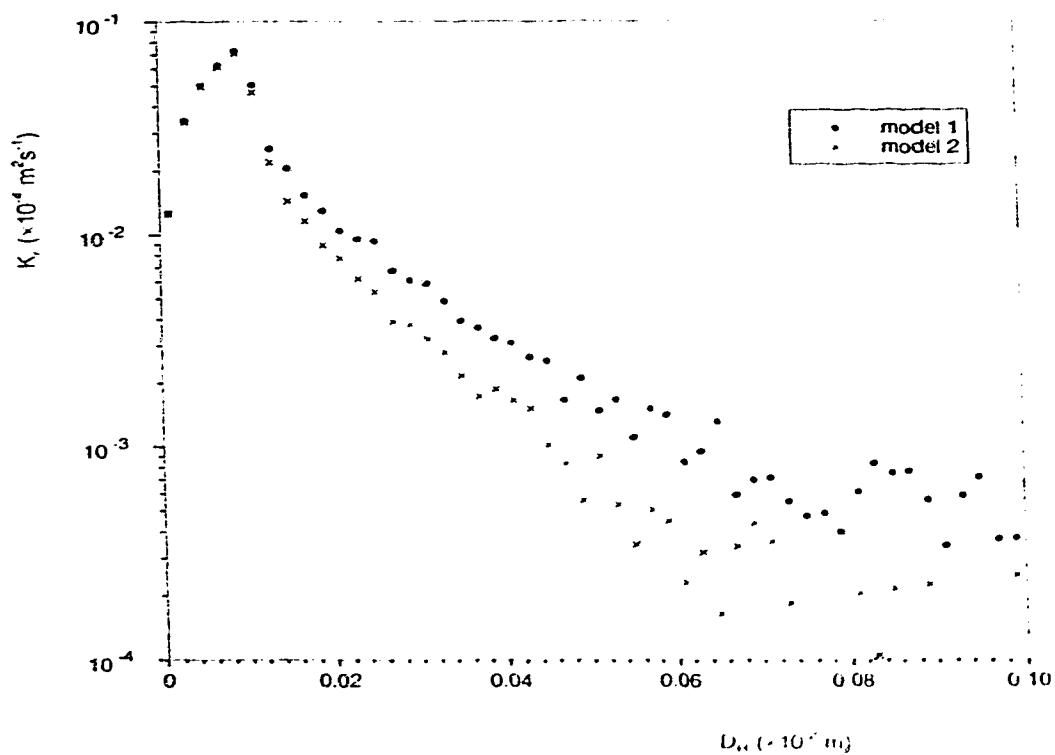


Figure 4.1.2. Distribution of the collection kernel according to models 1, 2 for droplets of equal radii ($50 \mu\text{m}$) in strong turbulence.

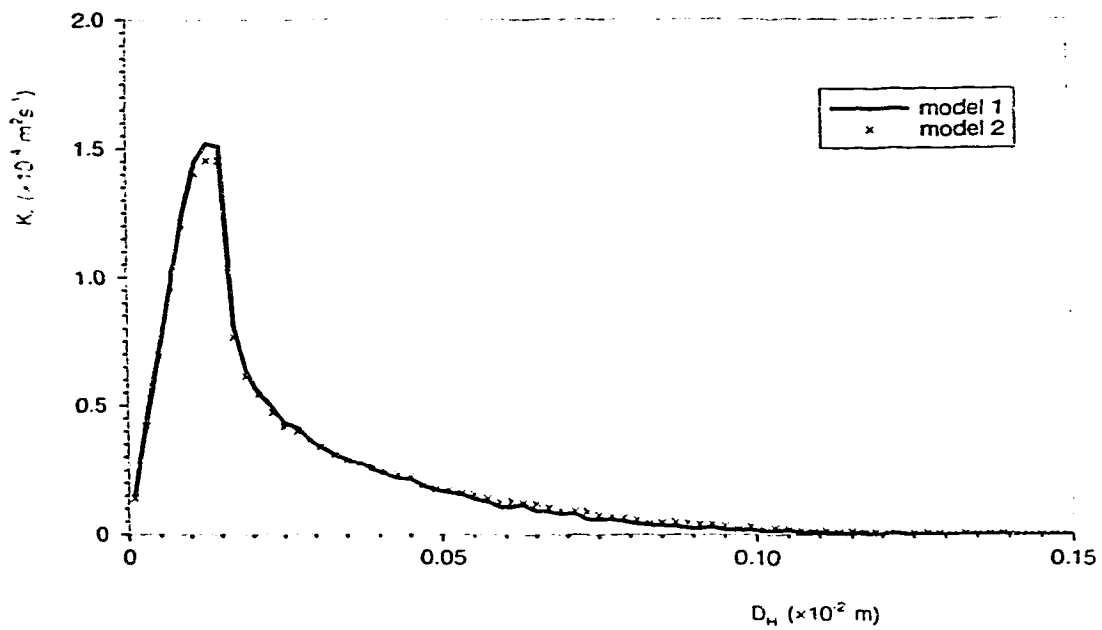


Figure 4.1.3. Distribution of the collection kernel according to models 1, 2 for droplets of radii 50 μm , 100 μm in weak turbulence ($\sigma_v=0.5 \text{ ms}^{-1}$; $\epsilon=0.01 \text{ m}^2\text{s}^{-3}$).

Table 4.1.1. Collection kernels from models 1, 2, 3 for droplets of radii 50 μm and 100 μm in strong turbulence ($\sigma_v=2.0 \text{ ms}^{-1}$; $\epsilon=0.1 \text{ m}^2\text{s}^{-3}$). The pure gravitational collection kernel for this case is 0.02827. The unit is $10^{-6} \text{ m}^3\text{s}^{-1}$.

model	model 1	model 2	model 3
collection kernel	0.03332	0.03464	0.05852
enhancement factor [†]	1.178	1.225	2.070

[†] Defined as the ratio of collection kernel to the pure gravitational collection kernel.

Table 4.1.2. Collection kernels from models 1, 2 for weak turbulence driving large droplets of (a) different radii (50 μm , 100 μm); and (b) equal radii (50 μm). The unit is $10^{-6} \text{ m}^3\text{s}^{-1}$.

model	model 1	model 2
a. Collection kernel (different size)	0.03236	0.03237
a. Enhancement factor (different size)	1.1447	1.1450
b. Collection kernel (identical size)	0.000465	0.000455

4.2. A STOCHASTIC MODEL OF CONCENTRATION FLUCTUATIONS IN PLUMES

4.2.1. Introduction

In the analysis of some important atmospheric diffusion processes, a knowledge of the (time or space) average concentration is insufficient. For example, to assess the impact of toxic and/or flammable materials released into the atmosphere, one may require to know recurrence statistics, specifying the frequency of exceedence of a specified threshold value c_t (of concentration),- the "upcrossing rate," $N^+(c_t)$. Once the upcrossing rate is known, other quantities of interest, such as peak concentration, mean duration of exceedances, first crossing probability, and mean waiting time for the first upcrossing, can be obtained; see Yee et al (1993b); Wilson (1995).

Kristensen et al. (1989) and Yee et al. (1993b) have modelled concentration upcrossing rate N^+ , on the basis of Rice's (1945) theory, that relates upcrossing rate to the joint probability density function (pdf) of concentration (c) and its time derivative (c'):

$$N^+(c_t) = \int_0^\infty c' p(c', c_t) dc' = p_c(c_t) \int_0^\infty c' p_{2|1}(c' | c_t) dc' \quad (4.2.1)$$

To apply Rice's theory, one has to know the form of the joint pdf $p(c', c)$, or of the conditional pdf $p_{2|1}(c' | c_t)$ of concentration derivative (c' , given c_t). We have scant knowledge of these pdf's, in general. Even if we have prior knowledge of the functional form of the joint pdf, the standard deviation of concentration derivative, conditioned on a specified threshold level, is difficult to measure because of its sensitivity to the data processing procedure used to produce smooth fits to data points from which the derivative is calculated.

The objective of this study is to develop a direct numerical method for predicting the upcrossing rate, using what we will consider the minimum amount of given statistical information. What we consider "given" is the "single" probability density $p_c(c)$ function for

concentration (by "single" we intend to stress that this pdf is not the joint pdf $p(c', c_t)$ we mentioned earlier), and a timescale characterising the rate of evolution of concentration.

The simplest characteristic timescale is the Eulerian (fixed point) integral timescale of the (entire) concentration fluctuation time series: assuming a stationary, continuous, non-intermittent time series, $c(t)$, we can define the correlation coefficient as

$$R_c(\tau) = \frac{\langle c(t+\tau)c(t) \rangle}{\sigma_c^2}, \quad (4.2.2)$$

where $\langle \rangle$ denotes an ensemble average, and σ_c is the standard deviation of $c(t)$. The integral time scale, T_c , is related to $R_c(\tau)$ by

$$T_c = \int_0^\infty R_c(\tau) d\tau. \quad (4.2.3)$$

If we consider only the "in plume" time series of concentration, ie. if we discard concentration "zeroes," the resulting time series is not continuous. The time scale is then physically less meaningful, a point we will discuss later.

Assuming as *given* parameters the integral time scale and the single pdf of concentration, our approach is to develop a stochastic model for the time evolution of concentration, with which we can mimic the random time series of concentration at a fixed location, - in a way that is guaranteed to reproduce those salient properties. From such a simulated concentration time series, the upcrossing rate $N^+(c_t)$ can be calculated directly, for any or many threshold level(s), c_t . The Dugway experimental data (Yee et al. 1993a, 1993b, 1994) will be used to test the numerical model.

4.2.2. A stochastic model of the concentration time series

We assume that the *in-plume* concentration evolution at a given spatial point can be represented as a first-order Markov process, ie. by the stochastic differential equation (SDE)

$$dc = a(c,t)dt + b(c,t)d\zeta, \quad (4.2.4)$$

where $a(c,t)$ is the conditional mean time derivative of concentration, conditioned on concentration, c ; and $b d\zeta$ is a random forcing, in which $d\zeta$ is a Gaussian random number, with zero mean and variance dt . Physically, the first term represents the contribution to the change of concentration from factors that are correlated with the present state, while the second term is the contribution from random factors un-correlated with present state.

The SDE (4.2.4) can be shown to imply a deterministic equation for the evolution of the probability density function p_c , where $p_c dc$ is the probability that a random sample of the concentration lies in the range $c \pm \frac{1}{2}dc$. The deterministic equation is (Risken 1984; or Gardiner 1985):

$$\frac{\partial p_c}{\partial t} = -\frac{\partial}{\partial c}(ap_c) + \frac{1}{2} \frac{\partial^2}{\partial c^2}(b^2 p_c), \quad (4.2.5)$$

In the case of a steady source emitting into a stationary turbulent flow, the time derivative of p_c is identically zero; and (4.2.5) reduces to:

$$\frac{\partial}{\partial c}(b^2 p_c) = 2ap_c. \quad (4.2.6)$$

This equation yields a useful constraint on the coefficients $a(c,t)$ and $b(c,t)$ of the SDE (4.2.4). Assuming the simplest linear form

$$a(c,t) = -\frac{c}{T} \quad (4.2.7)$$

we have from (4.2.6) that

$$b^2 = \frac{2}{T p_c} \int_c^\infty c p_c(c) dc. \quad (4.2.8)$$

To progress, we need $p_c(c)$.

The shape of the (in plume) concentration pdf depends on the distance from the source (Yee et al. 1993a; Zelt 1992). Far downwind from the source, both studies found the pdf to be approximately log-normal; eg. for the Dugway experiment p_c at the point $(x/h, y/\sigma_y)=(20,0)$ is well represented (Yee et al. 1993a) by the log-normal distribution¹⁸

$$p_c(c) = \frac{1}{\sqrt{2\pi}\sigma_c} \exp\left[-\frac{\ln^2(c/m)}{2\sigma^2}\right], \quad (4.2.9)$$

where m and σ are related to the conditional mean concentration C_p and fluctuation intensity i_p by

$$m = \frac{C_p}{\sqrt{i_p^2 + 1}}, \quad (4.2.10)$$

$$\sigma^2 = \ln(i_p^2 + 1). \quad (4.2.11)$$

Substituting (4.2.9) into (4.2.8), we obtain an explicit specification for our second coefficient of the stochastic model, in terms of a set of "knowns,"

$$b^2 = \frac{m e^{\sigma^2/2}}{T p_c} \{1 - \operatorname{erf}\left[\frac{\ln(c/m) - \sigma^2}{\sqrt{2}\sigma}\right]\}. \quad (4.2.12)$$

We now turn to the time scale T in (4.2.7). In an ideal continuous, non-intermittent time series, T is identically T_c defined by eqn (4.2.2,4.2.3). This can be shown by solving (4.2.4) for $c(t+\tau)$ with the above specified $a(c,t)$ and $b(c,t)$, multiplying the solution by $c(t)$ and averaging the product to get the autocorrelation coefficient $R_c(\tau)$; since we obtain $R_c(\tau) = \exp(-\tau/T)$, it is obvious that T is the integral time scale of concentration fluctuations.

¹⁸ Later experiments with sensors that captured fluctuations over wider frequency and amplitude range (Yee et al. 1994) found a gamma function pdf gave best fit. We will consider both log-normal and gamma functions, and show the log-normal is most suitable.

Of course, (4.2.7) is but an assumption, the most important made in this study. Since $a(c,t)$ is the time derivative of concentration *conditioned on* the instantaneous concentration, adopting (4.2.7) implies the form of the conditional pdf $p_{21}(c'|c)$,— although we do not know what this pdf is. The good agreement we will demonstrate, between the predicted and measured upcrossing rate, suggests our assumption (4.2.7) is acceptable, at least from the viewpoint of predicting the upcrossing rate.

To determine whether the linear ("Langevin") assumption for $a(c,t)$ (eqn 4.2.7) is too strong, we have also examined a generalization of (4.2.7), a non-linear specification of the conditional mean concentration derivative $a(c,i)$,

$$a(c,t) = -\frac{c}{T_c} \left(\frac{c}{C_p}\right)^{-\alpha}, \quad (4.2.13)$$

where T_c is the integral time scale for concentration fluctuations¹⁹. The corresponding specification of the second model coefficient is, from (4.2.8),

$$b^2 = \frac{m}{T_c p_c} \left(\frac{C_p}{m}\right)^\alpha e^{\frac{\sigma^2}{2}(1-\alpha)^2} \left\{1 - \operatorname{erf}\left[\frac{\ln(c/m) - \sigma^2(1-\alpha)}{\sqrt{2}\sigma}\right]\right\}. \quad (4.2.14)$$

4.2.3. Application of the present model to an intermittent concentration time series

Dispersing plumes are usually intermittent, i.e., at a fixed sampling point, some readings of concentration will be zero (see Figure 4.2.1(a)). A common practice used in the air pollution community is to remove the zero readings from the series, and to form the conditional time series, as shown in Figure 4.2.1(b). However, in so doing the essentially uncorrelated segments (e.g. A, B, C, etc) become artificially correlated, so that in the conditional time series the high-frequency component originally contained in the total time

¹⁹ We can not prove rigorously that T_c is the Eulerian integral timescale for this particular non-linear model, but it will be approximately so provided $\alpha < O(1)$.

series will be “contaminated” by the artificially introduced high-frequency “kinks”. It is necessary to assume errors will be introduced to power spectra, time scales, and other properties calculated from the conditional time series.

It is our proposition that in predicting the upcrossing rate, the model developed in the last section can be used to approximate the conditional time series obtained by reduction (zeroes-elimination) of an intermittent series. However, since the conditional time series contains some artificial high frequency component, caused by removing of zeros from the total time series, the integral time scale calculated from the conditional time series may not give the best prediction.

4.2.4. Comparison of stochastic model with the Dugway data

Firstly, we investigate the (in-plume) concentration pdf given by the model. When b is specified by eqn (4.2.12), ie. under the *a-priori* assumption of a log-normal pdf, we require to set a minimum permissible concentration (c_{min}) in order to prevent unrealistic evolution of concentration: otherwise the *numerical* model can produce an extremely high concentration when the concentration at previous time step is extremely low. Our criterion for choosing c_{min} is simply that we should reproduce the desired pdf $p_c(c)$.

We simulated the concentration evolution of the Dugway experiment data obtained at point $x/h, y/\sigma_y = (20.0, 0.0)$, at which point $i_p = 1.4$ and $T_{c,p} = 0.164$ sec ($T_{c,p}$ is the integral time scale from analysing the measured conditional time series). Since the statistics of concentration derivative are controlled by high frequency fluctuations produced by small eddies, the upcrossing rate will be sensitive to the sampling cut-off frequency. The concentration time series generated by the stochastic model was filtered with a Butterworth digital filter, with the cut-off frequency set at 5 Hz or 100 Hz.

The linear model calculations (with “ a ” term from (4.2.7)) were carried out with several values for the time constant $T_{c,p}$, to obtain a family of threshold upcrossing rate N^+ for each of the two cut-off frequencies. Figure 4.2.2 shows, as expected, the upcrossing rate N^+ decreases monotonically with increasing $T_{c,p}$, showing that N^+ is indeed controlled

by small scale eddies.

Figure 4.2.3 compares the upcrossing intensities obtained from the linear model calculations (with $T_{c,p} = 0.164$ sec) with observations of the Dugway experiment. Overall the agreement is quite satisfactory (the maximum difference is within a factor of 2).

Figure 4.2.4 compares the non-linear model predictions of upcrossing rate for different α 's. The prediction is not very sensitive to the value of α , and it seems that $\alpha=0$ may be the optimal choice. This is a very good property of the model: the simplest model gives the best result.

4.2.5. Sensitivity of N^* to the shape of the concentration pdf

We also examined the sensitivity of N^* to the shape of the concentration pdf. The Gamma pdf

$$p_c(c) = \frac{k^k (c/C_p)^{k-1}}{C_p \Gamma(k)} \exp(-k \frac{c}{C_p}), \quad (4.2.15)$$

where $k=1/i_p^2$, approximates many of the available observations quite well. With $a(c,t)$ given by (4.2.7), we can derive by substituting (4.2.15) to (4.2.8) that

$$b^2 = \frac{2C_p k^k}{T_c p_c(c) \Gamma(k)} \int_0^\infty c^k e^{-kc} dc. \quad (4.2.16)$$

Figure 4.2.5 compares the predictions of N^* with (4.2.1) and with (4.2.16), respectively. Predicted N^* is somewhat sensitive to the shape of $p_c(c)$, which suggests that in predicting upcrossing intensity the functional form of p_c should be chosen with care, - a difficulty, since from experimental data it is often difficult to discriminate which pdf p_c is "best."

4.2.6. Conditional standard deviation of concentration time derivative

One of the most important findings of Yee et al. (1993b) is that for a stationary

concentration time series, the concentration derivative is *not independent* of concentration itself, although concentration and its time derivative are *uncorrelated* due to the steadiness of the concentration series. This of course is hardly surprising, and was anticipated by Kristensen et al. (1989). It explains in part why the Kristensen et al. model underestimates the upcrossing intensity for large concentrations.

For the Dugway field experiment, Yee et al. (1993b) obtained that at the sampling point $x/h=20.0$ on the plume centerline that the conditional standard deviation (σ_{ξ}) of normalized concentration derivative, $\xi=c/\sigma_c$, given a fixed normalized concentration level, c/C_p , can be represented well by the empirical formula

$$\sigma_{\xi}(c/C_p) = \frac{1}{\sqrt{2}} \left(\frac{c}{C_p} \right)^{1.7/2.0} \quad (0.5 < c/C_p < 6.0). \quad (4.2.17)$$

In obtaining (4.2.17), the cut-off frequency was chosen to be 100 Hz.

The stochastic model predictions for $T_{c,p} = 0.1 \sim 0.3$ s, cut-off frequency $f_c = 100$ Hz were compared with formula (4.2.17). Our results (Figure 4.2.6) support Yee et al's (1993b) finding that $\sigma_{\xi} = \sigma_{\xi}(c/C_p)$, but suggest a slightly different form

$$\sigma_{\xi}(c/C_p) = A_1 + A_2 \left(\frac{c}{C_p} \right)^{A_3}, \quad (4.2.18)$$

where the A's are constants for given T_c . We also calculated σ_{ξ} with the gamma single pdf, as shown in Figure 4.2.7. It seems that A_1 increases with $T_{c,p}$ for a given pdf, while A_2 and A_3 are controlled by the form of the single pdf $p_c(c)$. In general A_2 and A_3 could vary with location, concentration pdf and possibly other factors. Formula (4.2.18) seems more reasonable than (4.2.17) for small c/C_p ; the latter implies that when the concentration is zero (or near zero), concentration at the later time should remain zero (or near zero).

4.2.7. Considerations to improve the model

The concentration spectrum generated by our first-order Markovian model is

characterised by a "-6/3 law" in the high frequency range. Wilson and Zhuang (1989) demonstrate this for the parallel case of their Langevin model for the evolution of velocity, in contrast the Dugway field data exhibit a "-5/3 law." Wilson (1995) in his Appendix B studied the effect of the concentration spectrum shape on the upcrossing rate, finding that the distinction between the "-6/3" and "-5/3" spectral form is not important for frequencies of practical interest. But when the concentration spectrum differs substantially from the "-6/3" law, for example, the "-3/3" law for the diffusion process with Schmidt number $Sc \gg 1$ (Wilson et al. 1991), consideration must be given to this aspect if we intend to predict upcrossing intensity (or more broadly, to regenerate the concentration time series) with a stochastic model.

The other problem is how to define an in-plume conditional time scale. Usually the in-plume conditional time series is obtained from the total series by simply clipping off all the concentration readings smaller than some "zero" threshold level. In doing so, the segments of the process lying between non-zero segments are artificially replaced by a "faster" process, so that artificial high frequency components are introduced, and the time scales calculated from such a conditional time series are expected to be smaller than the true values. This may explain why a larger $T_{c,p}$ (in between 0.2~0.3) gives the best agreement between the model prediction and the measurement.

4.2.8. Conclusions

From a specification of the concentration pdf and the Eulerian integral time scale for concentration, we can specify a Markovian model for $c(t)$, simulate a concentration time series, and draw information from it to predict upcrossing intensity. The merit of this technique, in comparison with models based on the Rice (1945) theory, is that it demands less given-information, but nevertheless achieves a reasonably accurate prediction. The conditional standard deviation of the normalized concentration derivative calculated from this stochastic model is qualitatively consistent, over the range of $1.0 \leq c/C_p \leq 6.0$, with Yee et al.'s (1993b) field measurements that show that the standard deviation of the derivative

increases with the concentration level c_i at which it is measured, and may be more reasonable in the small concentration range $c/C_p < 1.0$. Our model calculation also shows that the upcrossing intensity has some dependence on the functional form of the single pdf, $p_c(c)$, with the upcrossing rate N^+ about a factor of two higher for the gamma pdf compared to the log-normal pdf.

Bibliography

- Gardiner, C.W., 1985: *Hand Book of Stochastic Methods*. 2nd ed. Springer-Verlag.
- Kristensen, L., J.C. Weil and J.C. Wyngaard, 1989: Recurrence of high concentration values in a diffusing, fluctuating scalar field. *Boundary-Layer Meteorol.*, **47**, 263-276.
- Rice, S.O., 1945: Mathematical analysis of random noise, *Bell Sysem. Tech. J.*, **24**, 46-156.
- Rockafellar, 1984: *The Fokker-Planck Equation*. Springer-Verlag.
- Wilson, D.J., 1995: *Averaging Time and Concentration Fluctuation Effects in Vapor Cloud Dispersion*. American Institute of Chemical Engineers, Centre for Chemical Process Safety, New York.
- Wilson, D.J., B.W. Zelt and W.E. Pittman, 1991: *Statistics of turbulent fluctuations of scalar in a water channel*. Technical Report for Defence Research Establishment Suffield (DRES-CR-31-91), University of Alberta, Canada.
- Wilson, J.D. and Y. Zhuang, 1989: Restriction on the timestep to be used in stochastic Lagrangian models of turbulent dispersion. *Boundary-Layer Meteorol.*, **49**, 309-316.
- Yee, E., R. Chan, P.R. Kosteniuk, G.M. Chandler, C.A. Biltoft and J.F. Bowers, 1994: Experimental measurements of concentration fluctuations and scales in a dispersing plume in the atmospheric surface layer obtained using a very fast response concentration detector. *J. Appl. Meteorol.*, **33**, 996-1016.
- Yee, E., P.R. Kosteniuk, G.M. Chandler, C.A. Biltoft and J.F. Bowers, 1993a: Statistical

characteristics of concentration fluctuations in dispersing plumes in the atmospheric surface layer. *Boundary-Layer Meteorol.*, **65**, 69-109.

Yee, E., P.R. Kosteniuk, G.M. Chandler, C.A. Biltoft and J.F. Bowers, 1993b: Recurrence statistics of concentration fluctuations in plumes within a near-neutral atmospheric surface layer., *Boundary-Layer Meteorol.*, **66**, 127-153.

Zelt, B.W., 1992: *Concentration fluctuations and their probability distribution in laboratory plumes*. Ph.D. thesis, Dept. of Mechanical Engineering, University of Alberta, Canada.

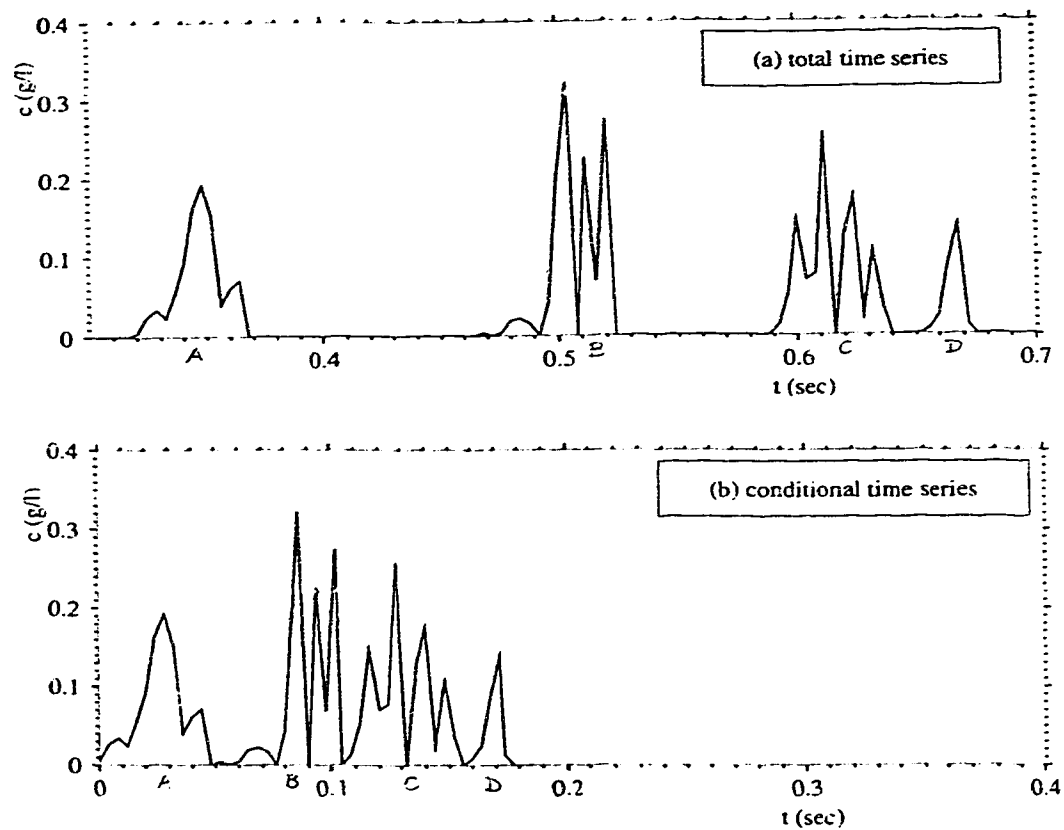


Figure 4.2.1. An example showing how essentially uncorrelated segments in the total time series become correlated in the conditional in-plume time series which is obtained by removing "zero" readings from the total time series. (a) total time series; (b) conditional time series.

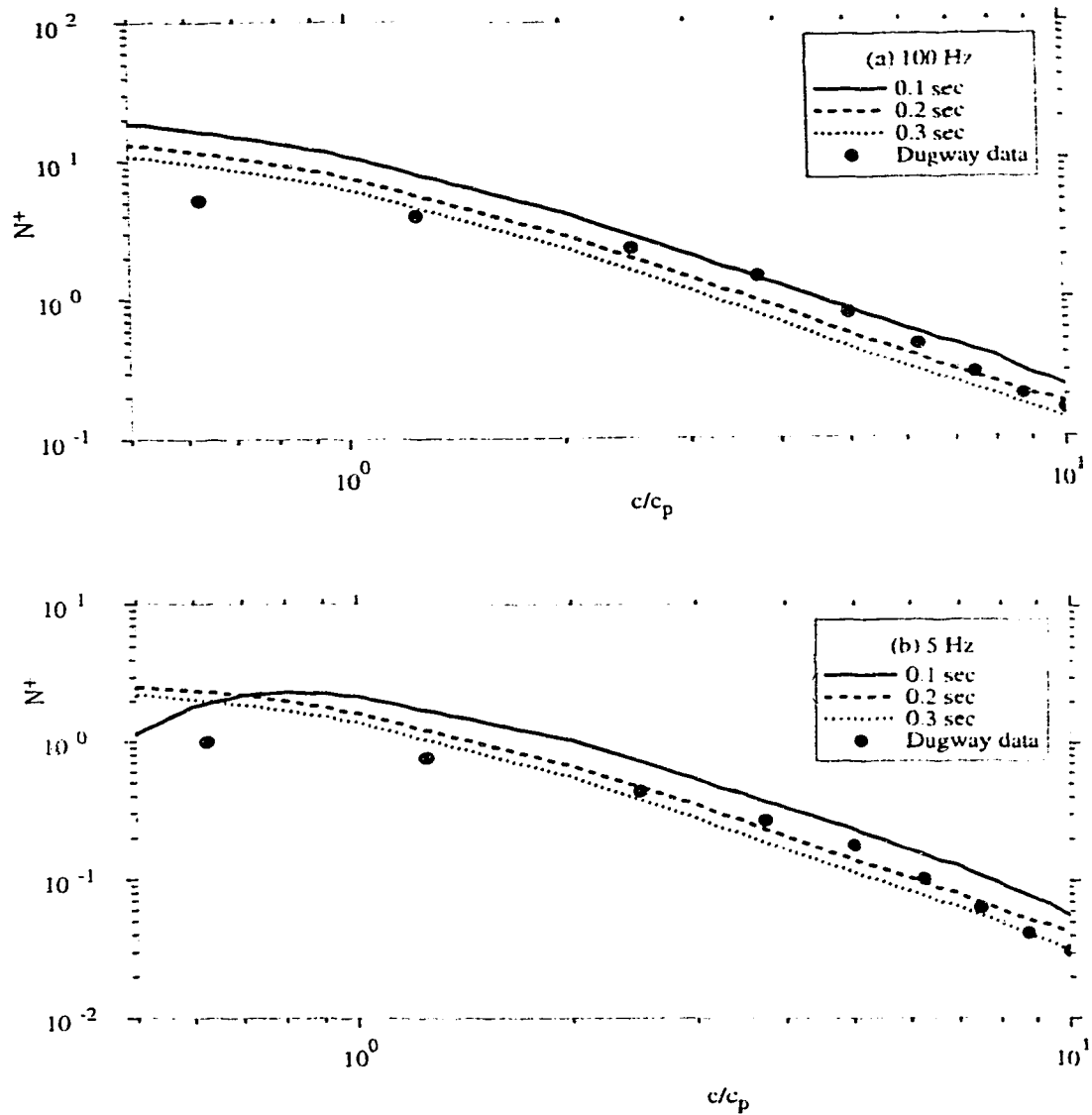


Figure 4.2.2. A family of the predicted upcrossing intensity from Log-normal concentration pdf. Also shown is the measured upcrossing intensity from Dugway experiment. Curves for different values of $T_{c,p}$.

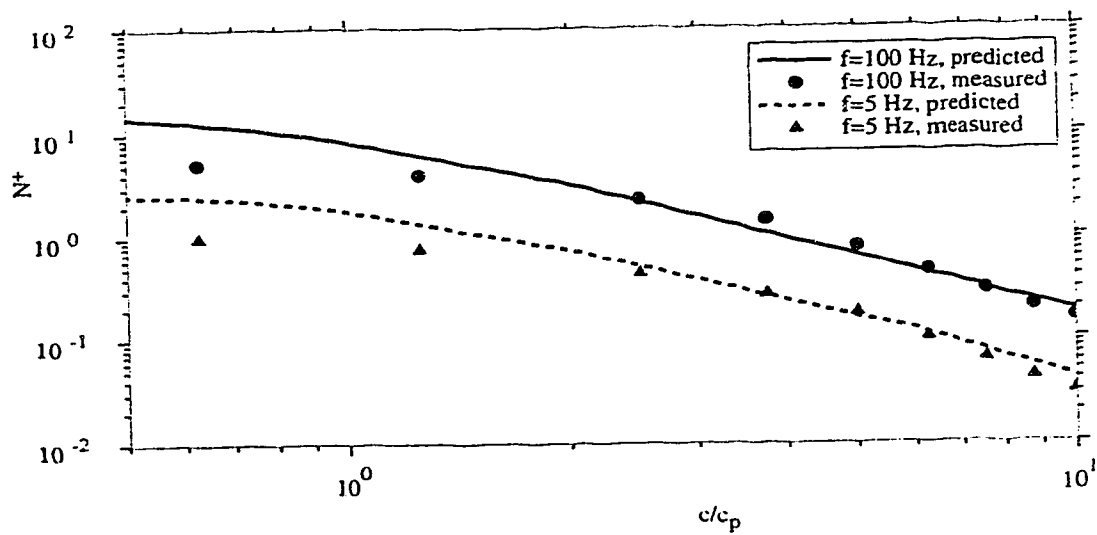


Figure 4.2.3. Comparison of model predicted upcrossing intensity with the Dugway field experiment data for two cut-off frequencies: 100 Hz and 5 Hz.

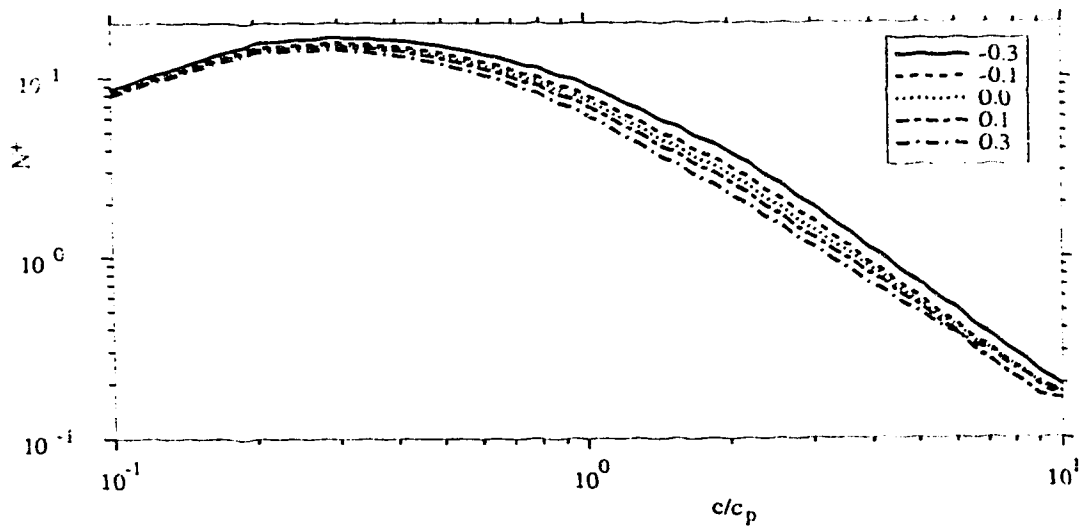


Figure 4.2.4. The sensitivity of the upcrossing intensity to the non-linearity exponent α .
Curves for α from -0.3 to 0.3.

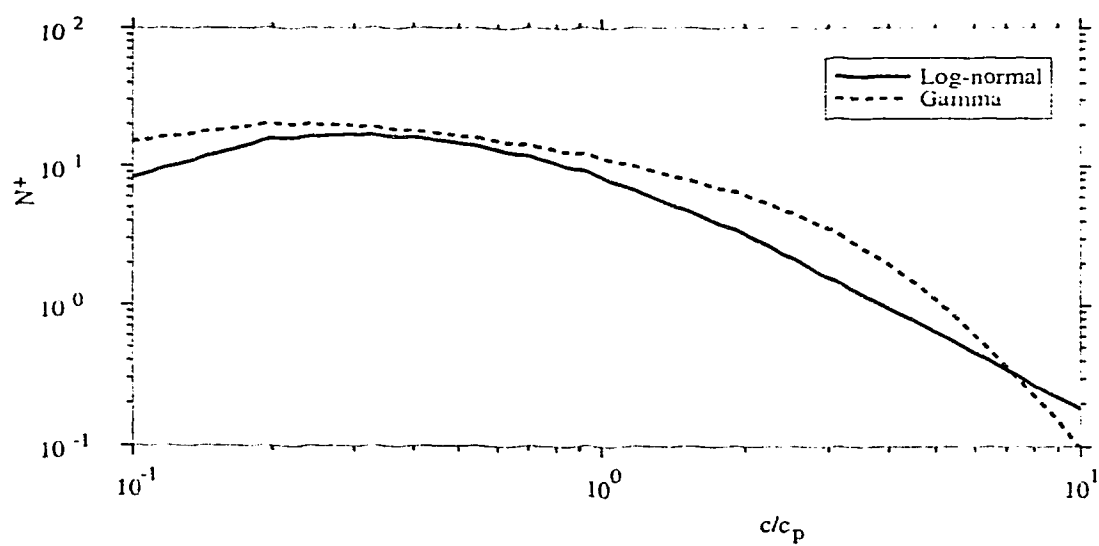


Figure 4.2.5. Upcrossing intensity N^+ predictions with different concentration pdf's: Log-normal pdf and Gamma pdf.

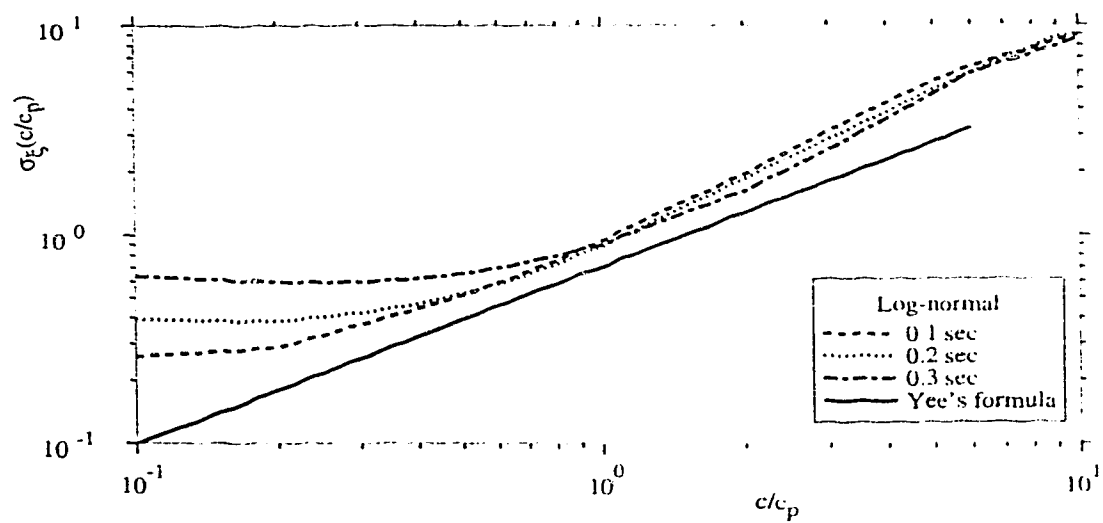


Figure 4.2.6. A family of conditional standard deviation of concentration derivative (see text for the exact definition), $\sigma_{\xi}(c/C_p)$, obtained from model calculation with Log-normal pdf. Also shown is the Dugway data fit reported by Yee et al. (1993b). Curves for $T_{c,p}$ from 0.1 to 0.3 sec.

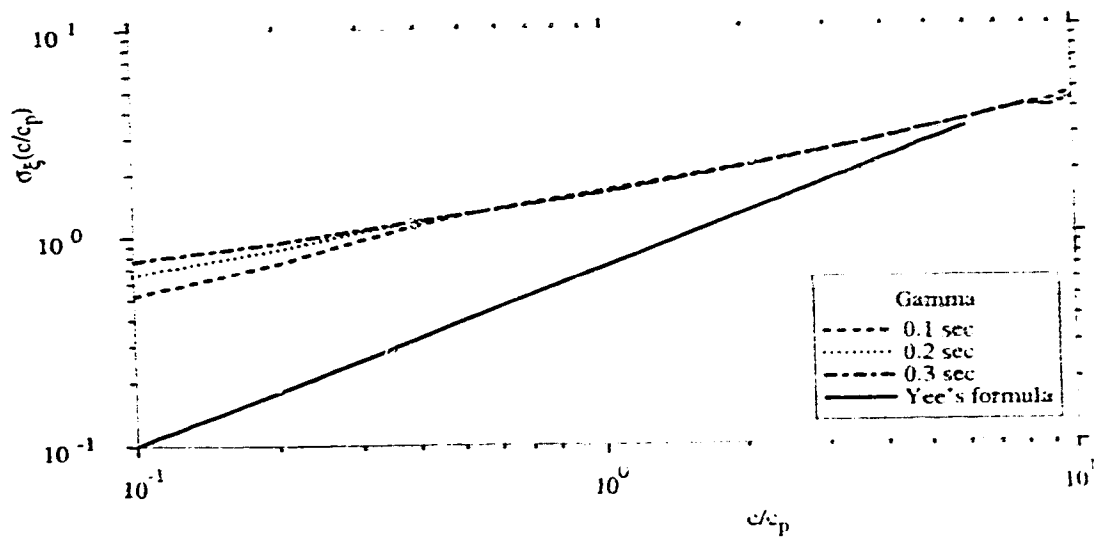


Figure 4.2.7. A family of conditional standard deviation of concentration derivative (see text for the exact definition), $\sigma_{\xi}(c/C_p)$, obtained from model calculation with Gamma pdf. Also shown is the Dugway data fit reported by Yee et al. (1993b). Curves for $T_{c,p}$ from 0.1 to 0.3 sec.

Chapter 5

Concluding Remarks

Two Lagrangian stochastic models are developed in this thesis: a first-order single particle model for non-Gaussian turbulence, and a second-order single particle model for Gaussian, low-Reynolds-number flow.

Some turbulent dispersion problems are studied by making use of these models and models developed by others: the distribution of mean concentration in the convective boundary layer; the effect of higher-order velocity moments on the mean concentration distribution; the validity of the moments approximation method developed by Kaplan and Dinar; determination of the Kolmogorov constant for the Lagrangian velocity structure function. The stochastic simulation technique is also used to study droplet collisions in a cloud, and the rate of upcrossing over certain threshold levels of concentration at a given spacial point downwind of a contaminant source.

A brief summary of the findings/contributions is as follows:

1. Rather than adopt an *ad hoc* velocity pdf, the maximum missing information (mmi) principle should be used when constructing the Eulerian velocity pdf from known velocity moments, otherwise the pdf may have unphysical properties.
2. There is no guarantee that an LS model derived by using the Kaplan-Dinar moments approximation method is well-mixed, and the model can give an inferior prediction for the mean concentration.
3. The third and fourth order velocity moments can affect the concentration distribution. The mean concentration distribution is sensitive to the velocity skewness S when S is large ($S > 0.6$), and to the velocity kurtosis K when K is small ($K < 3.0$). Hunt's small-time analytic predictions for the plume centerline position and the plume width are valid for $t \leq 0.5(2\sigma_w^2/C_0\epsilon)$; but his inference that near a ground-level source the vertical spread is dominated by the gradient of third-order velocity moment, is not correct.
4. The Sawford second-order model is exact for isotropic, homogeneous,

stationary and Gaussian turbulence (wherein both velocity and acceleration pdf's are Gaussian); an extended version of the Sawford model for isotropic, homogeneous, Gaussian and *decaying* turbulence is derived.

5. The Kolmogorov constant (C_0) for Lagrangian velocity structure function has numerical value $C_0=3.0\pm0.5$, universal across grid turbulence, laboratory boundary layer flow and (full-scale) atmospheric boundary layer flow.

6. Turbulence can enhance the collision probability of cloud droplets when fluctuations are strong and the size difference of cloud droplets is not large.

7. A stochastic simulation technique is developed to predict the rate of upcrossing over concentration threshold levels at a given spacial point. The model is tested against experimental data from the Dugway Proving Grounds, and is shown to be satisfactory.

The present work has dealt with both the deterministic term $a_i(\mathbf{u}, \mathbf{x}, t)$ and the random forcing term $b_{ij}(\mathbf{u}, \mathbf{x}, t) d\zeta_j$ of the Langevin equation for the evolution of particle's velocity. By applying appropriate models to several different turbulent flows, the Kolmogorov constant C_0 appears to be universal with a value of 3.0 ± 0.5 . Therefore the non-universality problem raised by Sawford and Guest (1988) has been solved. However, I want to stress that a discrepancy in the apparent value of C_0 still exists, between the present study and studies based on other methods (eg., Fung et al. 1992; Pope 1994); that is, to completely settle the non-universality problem, further investigation is needed. With respect to the deterministic term, I studied how to construct the Eulerian velocity pdf from given low order moments so that the well-mixed constraint can be used to derive the coefficient $a_i(\mathbf{u}, \mathbf{x}, t)$ - which is of great importance in practical applications: but the outstanding non-uniqueness problem is yet to be solved. Solving the non-uniqueness problem is imperative, because frequently diffusion must be calculated in multiple dimensions.

Speaking of practical applications, few real plumes/puffs can be treated as "passive tracers"; real pollutants are either buoyant or heavy, in comparison with the ambient air. Diffusion models are less developed for those non-passive contaminants, the main difficulty in the Lagrangian stochastic modeling being a lack of sound physical

constraint(s) parallel to the well-mixed constraint for passive tracer.

Though it is presumably the most natural and appropriate means to study droplet collisions in turbulent clouds, a second-order two-particle Lagrangian stochastic model is not yet available. The present study in this respect is intended only to draw the attention of the cloud physics research community to the fact that if the LS modeling technique is used inappropriately, results could be in serious error.

A novel attempt made in this thesis is to apply the stochastic modeling technique to simulate the time evolution of concentration (ie. to simulate statistically the concentration time series) at a given spatial point. To my knowledge this is the first work of its kind reported. The preliminary results show this technique can be very successful. *If further tested (confirmed) the model will be very useful in many practical applications.*

Finally, it may be helpful to discuss the fundamental assumption underlying Lagrangian stochastic simulation: each fluid element/particle conserves its species concentration and does not mix with other fluid elements. If this assumption were exactly true, then the distribution of concentration moments will be uniquely determined by the source distribution and the time-space distribution of tracer particles - for example, under that assumption, the mean concentration distribution due to a point source will be uniquely determined by source strength and by the number density function of tracer particles. But there is evidence showing this is not the case in reality: the shape of the mean concentration distribution is not identical to the shape of the concentration intermittency factor (Mylne 1993); and the in-plume conditional mean concentration decreases with downstream distance (Chatwin and Sullivan 1990). One may expect LS methods to require further development for application to problems in which molecular effects play an important role.

Bibliography

- Chatwin, P.C. and P.J. Sullivan, 1990: A simple and unifying physical interpretation of scalar fluctuation measurements from many turbulent shear flows. *J. Fluid Mech.* **212**, 533-556.
- Fung, J.C.H., J.C.R. Hunt, N.A. Malik and R.J. Perkins, 1992: Kinematic simulation of homogeneous turbulence by unsteady random Fourier modes. *J. Fluid Mech.* **236**, 281-318.
- Mylne, K.R., 1993: The vertical profile of concentration fluctuations in near-surface plumes. *Boundary-layer Meteorol.* **65**, 111-136.
- Pope, S.B., 1994: Lagrangian pdf methods for turbulent flows. *Annual Review of Fluid Mechanics*, Vol. **26**, 23-63.
- Sawford, B.L. and F.M. Guest, 1988: Uniqueness and universality of Lagrangian stochastic models of turbulent dispersion. *8th Symp. Turbulence and Diffusion*. American Meteorol. Soc. pp96-99.